

EDDY BAR RESPONSES TO THE
SEDIMENT DYNAMICS OF POOL-RIFFLE ENVIRONMENTS
- FINAL REPORT -

APRIL 10, 1997

BY

BRIAN L. CLUER, HYDROLOGIST

NATIONAL PARK SERVICE

WATER RESOURCES DIVISION

FORT COLLINS, COLORADO

442.00
RES-3.20
G649c

EDDY BAR RESPONSES TO THE
SEDIMENT DYNAMICS OF POOL-RIFFLE ENVIRONMENTS

- FINAL REPORT -

APRIL 10, 1997

BY

BRIAN L CLUER, HYDROLOGIST

NATIONAL PARK SERVICE

WATER RESOURCES DIVISION

FORT COLLINS, COLORADO

COOPERATIVE AGREEMENT NUMBER #9AA-40-07920 MOD 11

PROJECT NAME: [A PROPOSAL TO] DETERMINE THE PROCESSES OF RAPID EROSION AND
THE EFFECTS ON EVOLUTION AND LONGEVITY OF CHANNEL MARGIN
DEPOSITS

[FINAL REPORT] ENTITLED: EDDY BAR RESPONSES TO THE SEDIMENT
DYNAMICS OF POOL-RIFFLE ENVIRONMENTS

PRINCIPAL INVESTIGATOR: BRIAN L CLUER

EFFECTIVE DATE OF COOPERATIVE AGREEMENT: JANUARY 15, 1993

COOPERATIVE AGREEMENT TERMINATION DATE: DECEMBER 31, 1996

FUNDED BY: US BUREAU OF RECLAMATION, GLEN CANYON ENVIRONMENTAL
STUDIES OFFICE, FLAGSTAFF, AZ

SPONSORED BY: NATIONAL PARK SERVICE, GRAND CANYON NATIONAL PARK, AZ

ABSTRACT

EDDY BAR RESPONSES TO THE SEDIMENT DYNAMICS OF POOL-RIFFLE ENVIRONMENTS

Rivers in bedrock channels often contain debris fans that create sand deposits in lateral flow separation zones. Debris fans are reworked by infrequent flood flows, which are more infrequent downstream from dams. Dams also reduce downstream sediment supply and the riparian environment suffers from a lack of rejuvenating floods and degradation of alluvial deposits.

During this investigation, one eddy bar in the dam-regulated Colorado River in Grand Canyon was stripped of 11,500 m³ of sand in a few hours. Monitoring programs have documented dozens of rapid erosion events throughout the Grand Canyon. This investigation was undertaken to determine (1) if the process occurs only in the regulated river environment, (2) the fate of sediment stripped from eddy deposits, and (3) what causes rapid erosion.

Investigation of similar deposits along the near-naturally flowing Colorado River near Moab, Utah, showed that eddy deposit stripping occurs annually, during the rising limb of annual floods. Stripping was preceded by deformation of the pool adjacent to the eddy. Repeated channel mapping in the Grand Canyon showed the same pattern of pool deformation preceding scour of an eddy bar. The sediment stripped from eddies is transported downstream. Therefore, new eddy bars form from sand delivered from upstream.

Velocity field measurements, concurrent with repeated channel mapping, showed that high boundary shear stress exists along the toe of large bars. Large bars have slopes at or exceeding the angle of internal friction, so minor changes in the flow field can trigger slope failure. A calibrated two-dimensional flow model confirmed that minor

deformation of the pool exit and entry slopes results in increasing shear stress beyond particle stability along the toe of the eddy bar.

Variation in sediment load between rising and falling limbs of flood flows causes temporary pool deformation. This process was documented in the natural river undergoing an annual flood flow and in the regulated river undergoing a daily hydropower flood flow. Slope failure, if sufficiently voluminous, may augment a rapid erosion event by increasing the sediment supply in the pool.

ACKNOWLEDGMENTS

The National Park Service, Water Resources Division suggested and initiated the comparative study between channel margin sand deposits occurring on regulated and unregulated incised bedrock rivers. NPS-WRD continued to provide equipment, supplies, personnel and technical support for the duration of this investigation. Grand Canyon National Park and the US Bureau of Reclamation's Glen Canyon Environmental Studies Office provided financial support and logistical support for the Grand Canyon studies. Numerous volunteers from NPS-WRD, Canyonlands National Park, Colorado State University and friends contributed to the field surveys and camera maintenance. The value of their assistance was, as usual, far greater than an acknowledgment recognizes. The Graduate Committee, consisting of Drs. Ellen Wohl, Deb Anthony, Pierre Julien, Stanley Schumm, and William Jackson provided review comments on this report.

TABLE OF CONTENTS

Chapter	Page
Abstract	iii
Acknowledgments	v
Introduction	1
Project Background	1
Goals	5
Geomorphic Setting and Processes	6
The Rapids	6
Debris Fans	8
Cobble Bars	8
Channel Margin Sand Bars	10
Importance of Sand Bars	12
Previous Sand Bar Monitoring Investigations	13
Methods	19
Site Selection	19
Near-Naturally Flowing River Near Moab, UT	20
Regulated Colorado River in the Grand Canyon	23
Data Collection	27
Moab Study Reach	27
Mohawk Study Reach in the Grand Canyon	29
Channel Surveying	29
Velocity Field Measurement	32
River Stage	35
Slope Motion	36
Particle Size	36
Shear Stress and Particle Stability Calculations	36
Computer Flow Modeling	39
Model Calibration and Verification	42
Mapping	45

Chapter	Page
Contour Maps and Slices	45
Results	46
Moab	46
Five to Ten Year Information	46
Seasonal Information	47
Continuous Information - The 1994 Flood	52
Results of the 1995 Flood	59
Mohawk	60
Capturing a Rapid Erosion Event	60
Tilt Sensor Data	62
Topographic Maps and Slices	64
Velocity Field - Particle Stability Maps	71
Particle Size	71
Particle Stability	71
Results From Hourly Surveys	76
Modeling Results	76
Discussion	95
Unregulated River Moab Reach	95
Regulated Mohawk Reach	99
The Causes of Rapid Sand Bar Erosion	100
Conceptual Model	108
Interpretation For Various Reaches	112
Conclusions	114
Summary	117
Recommended Improvements	117
Management Considerations	119
Investigating Natural Rivers	119
Monitoring Regulated River Sand Bars	120
Processes Missing On The Regulated River	122
Role Of Floods, Expectations Of Their Results	122
Additional Work	125
References	126

INTRODUCTION

Project Background and Objectives

The Glen Canyon Dam completely regulates the water flowing downstream through the Grand Canyon, which passes first through hydroelectric generators that respond to demand for peaking power in the interior western U.S. This type of power plant yields very unsteady discharge as demand varies with hourly home and industrial usage, and with daily and seasonal heating and cooling needs. A typical peaking power hydrograph for the Glen Canyon Dam is shown in figure 1. Discharges rarely exceed power plant capacity ($895 \text{ m}^3\text{s}^{-1}$) except for tests and spilling surplus inflow (figure 2). The high suspended sediment load, causing coloration for which the Colorado River was originally named, is trapped in Lake Powell behind the Glen Canyon Dam and no clastic sediment passes this structure.

As part of the Glen Canyon Dam Environmental Impact Statement (USBOR, 1995), a comprehensive set of environmental studies was conducted in the Grand Canyon in 1990-1991 to supply data on various dam operation alternatives. A series of test flows were run to examine the effects on the physical and biological systems. The test flows were all within power plant capacity and within water delivery legal agreements. They consisted of 11-days of releases followed by three days of low constant flow at $142 \text{ m}^3\text{s}^{-1}$ for evaluating the effects.

Sand bar surveys repeated at two-week intervals were confounded by measurement of unexpectedly large erosion and deposition (Beus and Avery, 1991). Having witnessed the large area and volume changes that occurred over two-week intervals, I monitored one study site with an automatic camera. Taking three photographs daily, it was discovered that the sand bar at river mile 68 underwent two cycles of very

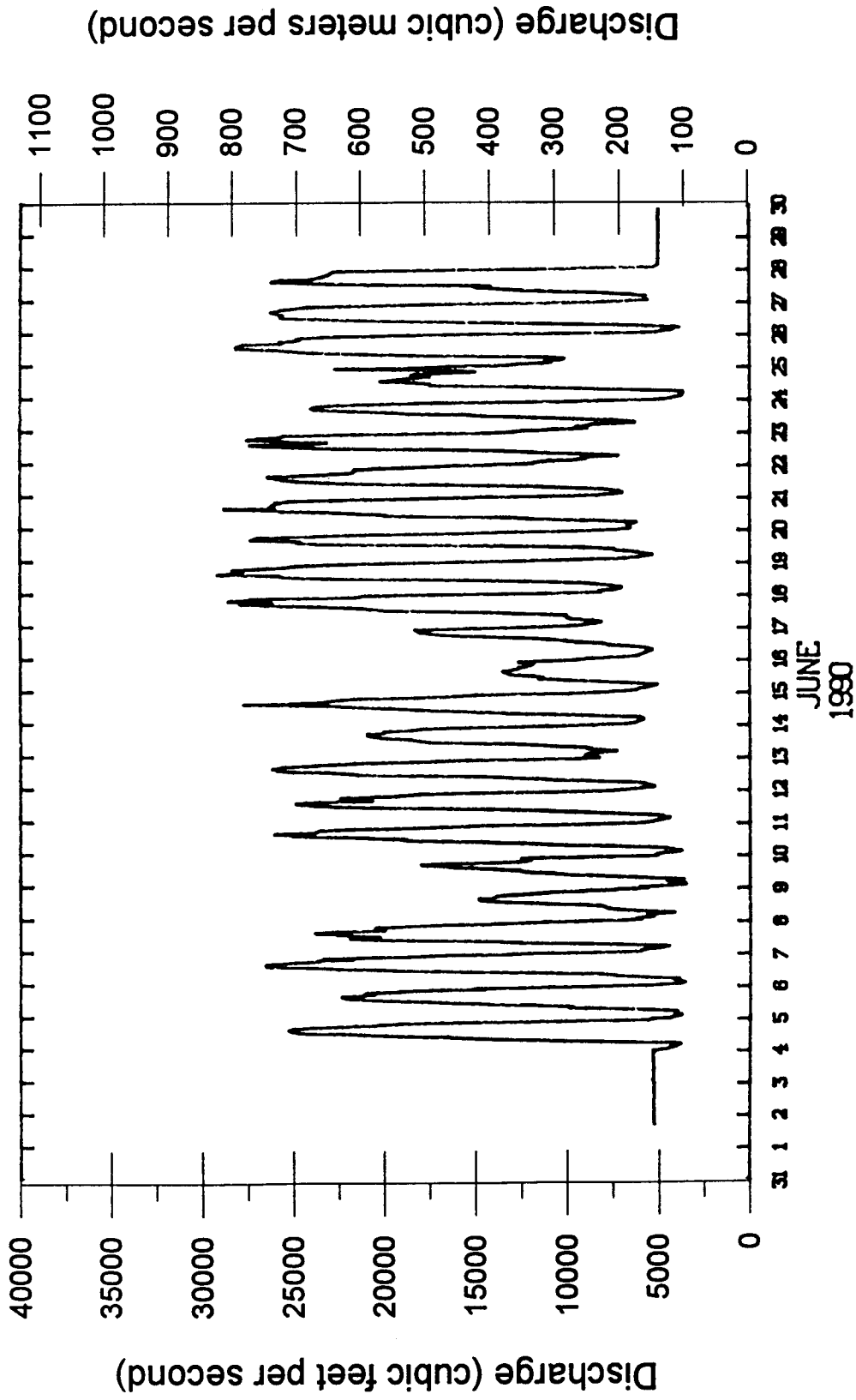


Figure 1. Example of post-dam hydrograph for peaking hydroelectric power production. Five days of large flow fluctuations (Monday-Friday) are typically followed by two days of lower flow fluctuations (Saturday-Sunday).

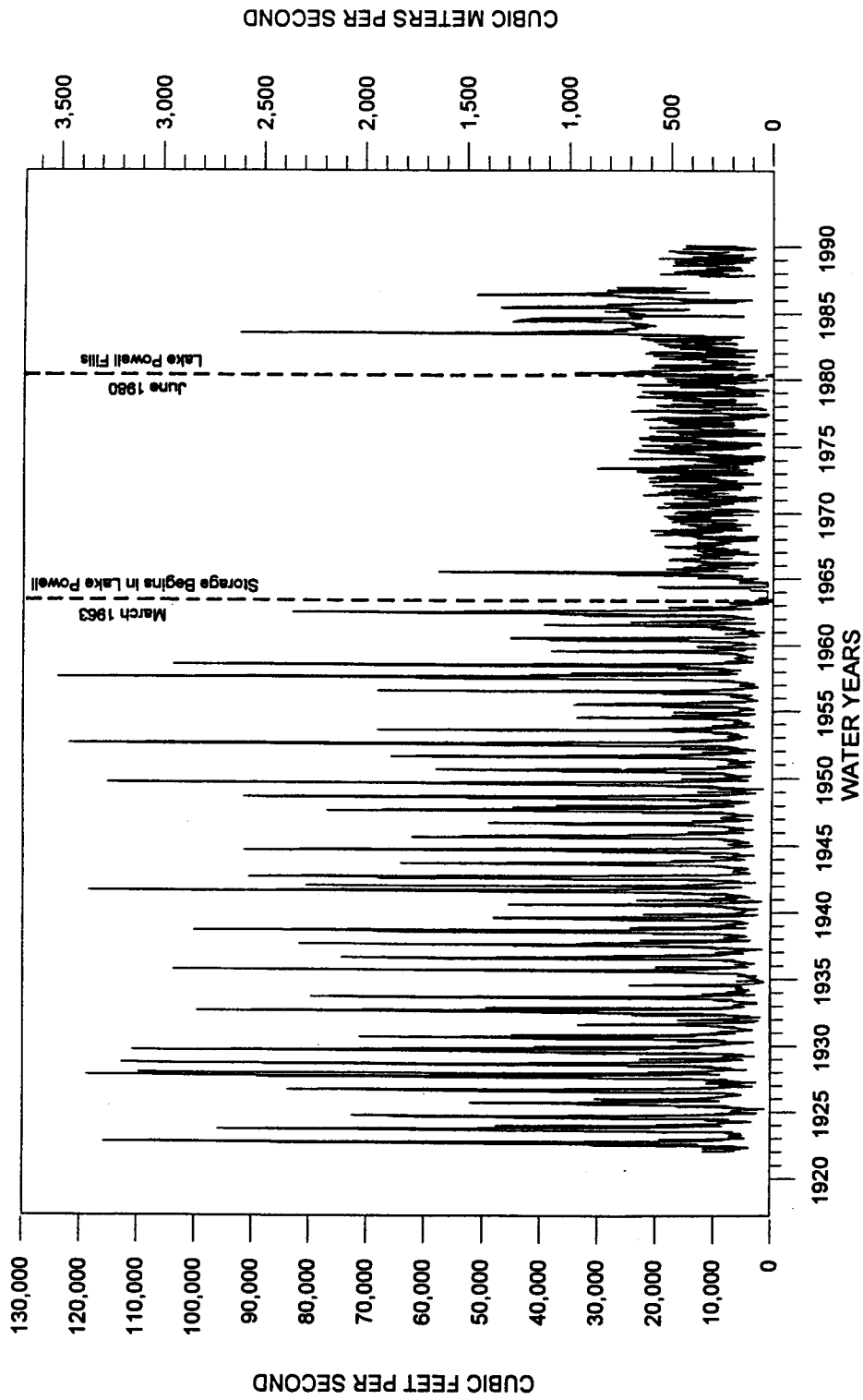


Figure 2. Daily mean discharge of Colorado River at Lees Ferry gage for water years 1922-90. Notice annual flood pattern in the pre-dam period, post-dam bypass flows 1983-1986, and regulated fluctuation patterns in the post-dam filling and post-dam full periods for hydropower production.

rapid erosion and deposition during the period between repeated two-week surveys (Cluer, 1991). Automatic camera systems were installed at seven study sites late in 1990, and in 1992 the sample was expanded to 43 sites as studies for the Environmental Impact Statement gave way to interim monitoring of the fluvial environment while awaiting the Secretary of Interior's Record of Decision (signed in 1996). Discharge during the interim period was constrained between the minimum of $227 \text{ m}^3\text{s}^{-1}$ and maximum of $567 \text{ m}^3\text{s}^{-1}$, and maximum daily variance of $227 \text{ m}^3\text{s}^{-1}$.

During the interim monitoring period, the automatic cameras documented several important and previously unknown fluvial processes on Colorado River sand bars. Between August 1990 and July 1993, 79 sudden losses of sand occurred at 28 sand bars distributed throughout the Grand Canyon (Dexter et al., 1995). The duration of erosion periods was generally less than one day, followed by a longer period of deposition lasting several weeks. Following a rapid erosion event and redeposition, it was impossible to deduce that a sand deposit had recently undergone the dramatic events documented on film.

Long-running records from two sites (river miles 68 and 172) showed 19 cycles of rapid erosion and deposition with mean return periods of approximately 100 days (Dexter et al., 1995). The processes causing rapid erosion appeared to be driven by particular patterns of flow fluctuation because 70% of all erosion events occurred within one or two days following a change in flow pattern, such as a low weekend flow, or other pattern adjustment coincident with changing dam releases to meet seasonally adjusted water delivery agreements (Cluer and Dexter, 1994). Ironically, many rapid erosion events coincided with changes to brief low constant flow patterns to obtain environmental measurements. Other contributions from automatic camera monitoring included the documentation of; 1) periods of sand deposition culminating in rapid erosion and repetition of the cycle, 2) unique cycle lengths for individual sand deposits, and 3) nearly all sand deposits being affected between Lees Ferry and Diamond Creek (between 29 and 390 kilometers downstream from the Glen Canyon Dam).

Rapid erosion was independently validated by continuous recording water level and land tilt instrumentation installed at several sites in Grand Canyon in 1991-1992. Several erosion events not revealed by photography were detected underwater by these methods (Carpenter et al. 1991; Cluer et al., 1993). The potential for rapid erosion of large volumes of sand out of these channel margin storage zones was recognized as an episodic process that was not previously documented or well understood. It was also recognized that the scour and fill histories of channel margin deposits were probably more complex than previous studies, using longer time intervals, were able to document.

The term 'rapid erosion event' was adopted to distinguish between the newly documented episodic process of erosion and the prevailing concept of gradual linear or logarithmic decay of channel margin deposits by 'erosion rates'. Finally, one rapid erosion event was witnessed by a group of scientists who were stationed for ten days at one location in 1991 (Cluer, 1991). Another erosion event was measured in detail in 1993 (Cluer et al., 1993) with channel bathymetry and three-dimensional acoustic Doppler velocity mapping equipment. The eddy deposit was scoured over five meters deep in the latter event, which lasted less than three hours. The results of that fortuitous investigation are presented in this report.

The observations listed above showed that sand deposits were cyclically eroded and deposited in the Grand Canyon by a wide variety of fluctuating hydropower discharges (Cluer and Dexter, 1994) and that previous measurement time scales probably biased the results of monitoring programs (Cluer, 1995a). Cyclic erosion processes primarily influence unvegetated eddy bars. However, because the low elevation eddy bars cover the toe and flank of older and higher elevation reattachment bars, there is an important secondary influence of rapid erosion processes that has longer term importance. During the time between scour and deposition of eddy bars, higher elevation sand deposits are exposed to erosion processes and steep banks retreat toward the angle of repose. For example, the July, 1993 rapid erosion event mentioned previously, scoured the toe of the reattachment bar which resulted in lateral erosion of approximately one meter into sand deposited prior to the germination of *baccarus* and *tamarisk* in 1986.

Thus, the erosion of high elevation deposits is periodic, with the period controlled by the cycle period of eddy bar erosion/deposition events. Cluer and Dexter (1994) found that the time period when sand deposits at higher elevations were susceptible to erosion from bank retreat varied in the Grand Canyon from two weeks to several months, and the susceptible erosion period was repeated several times annually at many of the locations studied.

Documentation that rapid erosion events were frequent, often involved entire eddy bars, and were spatially ubiquitous in the Grand Canyon invoked several questions about the processes of sand bar erosion. Short interval data suggested that the scour and fill histories of channel margin sand bars were more complex than previously described. Because of the increasing ecological and natural resource significance of the diminishing sand bars (or at least the diminishing sand supply) in Grand Canyon, the processes of erosion have potentially important management implications. Except for a study on wave erosion processes (Bauer and Schmidt, 1993), a demonstration study of seepage erosion (Werrell et al., 1993), and theoretical modeling of seepage induced sand bar failure (Budhu and Gobin, 1994), the process based studies have been focused on deposition (Andrews, 1991a; Nelson et al., 1994; Rubin et al., 1990, 1991, 1994; Schmidt, 1990; Schmidt and Graf, 1990; Schmidt et al., 1993). Managers and resource users have lamented the erosion of sand bars but the focus of scientists has been on deposition, or the lack of deposition (Smith and Andrews, 1993). One of the most important management questions is: how can the effective life of sand bars be prolonged? This question is especially opportune following the experimental sand bar/habitat rebuilding spike flow which occurred in March 1996 downstream from Glen Canyon Dam, which was a purposeful perturbation to the river ecosystem with the intent to increase sand stored on the channel margins and replenish sand bars.

Goals

The goals of this investigation were to; (1) determine if the processes of rapid erosion are unique to the regulated river environment, (2) determine if sediment eroded during rapid erosion of channel margin deposits is retained in the local eddy or transported downstream, and (3) determine the processes that result in rapid erosion events. It was hypothesized that transient deformation in the riffle-pool system could result in flow pattern changes that caused the observed eddy bar erosion.

Geomorphic Setting and Processes

Rivers in deeply incised bedrock canyons are often characterized by long, low velocity pooled reaches punctuated by short, abrupt drops through rapids and riffles. The Grand Canyon in Arizona is the classic example of bedrock canyons, and equally well known are the rapids of the Colorado River. The rapids of the Colorado River are constructed of angular, locally derived rocky debris and gravel, and bedrock in some cases. Leopold (1969) showed that 90% of the elevation loss in the Grand Canyon occurs in 10% of the horizontal distance, through the rapids. The rapids create the physical controls that provide the framework for transport, sorting and deposition of finer grained sediments, with unique time scales of stability and motion for the different particle size classes.

The Rapids

The first written descriptions of the Colorado River rapids come from pioneer explorer and geologist John Wesley Powell (1875) who, after his 1869 journey down the Green and Colorado Rivers, suggested that mass movement processes from tributary streams and steep side-canyons periodically delivered large volumes of coarse unsorted sediment to the river. Debris laden side-canyon floods merging into the Colorado River

lose competence and deposit coarse debris as localized obstructions in the main channel. Most rapids in the Grand Canyon occur at tributary and side-canyon mouths. Leopold (1969) made the first depth soundings of the channel in 1965 and presented the argument that rapids spacing was equidistant and rhythmic, related to uniform energy expenditure and a quasi-equilibrium condition of the graded river, not necessarily located at tributaries or side-canyons. This argument and observations of random rapids spacing on other canyon rivers started an interesting scientific discussion.

Dolan et al. (1978) demonstrated that the spatial controls on rapids coincide with geologic structures such as regional joints and faults that result in weaknesses in the bedrock and avenues for tributary and side-canyon formation. However, subsequent echo-sounder channel mapping (Howard and Dolan, 1981) revealed drowned riffle and pool sequences with quasi-rhythmic spacing in wide reaches where the river is free to meander and where geologic controls are not a factor. Graf (1987), looking at rapids in many other canyon rivers of the western U.S., agreed with the structural control conclusion of Dolan et al. (1978) for the Grand Canyon, but proposed that large boulders derived from rock falls could provide a mechanism for the development of randomly located rapids. This idea is similar to Clifford's (1993) autogenetic process of riffle-pool formation where roller eddies (eddies that rotate about an horizontal axis) form upstream and downstream from a major flow obstacle, such as an immobile rock or even a bridge pier. If the obstacle persists long enough it fixes the local flow pattern and causes modification of the channel form which is maintained by riffle-pool processes such as velocity reversals (Keller, 1971) or bed shear stress reversals (Lisle, 1979) at flows exceeding bankfull. Rapids formed by this process would be randomly spaced and located where geology and topography together produced and delivered large coherent blocks to the river.

Graf (1987) compared the spacing and location of rapids in canyon rivers of the Colorado Plateau and found different controls operating in different canyons. Webb et al. (1989) completed the debate's circle for the Colorado River in Grand Canyon by demonstrating that infrequent debris flows from tributaries and short steep side-canyons

deliver coarse sediment to the main channel in sufficient quantity to create rapids, thus corroborating Powell's 1875 theory. They also suggested that subsequent reworking of debris fans supplied cobbles and gravel to the river, and produced gravel-cobble bars resulting in secondary rapids and riffles.

Debris Fans

Debris fans in the Grand Canyon typically consist of a poorly sorted mixture of angular and rounded cobble to gravel material, derived from debris flows. On average, debris fans constrict the channel width by about 50% (Kieffer, 1985). Schmidt and Graf (1990) found that the channel expansion immediately downstream from debris fans is approximately 10% wider than the upstream channel width. They also noted that the channel constriction ratio is not particularly sensitive to stage changes. Channel constriction results in high flow velocity through the narrowed channel opening where flow can reach a supercritical state during infrequent high discharges.

Kieffer (1985) documented that reworking of the debris fan at Crystal Creek Rapid occurred during flows of approximately $2,600 \text{ m}^3\text{s}^{-1}$ in 1983. The pre-dam ten-year recurrence interval flood discharge was approximately $3,500 \text{ m}^3\text{s}^{-1}$. Since the completion of the Glen Canyon Dam in 1963, the mean annual peak discharge was reduced from $2,440 \text{ m}^3\text{s}^{-1}$ (1921-63) to $790 \text{ m}^3\text{s}^{-1}$, except for unavoidable spills (e.g., 1983) and brief tests of the Dam's outlet works. Howard and Dolan (1981), Kieffer (1985), Graf (1987), and Webb et al. (1989) concluded that the debris fans and rapids of incised rivers on the Colorado Plateau are stable geomorphic features because in the present climatic/hydrologic regime, the rivers are not powerful enough to rearrange the materials or alter the spacing of rapids. Consequently, these authors predicted that debris fan rapids would enlarge downstream from flow regulating engineering works and recent debris flow events in the Grand Canyon support this prediction (Webb, 1996).

Cobble Bars

Bars of well-rounded and well-sorted cobbles up to 0.5 meters in diameter occur throughout the Grand Canyon. The bars are primarily composed of rock from within the canyon (Howard and Dolan, 1981) delivered to the river by debris flow processes (Webb et al., 1989). Decrease in competence of flood flow where the river spreads into the wide sections of the canyon is the factor controlling cobble deposition. Cobble bar deposition is generally aided by a downstream constriction (such as bedrock or a tributary fan) and backwater effect. Isolated cobble bars occur below the plunge pools downstream from short, steep rapids (Howard and Dolan, 1981).

Cobble bars form secondary rapids and riffles downstream from debris fans. The cobbles are often imbricated and resist entrainment by flows less than pre-dam flood flows. Howard and Dolan (1981) reported that cobble-sized material is a conspicuous component of the fluvial deposits in Grand Canyon, but is weakly represented (less than 0.1%) downstream in deposits of Lake Powell (Smith et al., 1960). In the pre-dam river, cobbles were moved by only the largest pre-dam flood peaks, but under regulated flow conditions the cobbles are immobile (Howard and Dolan, 1981).

The consequence of debris fans and cobble bars in the river channel is to create hydraulic controls at sites of maximum width and depth constrictions of the channel (Smith and Wiele, in press). This leads to an upstream pool created by the damming effect of the hydraulic control followed by a rapid that begins at the site of least cross-sectional area and, in many cases, a pool downstream from the rapids (Leopold, 1969; Howard and Dolan, 1981; Wilson, 1986). The hydraulic controls create spatial variations in flow patterns and flow competence that result in sediment sorting and deposition processes along the channel margins. Schmidt and Rubin (1995) described the basic channel unit as a complex composed of a backwater upstream from the debris fan, a debris fan and channel constriction, an eddy or eddies and associated bars in the channel expansion downstream from the fan, and a downstream gravel bar. They called the basic channel unit the fan-eddy complex. This is a plan view description of what may be more

generally and more commonly described as a riffle-pool unit, the differences being in profile view rather than plan view and in the origin of fans versus riffles. The term fan-eddy complex emphasizes the large eddies that form in this type of riffle-pool channel.

Channel Margin Sand Bars

Low velocity zones are characteristic upstream from debris fan constrictions in backwater pools, and downstream in zones of lateral flow separation and recirculation associated with channel expansion and with deep scour holes immediately downstream from rapids. Lateral flow separation also occurs along the upstream lobe of debris fans (Schmidt, 1990). Lateral flow separation zones, because of their slow velocities, are depositional environments for sand.

Over longer time scales, environments conducive to sand deposition persist because the debris fans persist, as Webb (1996) shows in repeated century interval photographs. Sand bars persist in the same locations over long time periods although the sand forming these bars will be reworked and replenished many times on this time scale. Were this not the case, sand deposits would be covered with riparian vegetation.

The consistency of channel constrictions and zones of recirculating flow causes consistency in the location, form, and large-scale characteristics of bars forming in channel expansions (Schmidt, 1990). Deposition of bars occurs in areas where velocity is least--near the separation and reattachment points, and at the center of the eddy. Schmidt proposed the terms separation deposit, reattachment deposit, and eddy-center deposit for sand bars formed near the separation point, reattachment point, and center of the primary eddy, respectively (figure 3). Separation bars mantle the downstream parts of debris fans. Reattachment bars are located beneath the primary eddy recirculation cell and project upstream in the form of spits. When observed at low flow, eddy bars and reattachment bars are actually one continuous deposit (Schmidt, 1990). Other common deposits not found in such highly structured eddies occur as channel margin deposits that

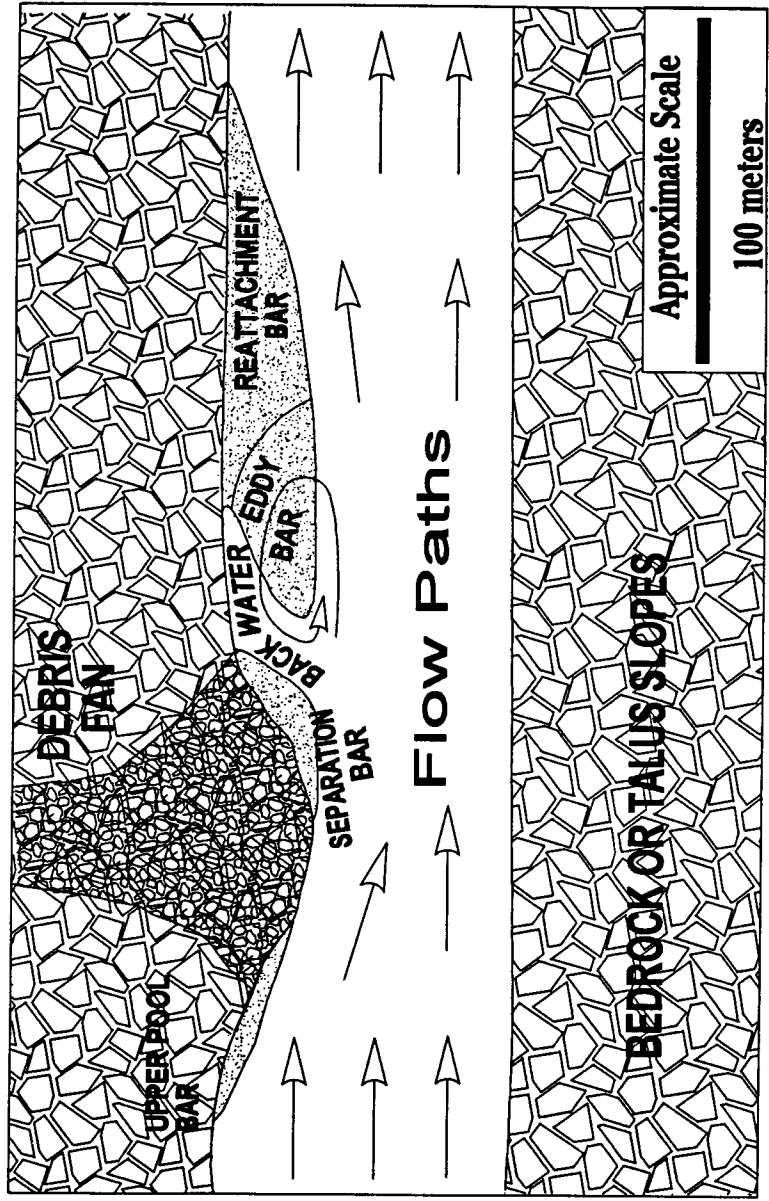


Figure 3. Sketch map and nomenclature used to describe sand bars commonly found in the Grand Canyon and other incised rivers with debris fan channel constrictions.

discontinuously line the banks. Separation, reattachment, and eddy bars are sub-categories of what are often called channel margin bars.

Lateral separation zones are typically efficient traps for the fraction of diffused suspended sand that is advected across the boundary between the primary and separated flow (Andrews, 1991a; Nelson et al., 1994). Sand particles transported into flow separation zones quickly deposit because of prolonged retention of water in the eddy, relative to the settling velocity of sand particles. The size distribution of measured sediment loads and eddy sand deposits are similar (Howard and Dolan, 1981; Schmidt et al., 1993).

Eddy sand bars account for as much as 75% of the total sand stored along the banks of the Colorado River (Schmidt and Rubin, 1995). The lateral sand bars are in areas of flow convergence, but grow or shrink in response to the supply of sand from upstream, the discharge history of the river, and the geometry of the channel (Smith and Wiele, in press). These responses can occur due to changes in roughness caused by changes in sand supply, changes in discharge caused by flow regulation or tributary flows, and by changes in channel geometry caused by tributary flows or debris fan deposition or erosion. Therefore, sand deposits in bedrock rivers are inherently unstable geomorphic features. The sand grains that constitute sand bars have time scales of residence, transport or deposition depending not only on the time scale of changes in channel geometry but on the time scale of individual changes in discharge and sand supply (Smith and Wiele, in press).

Importance of Sand Bars

The sand and finer alluvial deposits are important in National Park Service (NPS) managed lands because the NPS mandate is to manage for environmental values. Specifically, alluvial deposits provide the physical substrate for diverse and dynamic riparian and aquatic ecosystems that provide habitat for endangered bird species and

possibly rearing habitat for endangered fish species (Stevens et al., 1995). Sand deposits themselves are depended on for camping by hikers and by rafters in the well established white-water recreation industry (Kearsley et al., 1994). Channel margin sand deposits also provide base level control for drainage systems developed on higher alluvium that contains archaeological sites (Hereford et al., 1993).

Over the last three to four decades, all major rivers in the western U. S. have been affected by engineering structures (Gore and Petts, 1989; Dynesius and Nilsson, 1994) that store and regulate flow, and trap the mobile alluvial components in deep reservoirs. Hirsch et al. (1990) have shown that the Colorado River is the most highly regulated river system in North America. As society realizes the value of river ecosystems and the damages caused by flow regulation (National Research Council, 1996), agencies responsible for resource management have tried to control the erosion and deposition of fine grained sediment in the Colorado River through dam re-operation (USBOR, 1995), and designed floods (Wegner et al., 1996).

Previous Sand Bar Monitoring Investigations

Fluvial geomorphologists have described, quantified and monitored changes in the alluvial components of bedrock canyon rivers. Beginning in 1974, pioneering studies of sand bar responses to river regulation were conducted on the Colorado River downstream from the Glen Canyon Dam in the Grand Canyon. Early investigations used various time scales ranging from eight years to three months to repeat measurements (table 1). To some extent, the chosen repeat intervals were probably driven by budget and permit limitations, but also depended on the perceived rates of change to hydropower flow patterns and the diminished sand supply.

The first monitoring program for Colorado River sand bars in Grand Canyon was initiated in 1974 by Howard (1975), who established permanent benchmarks and surveyed topographic profiles on 20 channel margin deposits. Lateral erosion and

deposition (changes in sand bar width) were documented when the profiles were resurveyed in 1975 and 1976 (Howard and Dolan, 1976). The maximum lateral erosion measured between 1975 and 1976 was 4.9 meters (Howard and Dolan, 1976).

Table 1. Summary of sand bar monitoring studies in the Grand Canyon.

Reference	Study Period	Time Interval	Sample Size	Method	Lateral Erosion, Maximum (meters)	Lateral Deposition Maximum (meters)
Howard and Dolan 1976	1965-1973	8 years	whole population along 360 km	Aerial Photography	80	15
Howard and Dolan 1976	1974-1976	1 year	20	Surface Profiles	4.9	0.7
Beus et al. 1984a	1974-1983	10 years	20	Surface Profiles	8.0	16.7
---- 1984b	1983-1984	1 year	20	Surface Profiles and Topography	3.5	
---- 1986	1984-1985	"	"	"	12	5
---- 1987	1985-1986	"	"	"	12	17
---- 1988a	1986-1987	"	"	"	22	8
---- 1988b	1987-1988	"	"	"	18	26
---- 1989	1988-1989	"	"	"	10	8
---- 1991a	1989-1990	"	"	"	15	15
Schmidt and Graf 1990	1965-1973	8 years	whole population along 360 km	Aerial Photography	na	na
"	1973-1984	12 years	population =350 along 270 km	Inventory	na	na
"	1985	2.3 months	5	Surface Profiles and Topography	12	
"	1985-1986	3.2 months	20	"	13	10
Beus et al. 1991b	1990-1991	2 weeks	30	"	20	15
Cluer 1995b	1990-1991	2 weeks	65	Aerial Photography	30	20
Cluer 1991	1990-1991	1 day	7	Time-lapse Photography	40	7
"	April, 1991	6 hours	1	Field Observation	20	
Carpenter et al. 1991	1991	20 minutes	1	Water Levels	Displacement of water level sensors suggests that one or more erosion events documented with time-lapse photography in 24-hour periods may have occurred in 1 or 2 20-minute intervals.	
Cluer 1995a	July, 1993	6 hours	1	Bathymetric and Surface Topography	25	4

Howard and Dolan (1976) also compared aerial photographs taken in 1965 and 1973 for the entire population of channel margin deposits along the river corridor between the Glen Canyon Dam and Lake Mead. Maximum lateral erosion rates

documented over this time-span were on the order of 10 meters per year [apparently determined from erosion of about 80 meters between 1965 and 1973 at one deposit].

The observation of high erosion rates, made in the context of the substantial decrease in sediment supply following construction of Glen Canyon Dam, led Howard and Dolan (1976) to predict the eventual scour of sandy banks throughout Grand Canyon, consistent with observations between 1956 and 1975 for the 24 kilometer reach downstream from Glen Canyon Dam (Pemberton, 1976). Twenty years after the dam began trapping sediment and regulating discharge, Howard and Dolan (1981) reversed their opinion and stated that channel margin deposits had reached an equilibrium with peaking power discharge patterns by the late 1970's. They suggested continued monitoring of a small sample of channel margin deposits at three to six year intervals (Howard and Dolan, 1976, pg. 26).

In the spring of 1983, high flows from the Rocky Mountains coincided with near maximum water storage in Lake Powell. These two events culminated in emergency water releases through Glen Canyon Dam of approximately $2,800 \text{ m}^3\text{s}^{-1}$ in 1983 and nearly continuous high flows throughout 1984-1986 that greatly exceeded post-dam flows for power production (figure 2). The floods of the 1980s renewed concerns about the impacts of Glen Canyon Dam on National Park and other resources downstream (National Research Council, 1987). Short-term process oriented studies and long-term monitoring programs were initiated following the flood releases.

Schmidt and Graf (1990) reevaluated the 1965 and 1973 air photos previously analyzed by Howard and Dolan (1976) and agreed with their interpretation that initially high erosion rates in the first ten years of river regulation were substantially reduced by the late 1970s. The effects of the 1983 flood were evaluated using aerial photographs taken in 1973 and 1984 by simply inventorying the total number of channel margin deposits existing within 270 kilometers of Glen Canyon Dam. From comparing these photographs separated by 11 years, Schmidt and Graf (1990) concluded that the 1983

flood resulted in net aggradation of channel margin deposits in wide reaches and net degradation in narrow reaches.

Schmidt and Graf (1990) also surveyed a small population of channel margin deposits prior to and after the 1985 peak flow and measured approximately 12 meters maximum erosion over 2.3 months. In the first attempt to directly determine the effects of fluctuating power plant discharges on channel margin deposits, they surveyed 20 sand bars in October 1985 (four months after the 1985 flood peak) and resurveyed them in January 1986. Over the 3.2 month fluctuating-flow period these resurveys recorded maximum lateral erosion of 13 meters, as well as substantial deposition. They hypothesized that deposition measured during the fluctuating flow period was an anomaly, perhaps a local response to locally increased sediment supply. Schmidt and Graf (1990) proposed that the floods of the early 1980s caused a depositional perturbation in the previously established state of gradual erosion, a state that would return as channel margin deposits readjusted to fluctuating discharges through initially high erosion rates that would diminish with time. Year-round daily fluctuating discharges for power optimization resumed following the 1980s flood flows.

A parallel long-term monitoring program was conducted throughout the 1980s by Beus et al. (1982, 1984a, 1984b, 1985, 1986, 1987, 1988a, 1988b, 1989, and 1991b) who annually resurveyed approximately 20 sand bars established as monitoring sites in 1974 by Howard (1975). Following the 1984 surveys, Beus et al. (1985) concluded that the flood of 1983 caused erosion at some sites and deposition at others, with a tendency for greater deposition at the larger deposits (consistent with Schmidt and Graf, 1990). In the years following the 1980s flood flow period, Beus et al. measured maximum lateral erosion rates of 10 to 22 meters per year (table 1). However, maximum lateral deposition rates during the same period ranged from 5 to 26 meters per year. During this period, the randomness of the variation in sand bar size made it difficult to identify a general response or trend. From the annual data there were about equal numbers of sites showing deposition and erosion, and erosion at a site was often followed by deposition, or vice versa, from year to year.

Recent studies that measure alluvial deposit changes in other bedrock gorge rivers continue to rely heavily on decade scale aerial photography (e.g. Lyons et al, 1992; Schmidt et al., 1995) largely because this is often the only antecedent information available, but also because image processing and analysis techniques are now readily available. Such decade scale information can be supplemented with annual or seasonal channel measurements from U.S. Geological Survey (USGS) gaging stations, although these gages are widely separated and continue to be decommissioned.

METHODS

Site Selection

Two widely separated reaches of the Colorado River were selected for this investigation to compare processes and rates of processes between the near-natural and regulated river environments. The similarities and differences of the two study sites are summarized in table 2.

Table 2. List of basic climatic, geologic and hydrologic attributes for two reaches of the Colorado River.

Attribute	Regulated River - "Mohawk Site", Grand Canyon	Near-Natural River - "Moab Site" near Moab, UT
Location	303 km downstream from Glen Canyon Dam, 1.6 km downstream from Mohawk Canyon	50 km upstream from Moab, UT, 9 km downstream from Dolores River confluence
Elevation (above sea level)	521 m (1,710 ft)	1,242 m (4,075 ft)
Vegetation, riparian zone	Riparian Woodland; tamarisk, arrow weed, willows	Riparian Woodland; tamarisk, willows, cottonwood
outside riparian zone	Mojave Desert Scrub	Pinyon-Juniper Woodland
Climate, precipitation (mean annual) temperature (mean annual)	20 cm (8 in) 19°C (66°F)	23 cm (9 in) 14°C (57°F)
Reference Stream Gage	135 km upstream from study site; Colorado River near Grand Canyon, (near Phantom Ranch) Station # 09402500	9 km upstream from study site; Colorado River near Cisco, UT Station # 09180500
Drainage Area	366,744 km ²	62,420 km ²
Discharge Data, Period:	1922 to present	1895 to present
peak flow (pre-dam)	3,600 m ³ s ⁻¹	2,176 m ³ s ⁻¹
peak flow (post-dam)	2,725 m ³ s ⁻¹	
10-year flood (pre-dam)	2,460 m ³ s ⁻¹	1,784 m ³ s ⁻¹
10-year flood (post-dam)	1,130 m ³ s ⁻¹	
mean annual flow (pre-dam)	480 m ³ s ⁻¹	209 m ³ s ⁻¹
mean annual flow (post-dam)	417 m ³ s ⁻¹	
Sediment Discharge Data:	<i>at Lees Ferry</i>	1974-1984
mean annual load (pre-dam)	66 x 10 ⁶ metric tons	9 x 10 ⁶ metric tons
mean annual load (post-dam)	0 x 10 ⁶ metric tons	
mean annual load (post-dam)	10 x 10 ⁶ metric tons <i>at Phantom Ranch (Andrews, 1991b)</i>	
Lithology at River Level	Cambrian Bright Angel Shale	Jurassic Entrada Sandstone
Hydraulic Control	debris fan constriction and downstream riffle	debris fan constriction and downstream riffle
Length of Study Reach	900 meters	450 meters

Near-Naturally Flowing River near Moab, Utah

The Colorado River near Moab, Utah was selected for comparison to regulated river conditions, processes and rates of change downstream from Glen Canyon Dam. A fan-eddy sand bar complex with features very similar to many in Grand Canyon is located approximately 50 kilometers upstream from Moab, Utah, at the upstream end of Professor Valley in a deep bedrock gorge, 9 kilometers downstream from the confluence with the Dolores River (figure 4). The well-known West Water Canyon is a short distance upstream from the study area. This river reach is deeply incised into upper Jurassic Entrada Sandstone (Baars, 1972), with steep canyon walls and regularly spaced short side canyons and tributaries localized along regional joints, fractures or faults. The study reach is located adjacent to mile post 26 (MP26) on Utah highway 128 which follows the river's course for 50 kilometers from the historical Dewey Bridge to Moab, Utah. Seven kilometers upstream from the study reach an USGS stream gage has operated continuously since 1914, and intermittently from 1895 to 1914.

Channel geometry at MP26 is very similar to that in the Grand Canyon where channel widths are on the order of 80-100 meters and the low flow constriction/expansion ratio is approximately 0.5. Reattachment and eddy deposits occur downstream from the debris fan channel constriction. Debris forming the fan constriction originates from a short, steep, side-canyon entering from the west (figure 5). The debris fan is broad, low in elevation, and observations made during this study show that it is overtopped by flows in excess of $340 \text{ m}^3 \text{ s}^{-1}$.

Flow of the Colorado River through this reach is somewhat regulated as a number of storage reservoirs exist in the basin's headwaters along with numerous irrigation diversions lower in the basin. The largest flow regulation facility is Blue Mesa Reservoir on the Gunnison River. It was constructed in 1965 and is operated to store spring peak discharges for summer irrigation releases. McPhee Reservoir on the Dolores River was completed in 1986 and is operated similarly. However, the effects of headwaters development on this reach of the Colorado River are minor compared to the complete

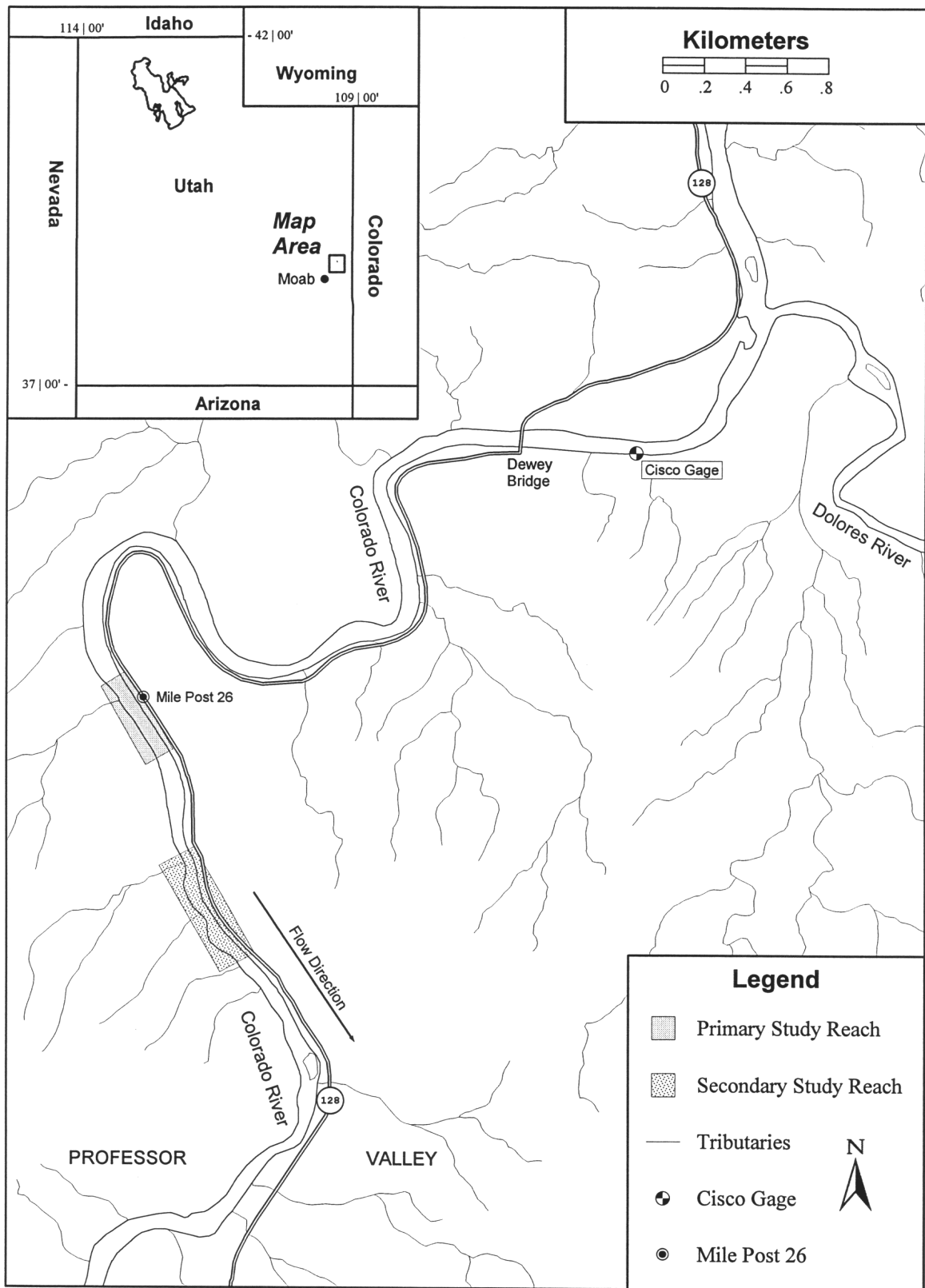


Figure 4. Location map of near-naturally flowing "Moab" study reach on the Colorado River near the Dolores River confluence, 50 km upstream from Moab, UT.



Figure 5. Aerial photograph of Moab study reach (outlined in red hatched box). Flow is from right to bottom, study sand bar is white area within box, the gray shaded debris fan is from the side-canyon entering from lower left corner. Photo width covers approximately 2 km.

flow and sediment regulation downstream from Glen Canyon Dam. The Colorado River near Moab is still characterized by a distinct annual flood cycle (see figure 15) and its natural sediment load (approximately 9×10^6 metric tons per year), thus satisfying the objective of comparing a naturally flowing river to the completely regulated river in Grand Canyon. The history of sand bar dynamics in the reach was analyzed by comparing aerial photographs that covered the primary study reach and two additional sand bars in a secondary study reach downstream.

Regulated Colorado River in the Grand Canyon

Through terrestrial surveying monitoring efforts (Beus and Avery, 1991) and aerial photogrammetry monitoring (Cluer, 1995b), both repeated at two-week intervals, the relative dynamics and cut and fill histories of approximately 75 sand bars were established during the test flow period 1990-1991. Daily photographic monitoring of sand bars during 1991-1993 further established the short-term scour and fill histories of 40 potential sites (Cluer and Dexter, 1994).

The most dynamic sand bar known in early 1993 was the eddy bar downstream from Mohawk Canyon at river mile 172.3. Between January 28, 1992 and January 27, 1996, 20 rapid erosion events were documented with automatic cameras (figure 6). The Mohawk site was selected for this investigation because it offered the greatest possibility to measure the hydrodynamics of flow and channel adjustment surrounding a rapid erosion event.

The Mohawk site is 303 kilometers downstream from Glen Canyon Dam and 1.6 kilometers downstream from Mohawk Canyon and Stairway Rapid (figure 7). The mean channel width is approximately 90 meters and Cambrian Bright Angel Shale (Breed, 1974) is exposed at river level. Talus slopes along the river are covered primarily with blocks from the overlying Cambrian Muav Limestone.

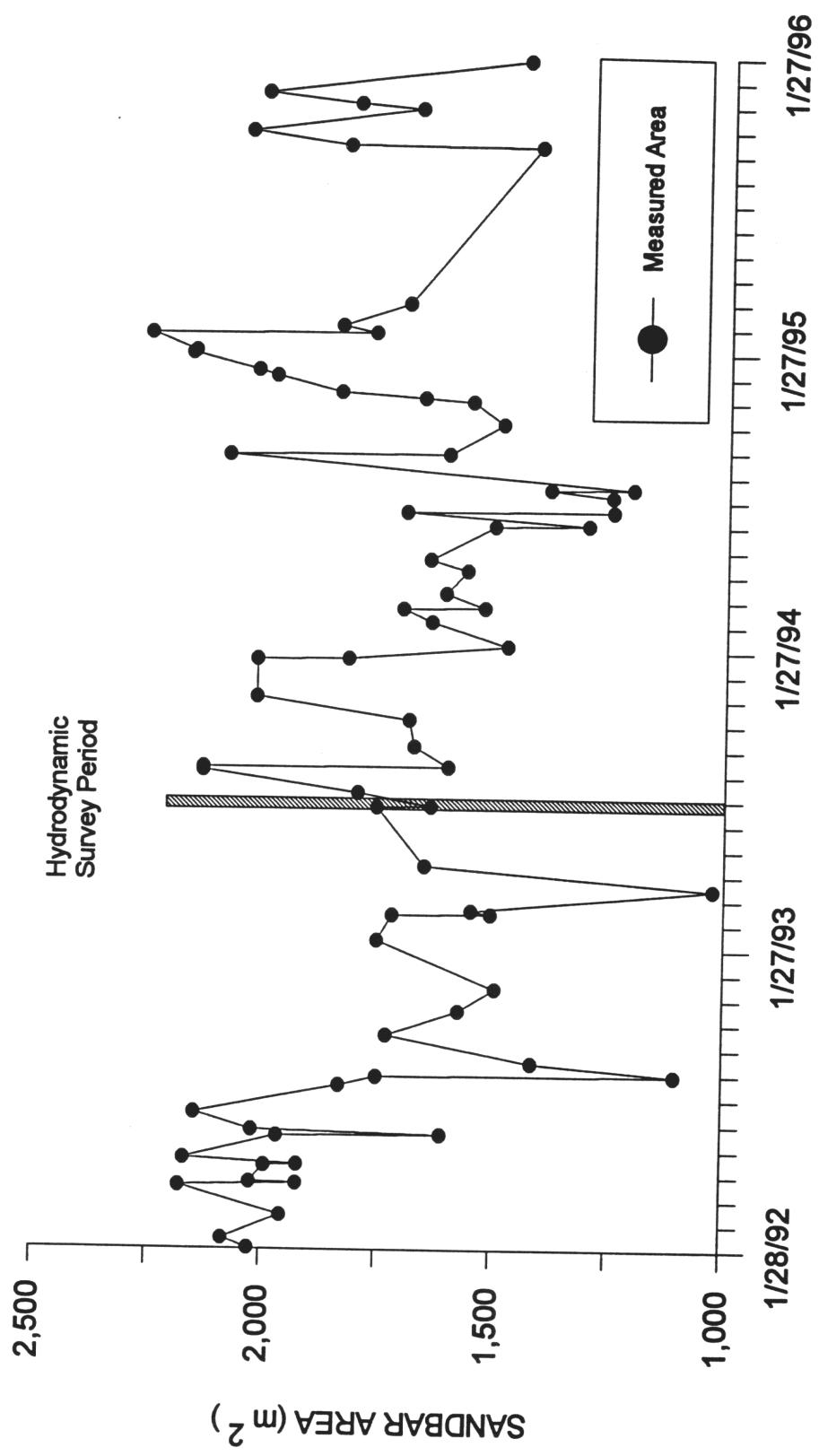


Figure 6. Time-series plot showing scour and fill history during powerplant discharges for the Mohawk eddy deposit in Grand Canyon. Data are from daily photographs (Cluer and Dexter, 1994). Shaded bar indicates period of field studies and rapid erosion event described in this report.

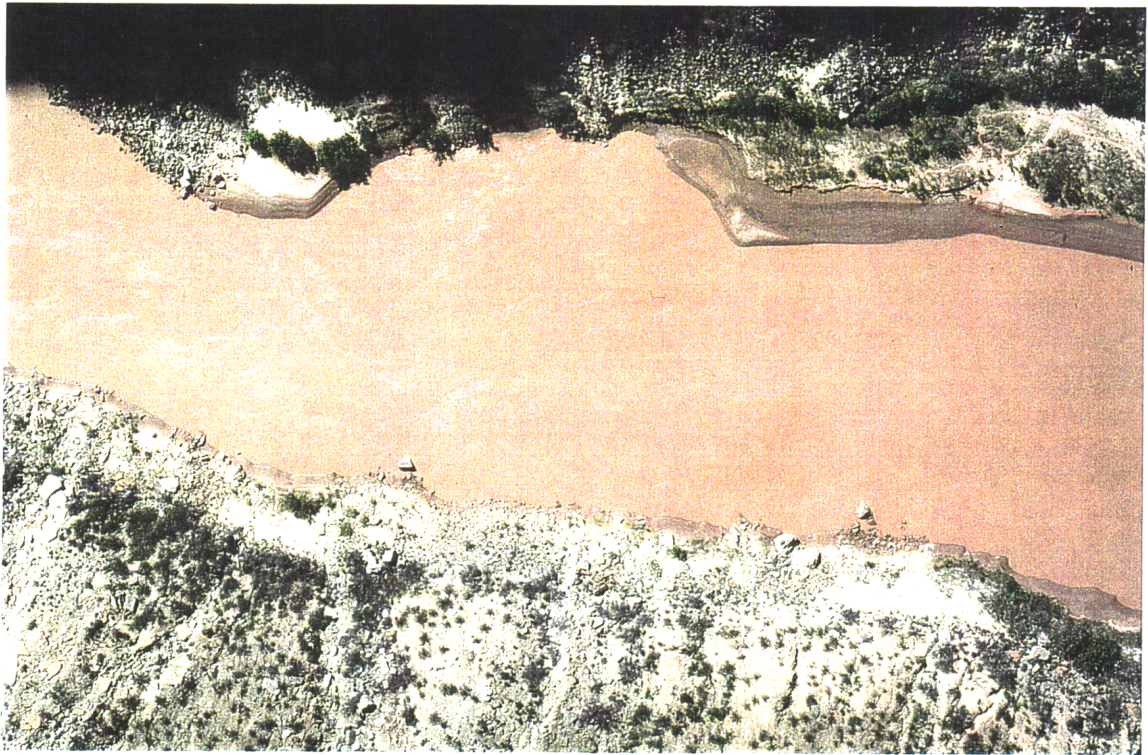


Figure 8. Aerial photograph of Mohawk study reach in Grand Canyon. Flow is from left to right. Debris-fan channel constriction is in upper left, unvegetated eddy bar and vegetated reattachment bar in upper middle and extending to right. Eddy bar was scoured three days prior to this photograph. Width of photograph is approximately 300 meters.

Data Collection

Data collection programs for the regulated and naturally flowing study reaches were designed to measure channel and sand bar changes at time scales shorter than the dominant hydrologic time scales. In the case of the Grand Canyon, that time scale is driven by daily flow fluctuations, whereas at Moab, the dominant hydrologic time scale is driven by the annual flood.

Moab Study Reach

The sand deposits associated with one channel constriction were selected for monitoring in March 1992 by staff of the National Park Service, Water Resources Division, who were familiar with channel constrictions and sand bar morphologies in the Grand Canyon. The initial monitoring activities consisted of establishing two locations for repeat photography of the exposed channel margin sand deposits. Photographs were repeated six times between March 1992 and March 1993, when periodic opportunistic photography was replaced by automatic daily photography. Except for brief periods during winter low flow, the automatic camera system was operated continuously until November 1995.

Following the spring 1992 flood, the exposed sandbars were topographically surveyed using a total station and approximately 500 points were measured around the perimeter and along topographic break-points. Topographic surveys of the exposed sand deposits were repeated twice annually through 1993. In September 1993 the local benchmark system was expanded to include 19 cross sections at 25-meter intervals. The cross sections were used to make bank-to-bank channel bathymetric surveys so that channel changes could be measured prior to, during and after the 1994 annual flood cycle. The Moab channel was surveyed eight times between September 1993 and July 1994.

Channel topography was measured using hydrographic surveying techniques and equipment developed specifically for this setting. For this study it was necessary to obtain sufficiently detailed topographic measurements over a reach 450 meters long, with minimal crew and field equipment, to create reliable topographic maps using automatic contouring algorithms. This was accomplished by navigating an inflatable kayak with reference to two or three vertical poles placed over surveyed cross section markers on the right bank.

Water surface elevation and horizontal position with respect to the cross section reference points were measured with a total station or tape and level, depending on personnel and equipment available for each survey. The kayak was equipped with an electric trolling motor and a Lowrance[®] echo sounder and chart recorder. A Hip Chain[®] string distance meter displayed distance along cross section from the reference starting point. Tick marks on the echo sounder chart were manually placed to correspond to even meter distance marks. At the end of each cross section, the distances were written on the corresponding chart tick marks.

The distance and depth data were digitized and transformed into local Cartesian coordinates in order to produce contour maps of channel topography. Precision of the hydrographic surveying measurements was within ± 5 meters horizontal and ± 0.1 meter vertical using these methods. The number of points on each cross section averaged about 50-60 and the topographic models for the 450 meter reach typically had at least 1000 points. This point density resulted in reliable creation of contour maps using micro computer contouring techniques and Surfer[®] software.

In addition to the detailed channel and sandbar monitoring conducted in the primary study reach during the period 1992-1995, aerial photographs (from 1952, 1956, 1975, 1980, 1987, and 1993) were obtained for the study reach from the USGS National Aerial Photography Program. Photo analyses included assessment of relative sandbar sizes, and changes in debris fans. The MP26 sand deposit and two additional debris fan-sand deposit complexes in a secondary study reach immediately downstream (figure 4)

were analyzed to better represent reach-scale adjustments to flow dynamics. The three deposits are all fan-eddy complexes and are representative of the population of deposits in the reach.

The 1952 aerial photograph was selected as the initial condition where the exposed sand deposits were assigned 100% size. The relative sizes of exposed sand deposits were measured by scaling each subsequent photograph to the 1952 scale and mapping the outline of exposed sand. The outlined areas were then measured and compared.

Stream flow data were obtained from the USGS stream flow gage (Colorado River near Cisco, Utah; station number 09180500) located 7.8 kilometers upstream from the study area near the historic Dewey Bridge. The Cisco gage was installed in 1914 and had 78 years of continuous record at the end of water year 1996. Sediment measurements were made beginning in 1930 and discontinued in 1984. A sediment rating curve has not been published for this gage station (Rod Tibbetts, Hydrologic Technician, USGS-Moab, personal communication 3/5/96), although the USGS State Office in Salt Lake City, Utah provided archived sediment data for the period 1974-1984.

Mohawk Study Reach in the Grand Canyon

Bathymetric and velocity surveying of the river channel were conducted from a 4.25-meter-long motorized pontoon raft that was outfitted specifically for channel surveying and equipment transport through the rapids of the Grand Canyon. The boat was crewed by a navigator, depth sounder operator and acoustic Doppler operator.

Channel Surveying

A SuperHydro[®] bathymetric surveying system was used, which consisted of a shore station and a boat station. Boat station equipment included an InnerSpace[®] 448 depth sounder with chart recorder, splash-proof PC for data collection and navigation,

navigator's display, omni-directional reflective laser target, radio data modem for communication with the shore station, and power supplies. Vessel position was determined from a shore station that consisted of a five-second Pentax® theodolite modified with a continuous tracking crank on the horizontal axis. Mounted through linkages on top of the theodolite were a high power-high speed laser distance meter and a spotting telescope. The shore station components were integrated by a small computer that converted bearing and distance data to the local coordinate system.

Boat position data were transmitted from the shore station to the ship station by radio modem where the position data were combined with water depth data and written to files. This system was built specifically for channel surveying in the Grand Canyon on a dynamic water surface, and for recording the water surface elevation in addition to the channel elevation. Hypack® navigation software controlled data collection functions and displayed steering corrections to the navigator to aid guiding the boat along pre-defined navigation lines.

At the Mohawk site the shore station position was established within an existing survey grid and 800 meters of river channel were surveyed along 32 cross-sections spaced 25 meters apart and along three profiles parallel to the channel. The center profile followed the thalweg defined by the lowest topography and two profiles paralleled the thalweg 25 meters on either side. Contour maps were made after the first survey so that the thalweg could be defined for navigation in subsequent surveys. The eddy shear zone was also surveyed during most time steps.

This bathymetric surveying system is capable of resolving positions at the rate of four Hz with accuracy within 10 centimeters in all three dimensions. In practice sessions it was found that data collection at the rate of two positions per second was more than adequate. The high rate of data collection was useful for improving boat navigation accuracy. Practice sessions also found that 10 centimeter accuracy was obtained only under ideal conditions. The most challenging conditions were during night surveys at distances of 600-700 meters. Under these conditions individual point accuracy was

probably within 25 centimeters but at closer ranges the accuracy achieved daytime accuracy. Night surveys were facilitated by the use of chemical light sticks on backsights and the ship station target, flashlights on displays, and reflective tape on lath at each cross section. Although risky, in some respects the night surveys were executed with relative ease compared to the daytime surveys where temperatures in excess of 49°C (120°F) taxed the equipment, power supplies and personnel.

Due to entrained air bubbles and other sporadic depths recorded by the echo sounder, it was necessary to edit each survey file. This was done in the field on portable PC's by the personnel who operated the equipment and collected the data, and were best qualified to make corrections after each survey. Editing consisted of comparing graphical images of the digital depth files to the corresponding paper charts and making adjustments as needed. It was adequate to simply delete erroneous depths from the digital files because of the large number of data points collected.

Post-processing of the survey data was more problematic because an unknown vertical angle error was found in some files when water-surface maps were made. The solution to this problem was difficult to determine because the problem was sporadic and the error was not always the same. It took two years of trial and error application of different corrections to derive and verify an algorithm, that could be applied globally to all files, that corrected only the corrupt files and retained the integrity of the uncorrupted files.

Once the survey files were corrected, data processing involved conversion to a Cartesian coordinate format containing x , y , z_1 for the water surface and z_2 for the channel surface. The number of data points in a typical survey ranged from approximately 4,000 to 6,500, so a logical filtering process was applied that selected one position per meter across the channel where the topography was relatively flat or one position for every 0.1 meters change in elevation. This technique insured accurate representation of channel topography while minimizing file sizes. Filtered files contained approximately 1,500 data points for a 500-meter reach of the river channel.

Channel topography data were supplemented with conventional total station surveying data along both banks to define the channel boundary where the boat could not navigate. The channel was also surveyed approximately five meters above the contemporary high water mark along each cross section. The total station was also used to locate land tilt and stage sensors installed at the site. An example of channel surveying and definitions used to describe the site and surveys are illustrated in figure 9.

Velocity Field Measurement

A broadband acoustic Doppler current profiler (BB-ADCP) manufactured by RD Instruments was mounted to the surveying raft along with a power supply and PC for operation and data collection. The BB-ADCP is a sophisticated echo sounder that transmits sound energy into the water column in phase-encoded acoustic pulses along four narrow beams. These beams are positioned 90-degrees apart horizontally and 30-degrees from vertical. The BB-ADCP transmits and then receives the energy reflected back from suspended particles in the water. Using Doppler shift theory, the system software resolves the direction and magnitude of the water in three dimensions based on the change in phase and frequency between the transmitted and received energy. By varying the delay time between transmit and receive modes, the BB-ADCP can determine three-dimensional velocity at multiple depths (RD Instruments, 1993).

Motions of the boat were determined and corrected with a 2-axis tilt and yaw sensor and by tracking horizontal motion with additional bottom-tracking pings. Heading of the boat is determined through a flux-gate compass. These onboard instruments allow the measured water velocity to be corrected for boat motion in real time.

Because it operates at 1200 Hz, the BB-ADCP can measure velocity at multiple depths from a moving ship. It has recently seen increased use on remotely controlled boats for bridge pier scour studies and for stream flow gaging applications in remote

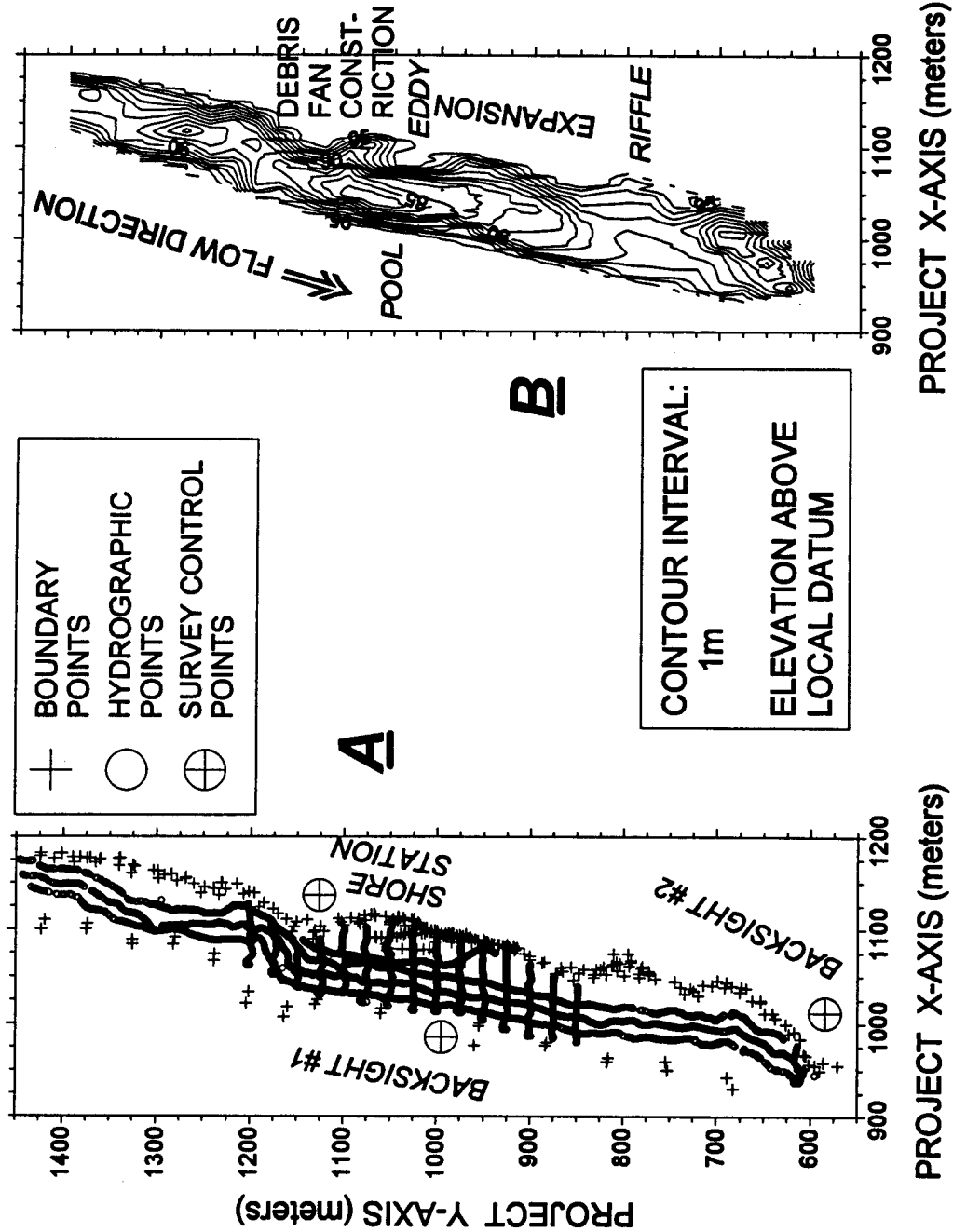


Figure 9. Data collection definition diagram and site description for the Mohawk study reach. (A) typical data coverage and survey control, and (B) resulting bathymetric contour map. All units are in meters.

areas(Oberg and Mueller, 1994). As deployed for this investigation, velocity was determined in 0.5-meter increments from 0.8 meters depth to approximately 85% of the total water depth. For example, if water depth was 10 meters, the first velocity data would be obtained from 1.3 meters depth (0.8+0.5 meters), the second data from 1.8 meters, the next at 2.3 meters and so on at 0.5-meter increments until the last velocity measurements were at 8.3 meters depth (or the nearest depth within 85% of the total depth [10 meters in this example]). The configuration used in this example would produce 15 sets (or bins) of three-dimensional measurements in one vertical. The BB-ADCP was programmed to average ten measurements per depth bin. The number of verticals per cross section ranged from 11 to 40 depending upon channel width and boat velocity, with the average number approximately 18 verticals per cross section.

During data collection, the PC connected to the BB-ADCP displays velocity structure and unit and cumulative discharge. As the boat crossed the channel from bank to bank the ADCP determined instantaneous discharge along the ship's path. The unmeasured zones were calculated using power equations for logarithmic velocity profiles and were automatically added to the discharge record (RD Instruments, 1993). Discharge measured by the ADCP compared to within $\pm 5\%$ of USGS stream gage discharges at the Colorado River near Lees Ferry and Colorado River near Grand Canyon (Phantom Ranch) in a series of trials. Because the velocity information is three-dimensional, one can discern areas of vertical upwelling and downwelling as well as zones of recirculating flow, which are actually subtracted from the discharge sum once the boat crosses an eddy shear zone.

Field editing of the velocity files was not necessary. They were simply backed up on floppy disks after each survey session. The ADCP operated simultaneously with the bathymetric mapping system but data were recorded independently on separate PC's. The beginning and ending of each velocity file was temporally correlated to the corresponding survey files by carefully starting and stopping data collection with both systems on the navigator's 'mark'. A notebook was kept that listed the names and starting times of corresponding velocity and survey files for post-processing integration.

Post-processing involved synchronizing the timing of velocity files with the bathymetry files in order to assign a position to each velocity measurement. A program was written in MS-Access[®] that compared pairs of velocity and bathymetry files, synchronized the time tags on the beginning record, and selected the nearest surveyed position to assign to velocity stacks. Because there were approximately 20 survey positions for each velocity position, this scheme provided reliable position accuracy to the velocity data. It was relatively simple to also interpolate between the two nearest survey positions, so this feature was added to the program.

The program was written to output two types of velocity files. The first file contained Cartesian coordinates and flow depth from the bathymetry files, and from the velocity files; velocity magnitude and direction for the upper-most measurement, the lower-most measurement, the depth-averaged velocity and the vertical components of flow at the greatest depth. The second output file contained Cartesian coordinates, water-surface elevation, channel bottom elevation and all velocity data collected for each position. The second file type could be used for visualization of flow patterns in three dimensions, which would be expected to show plunging and rising jets as well as other complex flow features, or for calculating velocity distributions with depth.

River Stage

The USGS had installed an array of temporary river stage gages at eight-kilometer intervals in 1990-1991 (Gauger, 1996). Data from the gages 3.7 kilometers upstream and 4.5 kilometers downstream from the Mohawk site were obtained at 15-minute intervals for a six-month period surrounding the field investigation.

River stage was measured continuously during the investigation at the Mohawk site with Motorola[®] MPX2200AS pressure sensors using equipment and techniques developed by Mike Carpenter (Carpenter et al., 1995). The pressure sensors were temporarily attached to rocks exposed along the left bank in the eddy return current

channel. Temperature and atmospheric pressure were also measured and appropriate water level corrections were made at the time of data storage in a Campbell Scientific® CR10 data logger and storage module. The spatial characteristics of the water-surface were also recorded by the hydrographic surveying system.

Slope Motion

An array of 12 biaxial Geometric® tilt sensors was placed at 0.2 meters depth along the crest of the eddy deposit facing the river. These sensors were installed in order to monitor deformation of the eddy deposit due to varying flow levels and to indicate the timing and sense of first motion upon failure of the deposit. The system was designed to help discriminate between rotational slumping by slope failure and undercutting by traction processes, and to obtain measurements of slope motion at 20-minute time intervals.

Particle Size

Bed sediment was sampled with a clam shell dredge in the eddy. Three 3.5-kg samples were combined and size distribution was determined by sieving a one-kg split of the 10.5-kg sample. A standard 1/4 phi sieve set (range 0.035-0.5 mm) was used with a Rotap® sieve shaker.

Shear Stress and Particle Stability Calculations

Bed shear stress was calculated using a formulation assuming a logarithmic velocity profile (Richardson et al., 1990)

$$\tau_o = \frac{\rho u^2}{\left[5.75 \log \left(12.27 \frac{y_o}{k_s}\right)\right]^2} \quad (1)$$

where u is mean velocity, ρ is density of the fluid, y_o is flow depth and k_s is height of roughness elements, taken as the sediment diameter. Bed shear stress was compared to the critical value of shear stress at incipient motion for the sand size sampled in the eddy. The critical value of the Shields parameter τ_{*c} was determined from the van Rijn (1984) sediment transport relationship

$$\tau_{*c} \cong 0.14 D_*^{-0.64} \quad (2)$$

where the sedimentation parameter D_* is determined from

$$D_* = d_s \left[\frac{(G-1)g}{\nu^2} \right]^{1/3} \quad (3)$$

and d_s is a selected sediment diameter, G is specific gravity of the particle, g is acceleration due to gravity, and ν is kinematic viscosity of the fluid. Critical shear stress for the sand diameter sampled was then determined by

$$\tau_c \cong \tau_{*c} (G-1) \rho g d_{50} \quad (4)$$

The threshold of incipient motion was then determined for flow on a plane bed under turbulent flow over hydraulically rough boundaries by comparing $\tau_o = \tau_c$.

Particle stability was defined as the ratio of bed shear stress to critical shear stress. Where the ratio = 1, particles are in a state of incipient motion. This equilibrium condition is exceeded and particles are entrained where the ratio is greater than 1. Where the ratio is less than 1, particles are stable. This method was used to predict the spatial

distribution of shear stress and predict where sand would be stable or deposited, and where it would be mobilized.

Applying the Shields plane bed critical shear stress in the eddy bar setting results in overestimating particle stability on slopes such as the eddy bar face, which can reach and exceed the angle of repose. However, the assumption of depth-averaged two-dimensional flow dominating the fluid motion, used to calculate the available bed shear stress, also biases particle stability analysis by ignoring vertical fluid motion which is directed upward over the steep eddy bar face when discharge is high enough to overtop the eddy bar. The vertical component of flow over the eddy bar face is the reason that the eddy bar face reaches slope angles exceeding the angle of repose. Although measurement of the velocity field included the vertical component of flow, measurements near the bed and banks were difficult to obtain without risking damage to the equipment. Therefore the velocity field measurements were simplified to vertically averaged two-dimensional flow. This had the advantage of comparison with computer modeled two-dimensional flow data described in the following section. The assumptions used in particle stability analysis tend to neutralize each other when flow recirculation exists in the eddy. During low flow, when flow recirculation has collapsed and upward flow along the eddy bar face is not occurring, the bias introduced by assuming a plane bed in determining particle stability has greatest effect.

A coupled three-dimensional hydraulic and sediment transport model would be required to more accurately predict particle stability in the area of the steep eddy bar face. This level of numerical modeling is beyond the scope of this investigation. The plane bed assumption of the Shields critical shear stress is replaced in more rigorous particle stability analyses (e.g. Stevens and Simons, 1971; Julien, 1995) that account for the reduced stability of particles on side slopes and subject to three-dimensional hydrodynamic forces. This analysis is difficult to apply over undulating topographic surfaces subject to turbulent flow patterns.

One strength of this field-based investigation is the detailed repeated channel topography measurements. Rather than simplify the field and model topographic and hydraulic data in order to apply more rigorous particle stability analyses, I chose the simpler particle stability analysis technique. The results show good agreement between predicted and mapped sand deposit locations and morphology including the formation of a return current channel between the bar and channel boundary. This result supports using the simpler method to determine particle stability over complex terrain underlying complex flow fields.

Computer Flow Modeling

Even with high speed data collection equipment, it was difficult and often impossible to obtain field data for the critical conditions of highest or lowest flow, or during maximum channel deformation and eddy bar erosion, especially during the rapidly varied flow conditions encountered during the Grand Canyon field investigation. The objective of using computer simulation modeling techniques was to fill in gaps between temporally and spatially widespread field data, in order to develop more comprehensive analyses. The large field data set obtained in this investigation provided ample opportunities to verify and calibrate numerical models at different flow levels. Once satisfactorily calibrated, the flow models were used to test the sensitivity of flow patterns and particle stability to observed changes in channel and pool geometry and eddy bar configurations.

The computer model RMA2 (version 4.35) was used to simulate free surface flows for discharge and channel geometry conditions that were not measured directly. RMA2 is a two-dimensional, depth-averaged, free surface, finite element program for solving subcritical hydrodynamic problems. It was originally developed by Norton et al. (1973) of Resource Management Associates, Inc., Davis, California. Various modifications to the original code have been made by a number of researchers at the U.S. Army Corps of Engineers Waterways Experiment Station (WES) (Thomas and

McAnally, 1991), and others (King, 1990). King (1990) discusses the solution techniques involved in using RMA2. SMS software (version 4.13) was used to prepare input boundary conditions, visualize data, analyze output results and print maps (Brigham Young University, 1995). SMS was developed by the Brigham Young University Engineering Computer Graphics Laboratory, in conjunction with WES.

RMA2 is based on the governing two-dimensional (depth-averaged) shallow water equations for continuity (5) and momentum equations in the x (6) and y (7) directions:

$$\frac{\partial h}{\partial t} + \frac{\partial(uh)}{\partial x} + \frac{\partial(vh)}{\partial y} = 0 \quad (5)$$

$$\frac{\partial u}{\partial t} + u \frac{\partial u}{\partial x} + v \frac{\partial u}{\partial y} + g \left(\frac{\partial h}{\partial x} + \frac{\partial \alpha_o}{\partial x} \right) - \frac{\epsilon_{xx}}{\rho} \frac{\partial^2 u}{\partial x^2} - \frac{\epsilon_{xy}}{\rho} \frac{\partial^2 u}{\partial y^2} + \frac{gu}{C^2 h} \sqrt{u^2 + v^2} = 0 \quad (6)$$

$$\frac{\partial v}{\partial t} + u \frac{\partial v}{\partial x} + v \frac{\partial v}{\partial y} + g \left(\frac{\partial h}{\partial y} + \frac{\partial \alpha_o}{\partial y} \right) - \frac{\epsilon_{yx}}{\rho} \frac{\partial^2 v}{\partial x^2} - \frac{\epsilon_{yy}}{\rho} \frac{\partial^2 v}{\partial y^2} + \frac{gv}{C^2 h} \sqrt{u^2 + v^2} = 0 \quad (7)$$

where

x = distance in the x -direction (longitudinal to flow)

u = horizontal flow velocity in the x -direction

y = distance in the y -direction (lateral to flow)

v = horizontal flow velocity in the y -direction

t = time

g = acceleration due to gravity

h = water depth

a_o = elevation of the profile bottom

ρ = fluid density

ε_{xx} = normal turbulent exchange coefficient in the x -direction

ε_{xy} = tangential turbulent exchange coefficient in the x -direction

ε_{yx} = tangential turbulent exchange coefficient in the y -direction

ε_{yy} = normal turbulent exchange coefficient in the y -direction

C = Chezy roughness coefficient (converted from Manning's n)

Model output includes flow depth and x and y components of depth-averaged velocity at each network node. The Boussinesq eddy-viscosity concept (LeMehaute, 1976) is used to simulate turbulent energy losses between elements, which are represented in equations 6 and 7 by the turbulent exchange coefficients ε_{mn} . RMA2 and similar two-dimensional flow models [i.e.; FESWMS-2DH (Froehlich, 1988), HIVEL2D (Stockstill and Berger, 1994)] have been successfully applied in a number of free surface flow simulation problems (e.g., Miller, 1994, 1995; Bates et al., 1992; Soong and Bhowmik, 1991).

Limitations of two-dimensional numerical models arise in representing three-dimensional processes. The application of vertically averaged flow models assumes that the vertical dimension of flow is negligible compared to flow in the horizontal dimensions and gravitational acceleration (right hand side of equations 6 and 7). These are reasonable assumptions, and the three-dimensional velocity profiles obtained in this study made it possible to test the validity of this modeling assumption.

The location of greatest vertical velocity is along the eddy shear zone. Here, depth-averaged velocity reached magnitude of 1.75 ms^{-1} in survey 16a. At this same

sampling location, near-bed vertical velocity of -0.35 ms^{-1} (down) was measured. Thus the vertical velocity magnitude at this location and discharge was 20% of the vertically averaged horizontal velocity.

Stratification of flow velocities in the water column is common, especially where topographic elements occur in the channel and where flow direction rapidly changes. Areas such as these are characterized by macro-scale turbulence which occurs in all three spatial dimensions. The vertical velocity component in areas of the channel where topography is flatter was found to be in the range of $\pm 0.05 \text{ ms}^{-1}$, or less than 5% of the average horizontal velocity magnitude. The adverse effects of the two-dimensional model assumption of negligible vertical velocity were minimized by constructing a very detailed mesh in areas of steep slopes and elsewhere that the greatest velocity gradients and flow turbulence were observed in the measured velocity fields.

Model Calibration and Verification

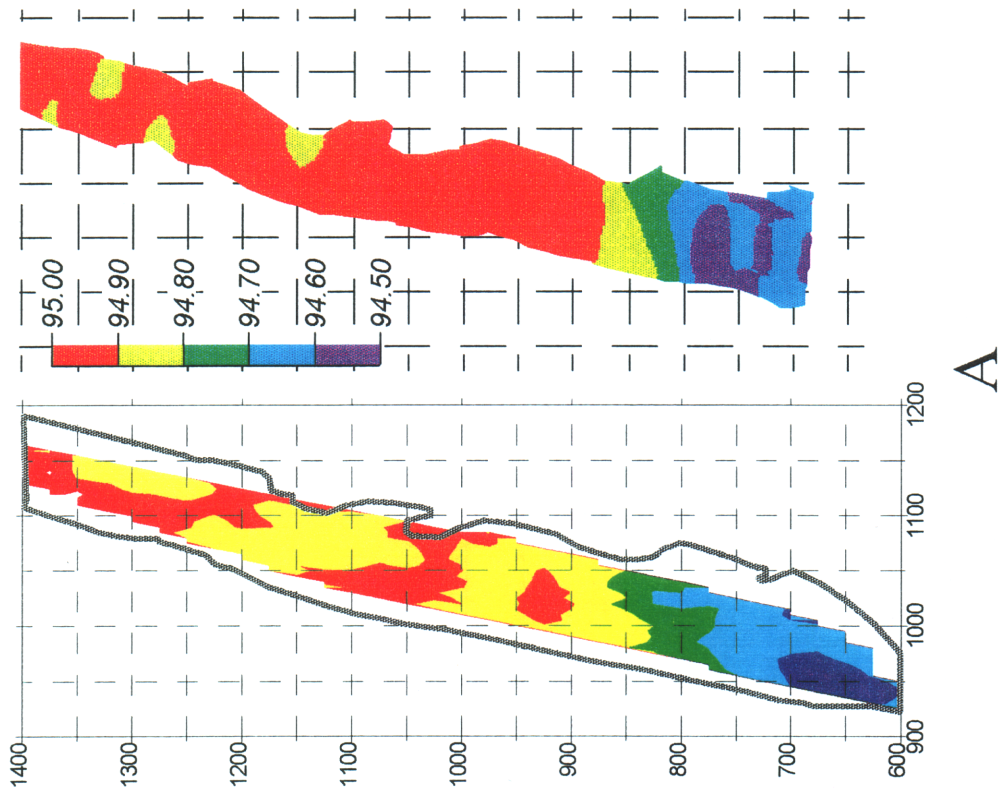
RMA2 calibration is accomplished by selecting values of water temperature (calculating fluid density), eddy viscosity and roughness of each element in the mesh. Water temperature was measured concurrently with velocity profiling and the average value of 15°C was used for all model runs.

Christiansen (1993) calculated roughness for the cross section at National Canyon gage (river mile 166.5) and found that effective roughness (n) increased inversely with discharge from 0.027 at $600 \text{ m}^3\text{s}^{-1}$ to 0.033 for $325 \text{ m}^3\text{s}^{-1}$. She compared this to recommended Manning's n of 0.025 for the range of discharges based on experience with wide alluvial channels (Richards, 1982). Lower roughness values in the upper pool environment of the National Canyon gage are expected where lower velocity results in greater percentages of sand versus gravel on the channel bed.

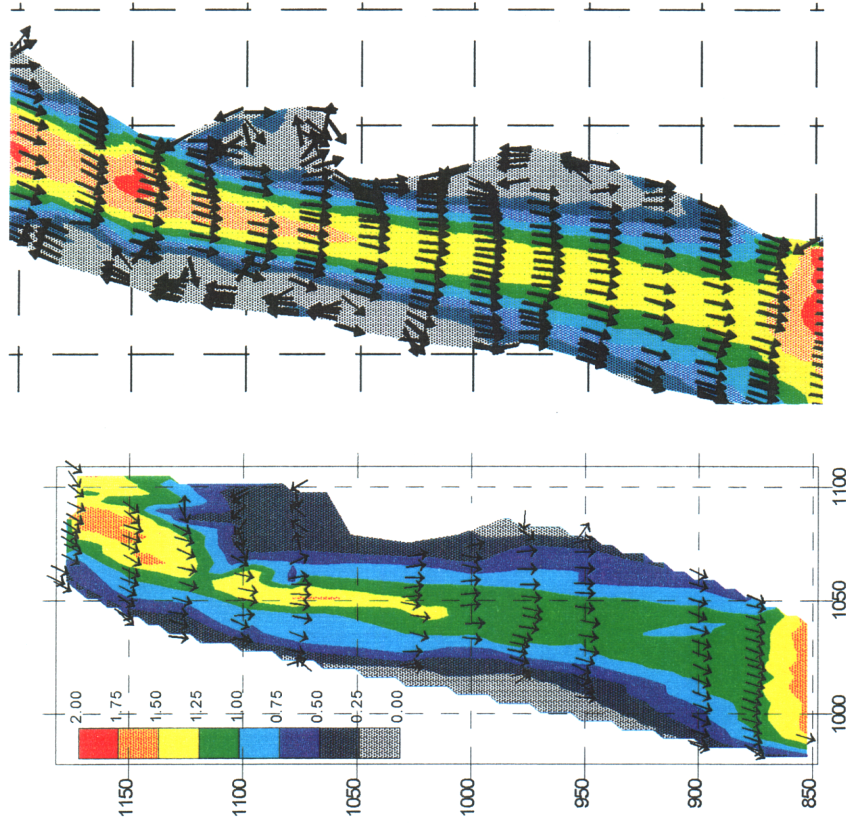
Roughness for each finite element can be specified and used to calibrate the model. A simple arrangement of three element roughness was used to discriminate between the banks, which consist of large angular and subangular rocks with interstitial sand ($n=0.035$), the partially sand covered gravel bedded main channel ($n=0.032$), and exclusively sandy areas ($n=0.020$).

Turbulent exchange coefficients, or eddy viscosities, describe the energy losses due to turbulence. The coefficients are semi-physical parameters in the flow model because they also include 'numerical viscosity' for stabilizing the model. Eddy viscosity can be specified in the x and y planes for each material type in the model. Guidelines in the model documentation recommend eddy viscosity values ranging between 1200-2400 Nsm^{-2} for shallow rivers with fast current and between 50-240 Nsm^{-2} for separation around structures. An isotropic eddy viscosity of 150 Nsm^{-2} was used for all material types and all model runs because it resulted in flow patterns matching the mapped flow patterns, especially in zones of lateral flow separation. Greater values greatly reduced the size of eddy recirculation zones and smaller values enlarged the recirculation zone beyond that measured, and made the model unstable. Eddy viscosity is a critical parameter in the model requiring calibration with field observations, just as is the water surface at the downstream boundary condition as well as water surface distribution throughout the modeled reach. The results from this investigation indicate that, in the absence of measurements on flow patterns, the minimum eddy viscosity that provides a stable model solution should be used.

The velocity distribution maps and water-surface maps from various field measurements provided several discharges and different eddy bar conditions for model calibration. Flow model calibration was accomplished by adjusting n values and eddy viscosity until model results agreed well with field measurements (figure 10). The calibrated model was then used to predict flow depth and velocity distribution for combinations of flow and channel conditions that were not measured in the field.



A



B

Figure 10. Water-surface (A) and velocity magnitude/vector maps (B) from depth-averaged field data (left) and two-dimensional model data (right). Labeled contours show water surface elevation in meters, colored contours show velocity magnitude in ms^{-1} . Arrows show velocity vectors.

Mapping

Contour Maps and Slices

The spatial topographic and velocity data were edited and analyzed primarily as contour maps. Surfer software was used to make contour maps, to overlay maps and to make velocity vector maps of the field data. Surfer was also used to calculate volumes from residual surface comparisons. Cross sections and profiles were sliced from contour maps along consistent lines to reduce the errors that navigation introduces. The SMS program was used to make contour maps and velocity vector maps of the model data, and to calculate and map particle stability.

RESULTS

Moab

The information from the near-naturally flowing river reaches is from three distinct time spans. Because the time span of the information determines the way in which it can be analyzed and interpreted, the results are presented and discussed in order of decreasing time span. Experience with sand bars in the Grand Canyon suggested that the shorter time step information has the greatest value for improving our understanding of processes, consequently the greatest effort was spent on the most frequent information.

Five to Ten Year Information

A series of aerial photographs was obtained and used for description and measurement of exposed sand deposit size and morphology, and changes in channel constriction caused by side-channel debris inputs. The photo series consists of high altitude images at various scales taken in 1952, 1956, 1975, 1980, 1987, and 1993 . All of the photographs were taken during late summer or fall low-flow periods. The MP26 site and two similar debris fan sand bar complexes downstream were included in this analysis (figure 7).

The areal extent and surface morphology of the three debris fans did not change during the 41-year period of time covered by the aerial photographs. Therefore change in channel hydraulics or local flow patterns caused by episodic debris flows was assumed to be negligible. However, sand deposit size varied markedly. The median was chosen rather than the mean to describe central tendency of the measurements because the sample distribution was strongly skewed toward the high end of the scale. One standard

deviation (STD) of the 5-10 year data was about 14%, whereas one STD determined from short time step monitoring over the period 1993-1994 for sand bar MP26 was about 25%. When error bars of the larger STD are plotted about the sample median of the 5-10 year data, it is evident that the changes that occurred over the period 1952-1993 for the three bar sample were not statistically significant (figure 11).

The range in median sand bar area for the three bar sample was $\pm 25\%$ of original area, whereas individually the deposits ranged $\pm 50\%$ of their original areas. It was common that each of the three neighboring deposits had unique responses at each of the time steps analyzed. Unique conclusions would be reached if these deposits were analyzed independently or not within the context of the large STD determined by more frequent measurement.

Stream flow for the period 1952-1993 is characterized by declining annual peak discharges as shown by an 11-year running average (figure 12). The 1984 peak discharge was the third largest flow recorded at the Cisco gage (figure 13), and the aerial photographs indicate that between 1980 and 1987, two out of three sand deposits in the MP26 reach decreased in size by approximately 10-15%. The actual response of the sand deposits to the 1984 high flow is unknown, but photographs from 1980 and 1987 show that the high flow was not a significant event in terms of sand bar size and geomorphology after three years.

Seasonal Information

The annual floods that occurred during this research/monitoring project are placed in perspective by graphs of the annual peak flow time series (figure 12) and the ranked return period (figure 13). Peak discharges in the range 280 to $1,000 \text{ m}^3\text{s}^{-1}$ have return periods of 1-2 years and the 1992 and 1994 floods were in this range. The 1993 and 1995 floods were in the range of 3-5 year return period flows. The highest flow recorded at the Cisco gage, $3,540 \text{ m}^3\text{s}^{-1}$, occurred on July 4, 1884. This flow record is an extreme outlier

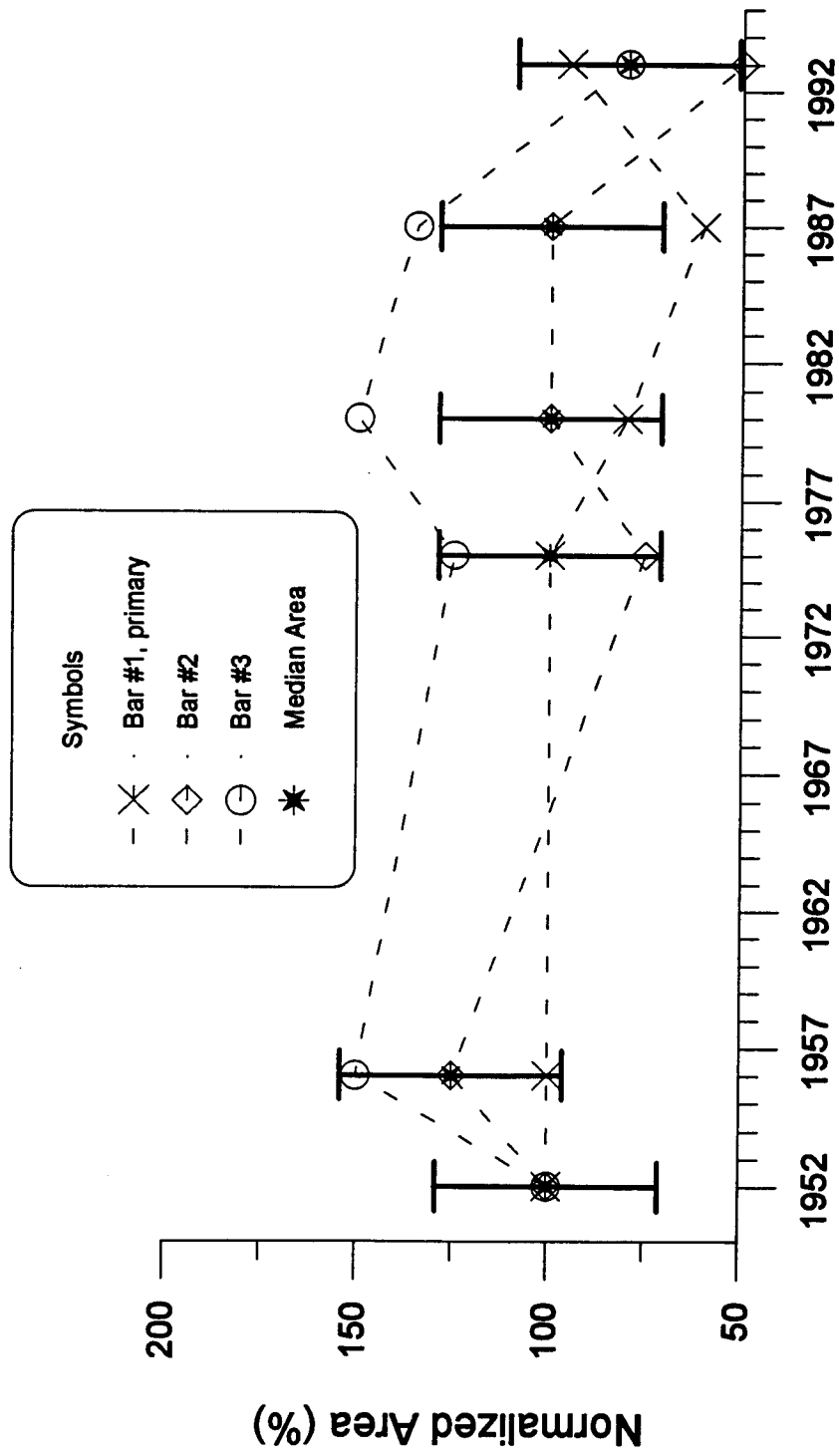


Figure 11. Results from aerial photography analysis for Moab study reaches. Bar #1 is the primary study bar and bars #2 and #3 are from the secondary study reach. See legend for explanation of symbols. Error bars were determined from one standard deviation from short time interval sampling.

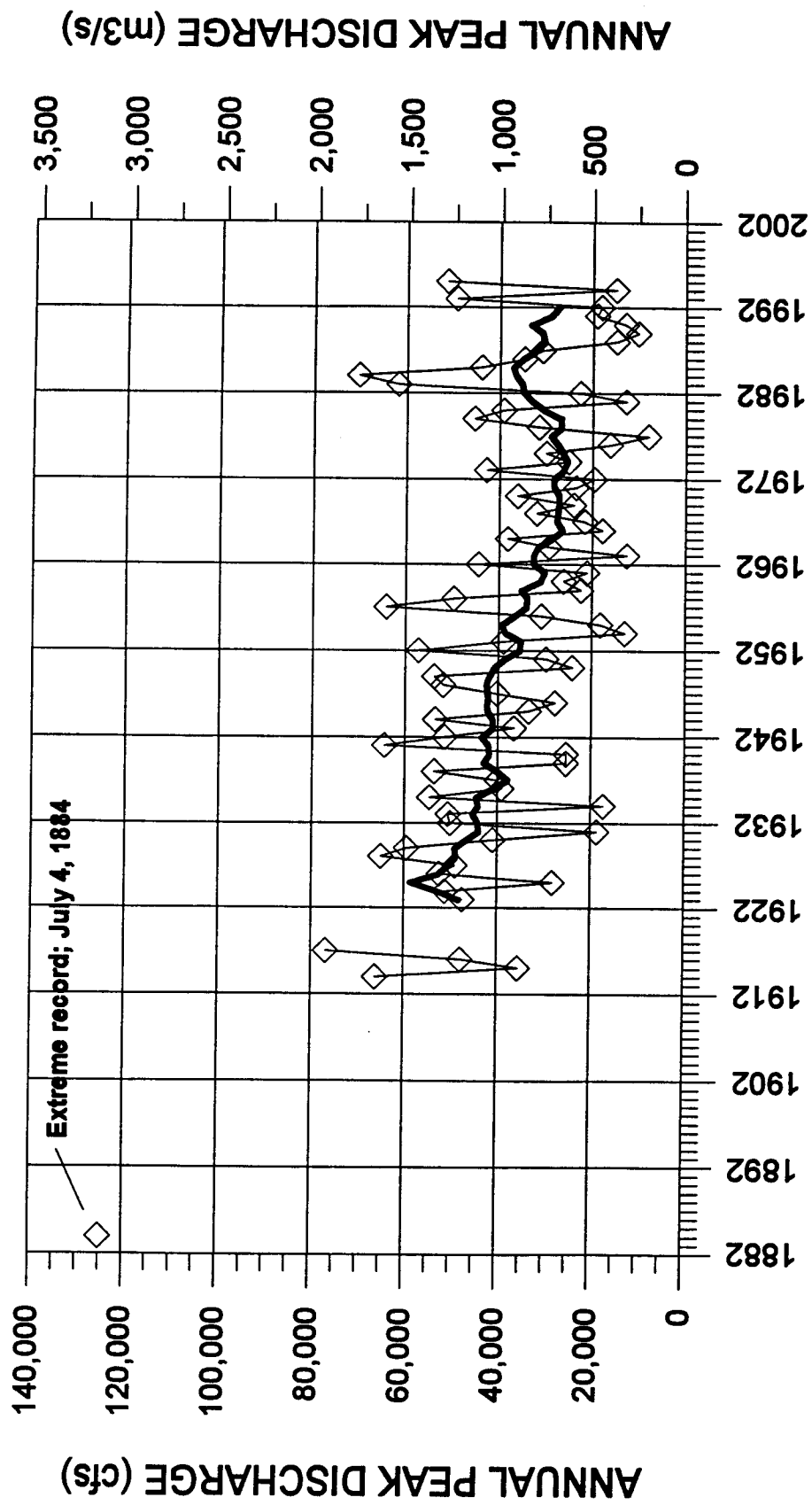


Figure 12. Annual peak discharge record for Colorado River near Cisco, UT. Heavy line is the 11-year running average. Note the outlying record from 1884.

and its accuracy is questionable because it was an indirect discharge measurement. The Cisco gage record began in water year 1914. Removing the 1884 flood peak from the flood frequency analysis would increase the ranking and return periods of the other flows recorded.

Peak values for the high flow years 1983-1984 and the period 1989-1995 are labeled on the return period graph (figure 13). The 1993 high flow of $1,397 \text{ m}^3\text{s}^{-1}$ ranks as a 3-4 year flood and it followed a four-year-period of peak discharges that did not exceed $567 \text{ m}^3\text{s}^{-1}$. The 1994 flood was in the 1-2 year return period range and was followed by the 1995 flood which peaked at $1,456 \text{ m}^3\text{s}^{-1}$. An 11-year running average of annual peak discharge shows a decreasing trend (figure 12). Peak discharges in 1983-1984 were the most significant departures from the trend in five decades.

Between March 1992 and March 1993, six repeated oblique photographs documented the relative size and morphology of the exposed sand bars. The first photographs of the sandy channel margin deposits at MP26 were taken on March 30, 1992, during late winter low flow conditions (figure 14a). The photograph shows a large vegetated reattachment deposit, a broad low elevation vegetated eddy deposit, and a narrow bare sand levee on the river side of the eddy deposit. The photographer's notes indicate that there was a thin veneer of sand overlying the downstream face of the cobble debris fan, where separation deposits occur. The reattachment bar had a vertical face and was undergoing erosion by bank retreat. This basic morphology, low elevation bars, was the result of four consecutive years of abnormally low peak discharges.

Systematic measurements of the sand bars began with the first topographic survey in July 1992. Photographs show that the bar was elongated, elevated and covered greater area as a result of the spring 1992 flood (from approximately $1,800 \text{ m}^2$, estimated from photographs, to $2,700 \text{ m}^2$, surveyed). Maps from topographic surveys indicated that the volume of sand temporarily stored in the 1992 eddy deposit was approximately $5,100 \text{ m}^3$ above the late July low flow level. At $484 \text{ m}^3\text{s}^{-1}$ peak discharge, the Spring 1992 flood was in the range of 1-2 year recurrence (figure 13). No information exists to describe if

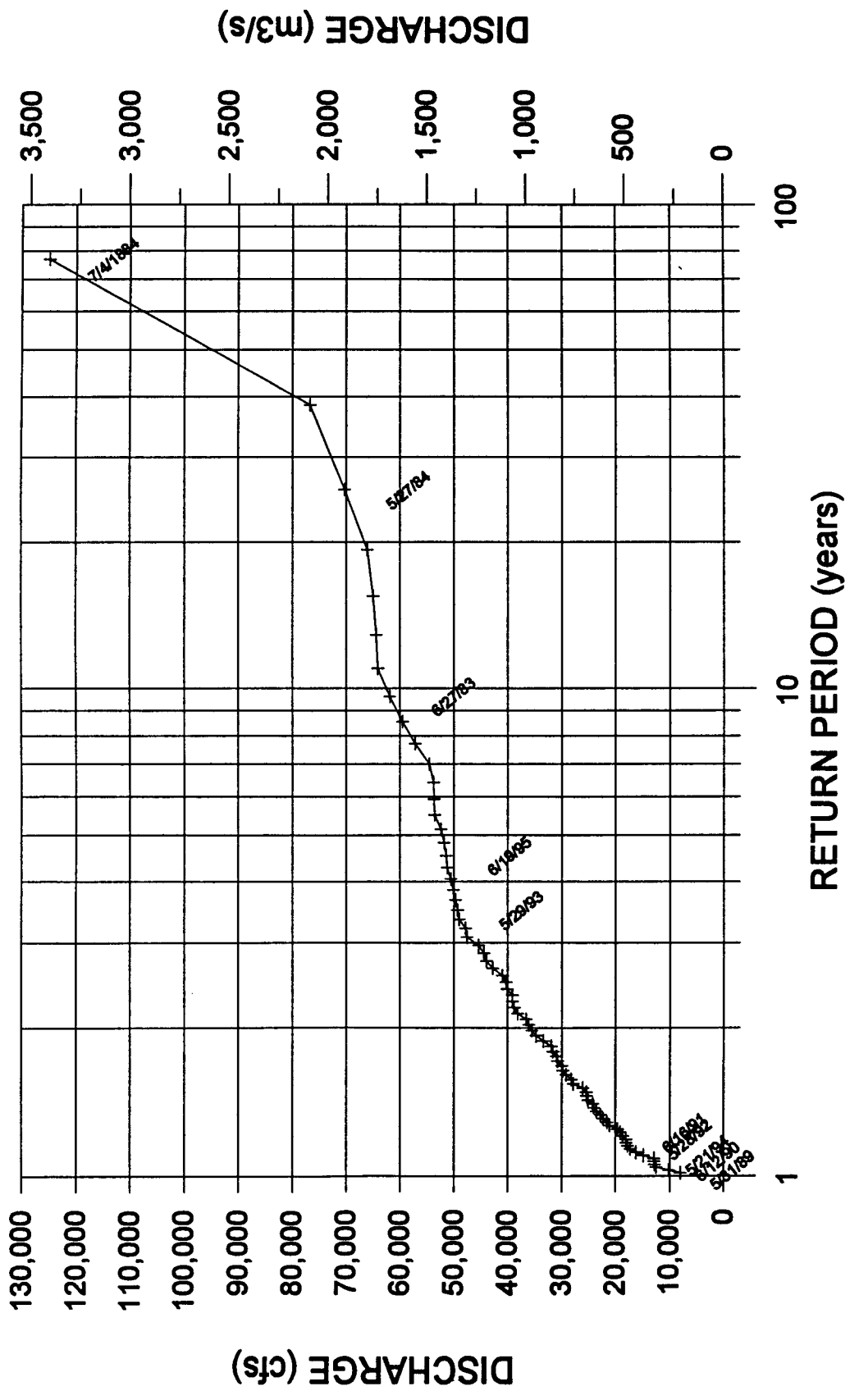


Figure 13. Return period graph for peak flows at the Colorado River near Cisco, UT stream gage.

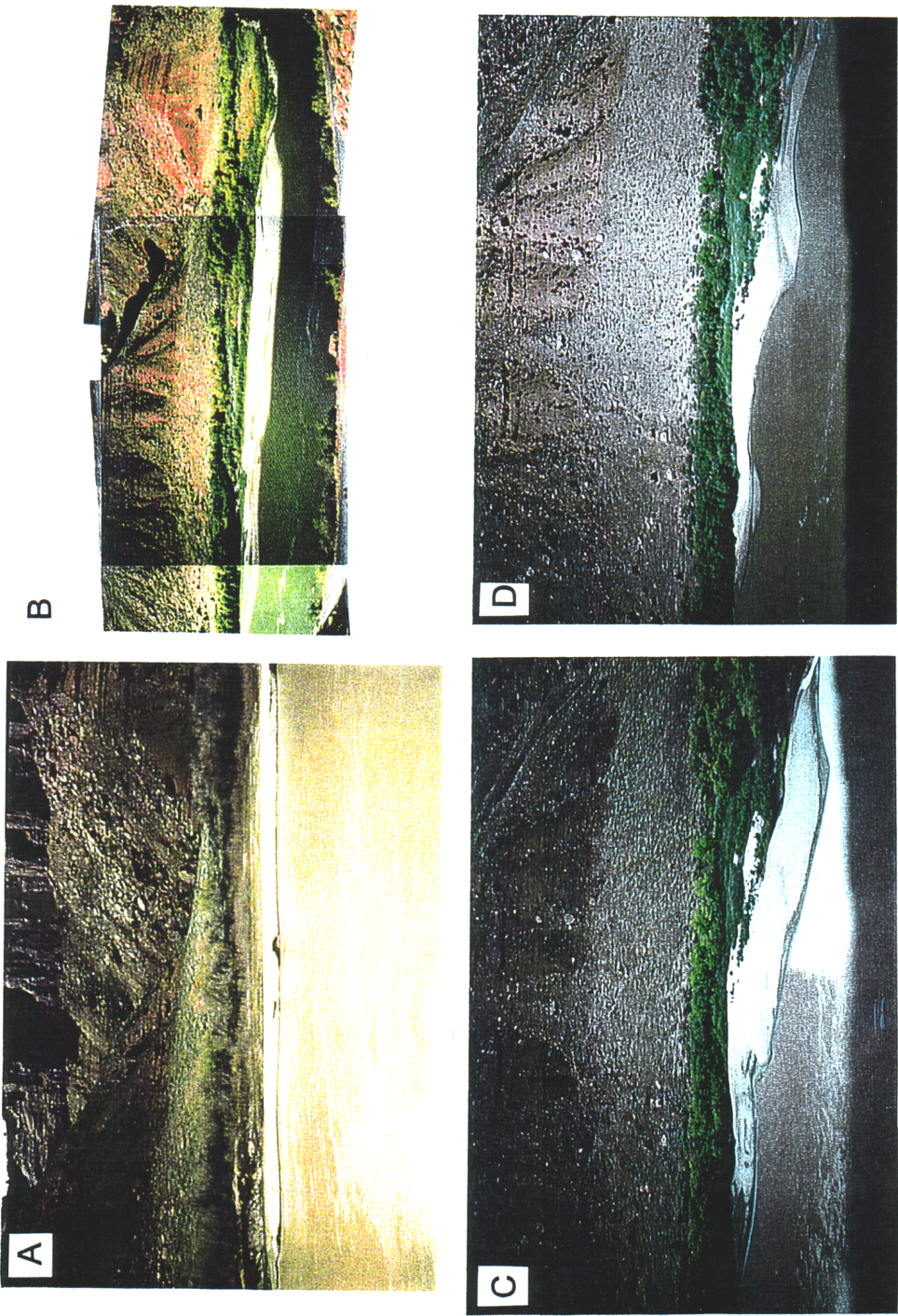


Figure 14. Photographs of the unregulated river sand bars at the primary study reach 50 km upstream from Moab, UT. Flow is to left. Images are approximately 300 m wide. (A) 3/30/1992, (B) 10/15/1992, (C) 10/11/1993, (D) 6/8/1994.

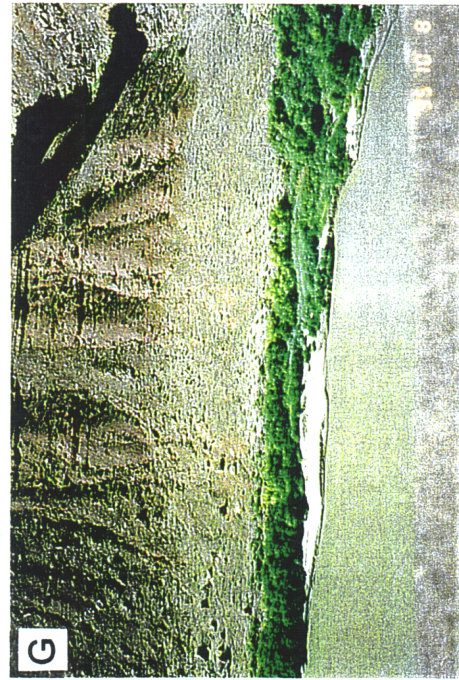


Figure 14, continued. Photographs of the unregulated river sand bars at the primary study reach 50 km upstream from Moab, UT. Flow is to left. Images are approximately 300 m wide. (E) 7/14/1994, (F) 5/19/1995, (G) 10/8/1995, (H) 10/14/1996.

the eddy bar was scoured and re-deposited by the 1992 flood. Figure 15 shows the results and corresponding flow conditions in time-series from April 1992 to October 1995.

Photographs taken in October 1992 (figure 14b) show that the deposits had not changed since flood recession in July. Sometime after October, 1992 and before January, 1993, the eddy deposit was scoured. The result was the elimination of the entire bare sand eddy bar and a small area of the vegetated reattachment bar. Photographs taken on January 10, 1993, at a discharge of approximately $68 \text{ m}^3\text{s}^{-1}$, show that ice had formed across the river. A meandering lead in the ice indicated that flow patterns were directed toward the eddy. Icing may have caused erosion of the eddy bar during low flow conditions. Topographic surveys in July 1992 and March 1993 allow estimation that the eddy bar area was reduced from approximately 2,700 to 100 m^2 during the winter scour event. The reattachment bar was largely unaffected by the winter scour event.

Spring 1993 peak discharge reached $1,397 \text{ m}^3\text{s}^{-1}$ (3-4 year recurrence) and photographs taken in August-October 1993 show that a significantly enlarged eddy bar was deposited (figure 14c). Compared to its previous morphology, the new eddy deposit was extended in the downstream direction and elevated so that it was fully connected to and overlying the reattachment bar. The eddy bar surveyed in September 1993 measured approximately $4,000 \text{ m}^2$. Daily time-lapse photography began in March 1993, and between March and October 1993 the eddy and reattachment deposits were stable.

Continuous Information - The 1994 Flood

The system of local surveying benchmarks was expanded in September 1993 to include channel cross sections. Nineteen cross sections spaced at 25-meter intervals provided thorough coverage of the channel topography and morphology from the apex of the debris fan and entry slope of the pool to the crest of the riffle downstream. The first channel topography survey was conducted in September 1993 and seven channel surveys were repeated between the 1993 and 1994 high flows. This detailed set of repeated

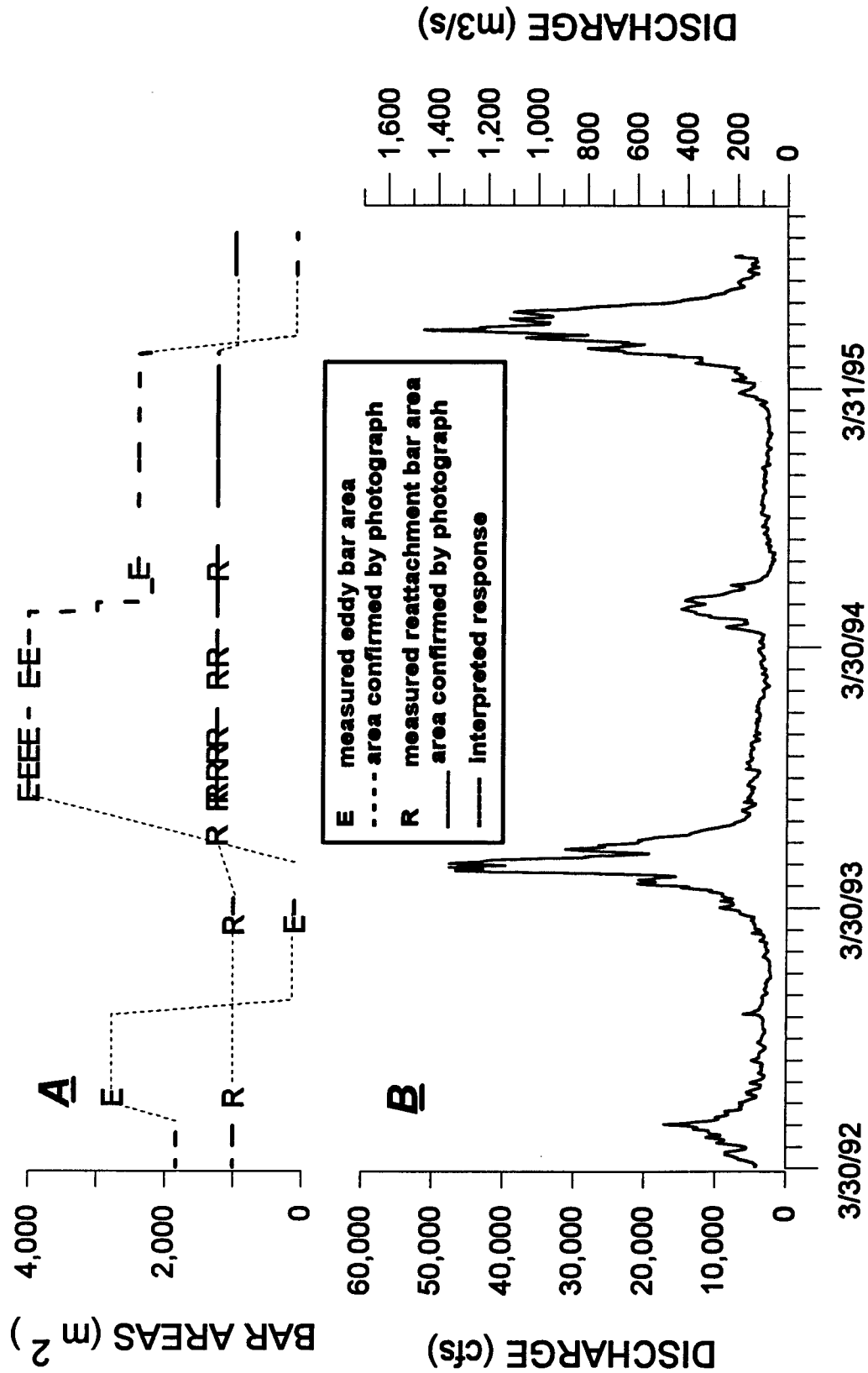


Figure 15. Time series of data collection and results for sand bars at the Moab study reach (A). Mean daily discharge for the study period (B).

bathymetric measurements documented an evolution of channel changes occurring throughout one annual flow cycle.

Repeated surveys and nearly continuous daily time-lapse photography show that the eddy and reattachment deposits were stable in their post-1993 flood morphologies for the remainder of the year. The 1994 flood flow peaked at about $425 \text{ m}^3 \text{ s}^{-1}$, and time-lapse photographs taken during May and June 1994 (figure 14d) show that the eddy deposit was eroding from recirculating flow during the rising limb, reducing to approximately 50% its pre-flood area before it became completely inundated.

Photographs taken after the July 1994 flood (figure 14e), at a discharge of approximately $76 \text{ m}^3 \text{ s}^{-1}$, show that the scoured eddy bar was re-deposited during the peak or receding limb of the flood hydrograph to approximately its pre-flood size and morphology. Its elevation was somewhat reduced consistent with the lower peak stage of the 1994 flood. No changes in size or morphology were observed during the remainder of 1994 and winter 1994-1995.

When the initial channel survey was conducted in October, 1993, the deepest part of the pool was located at range 1100, at 84 meters elevation (figure 16). During the fall low flow season, the pool lengthened and deepened in the upstream direction. By late winter an equilibrium condition existed where only minor channel changes would subsequently occur. During the rising limb of the flood, the mid-May survey shows that the mid-pool area (around range 1000-1100) deepened as much as 2 meters to an elevation of 83 meters. Also, a large dune approximately 3 meters thick and 50 meters long formed on the pool exit slope around range 1100-1150. The pool was deepened and contracted in the upstream direction by these two adjustments.

The eddy bar face obtained a maximum angle of 26 degrees near its crest (figure 17). This angle was maintained as minor deposition occurred along the face between March 16, 1994 and May 12, 1994. The eddy bar was scoured shortly after the May 12 survey and a new eddy bar was deposited at an angle of approximately 24 degrees, as measured on July 16, 1994.

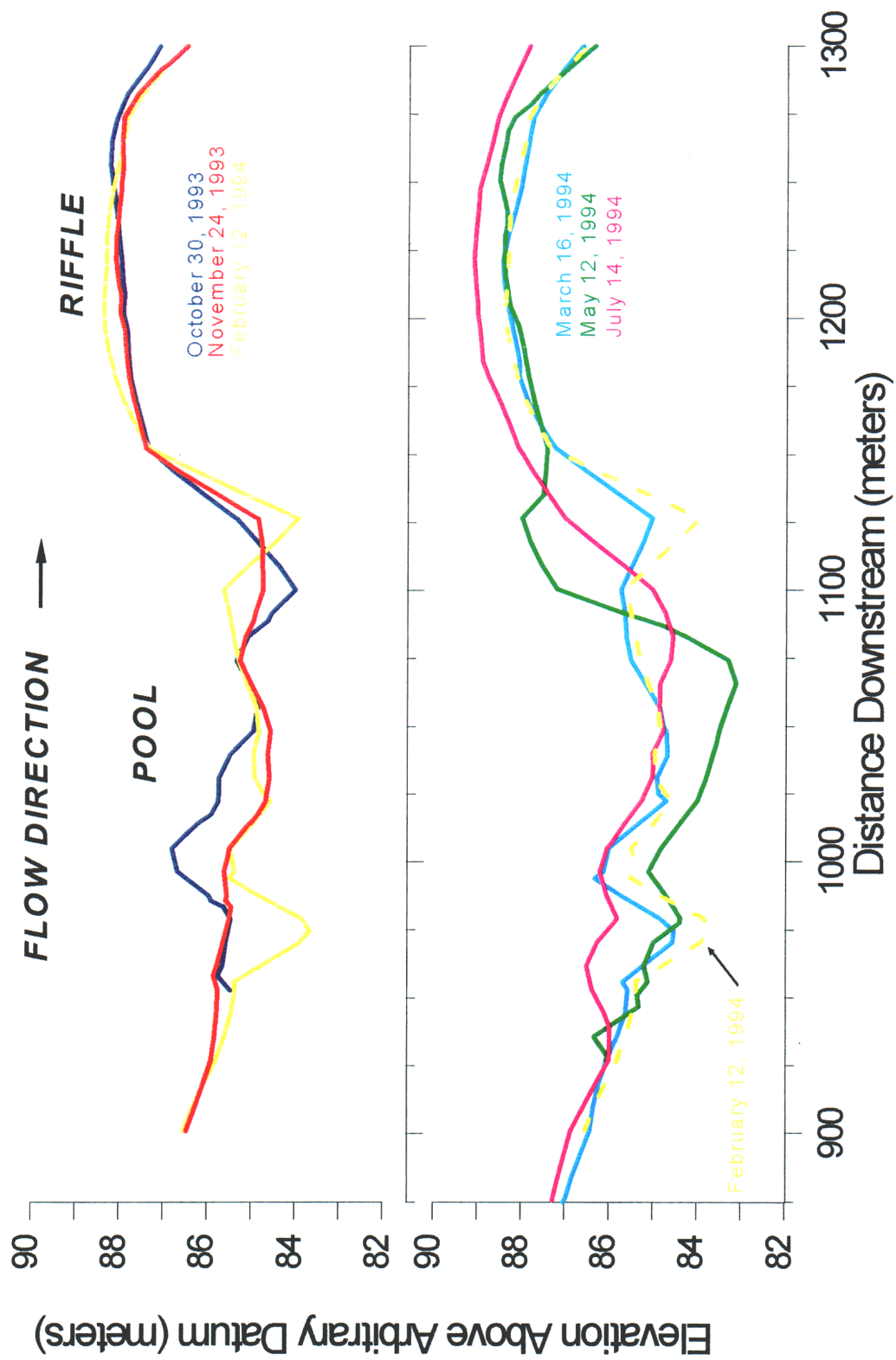


Figure 16. Thalweg profiles from Moab study reach for dates shown in legend, showing changes in the pool downstream from the debris fan riffle.

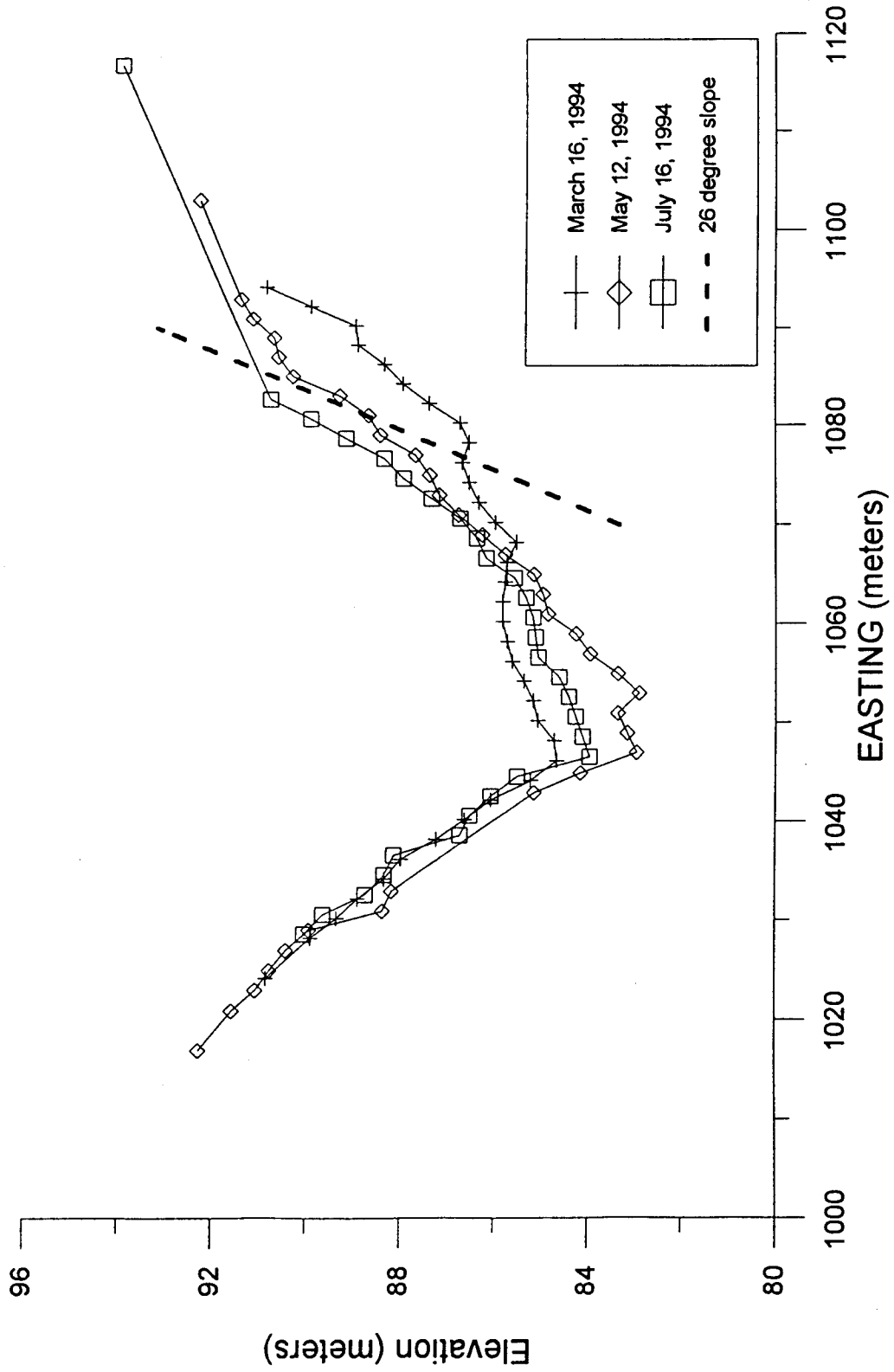


Figure 17. Cross sections at the Moab study reach for dates shown in legend. View is looking downstream across the pool and eddy bar. Heavy dashed line indicates slope at angle of repose.

Following flood recession in late June, the survey taken in July shows that the upstream pool area aggraded between ranges 950 and 1075 (figure 16). The dune-shaped body of sediment that was evident on the pool exit slope was eroded. These two changes expanded the pool in the downstream direction while making it slightly shallower. Consequently, the pool returned to a configuration similar to the post-flood configuration surveyed the previous October.

Results of the 1995 Flood

The highest flow observed during the study period occurred in Spring 1995 when flood flow reached $1,456 \text{ m}^3 \text{ s}^{-1}$ in June (4-5 year recurrence). Time-lapse photographs showed the eddy bar eroding during the rising limb of the flow (figure 14f). Erosion was occurring along an arc shape following the pattern of eddy recirculation. The relatively low elevation eddy bar became completely submerged during the early part of the rising limb of this flow on June 5 when discharge was $346 \text{ m}^3 \text{ s}^{-1}$. When flow had receded to approximately $142 \text{ m}^3 \text{ s}^{-1}$ in early September 1995, photographs showed that not only was the entire eddy deposit eroded during the flood, but a new bar was not deposited (figure 14g). Vertical cut banks extending into the large woody vegetation of the reattachment deposit indicate that the toe of that deposit was also eroded during the flood. Based on previous photographs of exposed deposits calibrated by topographic surveys, the Spring 1995 flood eroded an area approximately $2,500 \text{ m}^2$ (figure 15) and the minimum volume eroded is estimated at $8,000 \text{ m}^3$.

The anomalous response of the MP26 eddy bar to the 1995 flood flow differs markedly from the previously observed pattern where the rising limb of flood flows eroded the eddy bars but new eddy bars emerged as the floods receded. However, observations following the experimental spike flow in the Grand Canyon in spring 1996 also showed a similar variety of results at numerous sand bars. This was especially pronounced in reaches downstream from the Little Colorado River where sand supply is

approximately ten times greater than it is upstream. Observations made in the fall of 1996 at MP26 showed that a new eddy bar was deposited by the 1996 flood (figure 14h).

Mohawk

Channel topography and velocity field mapping began at Mohawk on July 24, 1993 and were repeated 61 times by August 5, 1993. The optimal design was to repeat the surveys twice daily, at low and high flow. However, high flow surveys were difficult to conduct because high flow occurred during the night and navigating in the dark is arduous and somewhat hazardous. After seven days and twelve surveys, we started a session of hourly surveys over a shortened 400-meter length of the channel centered around the eddy recirculation zone. Another hourly survey session was conducted two days later.

Instead of using dates and times to distinguish between the closely spaced surveys, a three-letter naming convention was established for the Mohawk surveys to aid file management. The first first survey was named "MOA" for Mohawk A. Subsequent surveys were named MOB, MOC, and so on. The hourly surveys were also given three character names counting down from hour 24. Thus "24A" is the first survey in the "A" session, followed by survey "23A", "22A", and so on. Figure 18 shows the timing relationship between surveys, their names and river stage. The 24A and 24B survey sessions were undertaken in order to measure channel changes and changes in the velocity field at hourly time scales during unsteady flow caused by variable power plant releases. Land tilt sensors were installed along the crest of the eddy deposit after survey MOB.

Capturing A Rapid Erosion Event

The Mohawk eddy deposit was known to be very dynamic, but the odds were small that a crew could measure the channel and flow field a few hours before and again a few hours after a rapid erosion event. However, this is exactly what happened on July 27 and tilt sensors obtained information throughout the event.

Tilt Sensor Data

Survey MOE was completed between 16:05 and 16:55 on July 27 (figure 18). At 20:30 two tilt sensors recorded slope motion. The motions of #82 and #84 were followed shortly by motion at tilt sensor #85 which inclined at 20:45. The other tilt sensors moved in a progressive manner with distance until 23:30. These data are summarized in table 3.

The sign and axis conventions of inclination assigned to the biaxial tilt sensors were: positive X axis is perpendicular to the river and +X is rotation toward the river when viewed from upstream; the Y axis is parallel with the river and +Y is when the sensor rotates downstream. A sensor within a slump block or rotational failure will tilt first in the +X direction. A sensor within a zone undergoing creep or within a zone on the riverward side of a fissure during early stages of a process similar to glacial calving will first tilt in the -X direction (figure 19).

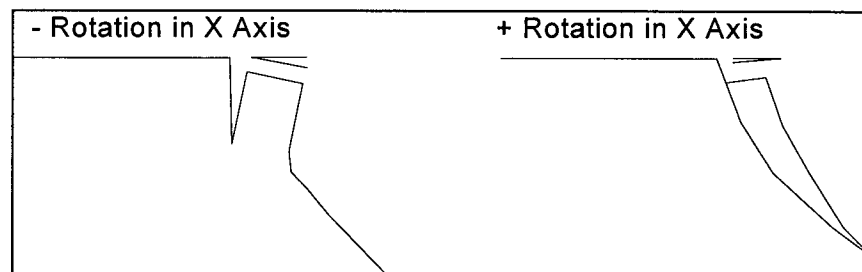


Figure 19. Definition sketch of tilt sensor axis conventions, in the X-axis, looking downstream at the left bank.

Table 3. Summary of tilt sensor data during rapid erosion event on July 27, 1993.

Sensor Number	Distance Along Crest of Eddy Bar (meters)	Time of First Motion	Motion in X-Axis (degrees)	Motion in Y-Axis (degrees)	Sense of Rotation in X-Axis	Sense of Rotation in Y-Axis
84	16.6	20:30	18	-3	Slump	Upstream
82	21.2	20:30	-12	-30	Calving	Upstream
85	16.6	20:45	-9	-22	Calving	Upstream
83	18.1	21:00	-2	-2	Calving	Upstream
83	18.1	21:15	-35	-15	Calving	Upstream
94	27.3	21:15	0	-37		Upstream
93	25.7	21:30	37	28	Slump	Downstream
80	16.6	21:45	18	27	Slump	Downstream
81	27.3	21:45	33	65	Slump	Downstream
99	27.3	22:00	18	35	Slump	Downstream
98	37.9	22:15	22	-32	Slump	Upstream
90	41.0	22:30	14	-47	Slump	Upstream
91	41.0	22:30	15	-32	Slump	Upstream
87	41.0	22:45	5	34	Slump	Downstream
96	41.0	22:45	-14	-14	Calving	Upstream
88	42.5	22:45	-19	-9	Calving	Upstream
92	60.8	23:30	-8	35	Calving	Downstream
		Sum:	81	-19		
		Mean:	4.8	-1.1	Slump	Upstream

The first slope motion detected by tilt sensor was recorded on July 27, 1993 at sensor #84, tilting +18 degrees in X and -3 degrees in Y between 20:15 and 20:30. These motions describe a rotational slump with upstream translation. The next five records showed initial motion describing blocks of sediment tilting toward the river and translating upstream. This same style of slope failure process was observed by a team of scientists at the Mohawk site on April 17, 1991 during the first documented rapid erosion event (Cluer, 1991). During that event, it appeared that the toe of the eddy bar was scoured and gravitational slope failure produced a vertical face which became saturated

and deformed under the weight of the overlying sand. Vertical cracks formed several centimeters away from the face as blocks of sand rotated toward the river. The unsaturated sand formed temporarily stable vertical slopes (probably due to capillary tension between the grains which was quickly destroyed upon wetting). The process continued in increments until the eddy deposit was largely removed.

In the July 27, 1993 rapid erosion event there were nine sensors indicating rotational slumping and seven indicating calving. Eleven showed translation upstream and six translation downstream. The sum and average of 16 first motions favor rotational slumping with upstream translation. However, it is now evident that first motion and total slope failure progressed at a rate faster than 15-minute sampling recorded. Therefore, the recorded motions averaged over 15-minutes probably mask the instantaneous first motion and may not help to distinguish between rotational slumping by internal stresses and calving processes by external stresses.

The tilt sensor array did record a progression of first motion starting at the downstream end of the eddy bar and advancing upstream, or in a direction from the high flow reattachment point to the upstream end of the eddy bar. The duration of the event was approximately 2.25 hours and comparison of pre- and post-event contour maps documents the effects of rapid erosion on sand storage, channel morphology and the resulting velocity fields.

Topographic Maps and Slices

Topographic maps of the channel were prepared for each survey at Mohawk. Channel changes are evident where contour lines follow different patterns between surveys. Maps from surveys MOE and MOF show the effect of the rapid erosion event (figure 20). A residual surface map and volume calculation shows that approximately 11,500 m³ of sand were scoured from the eddy during this event. Maps from surveys MOA, MOB, and MOC showed that the pool and eddy were both dynamic prior to the

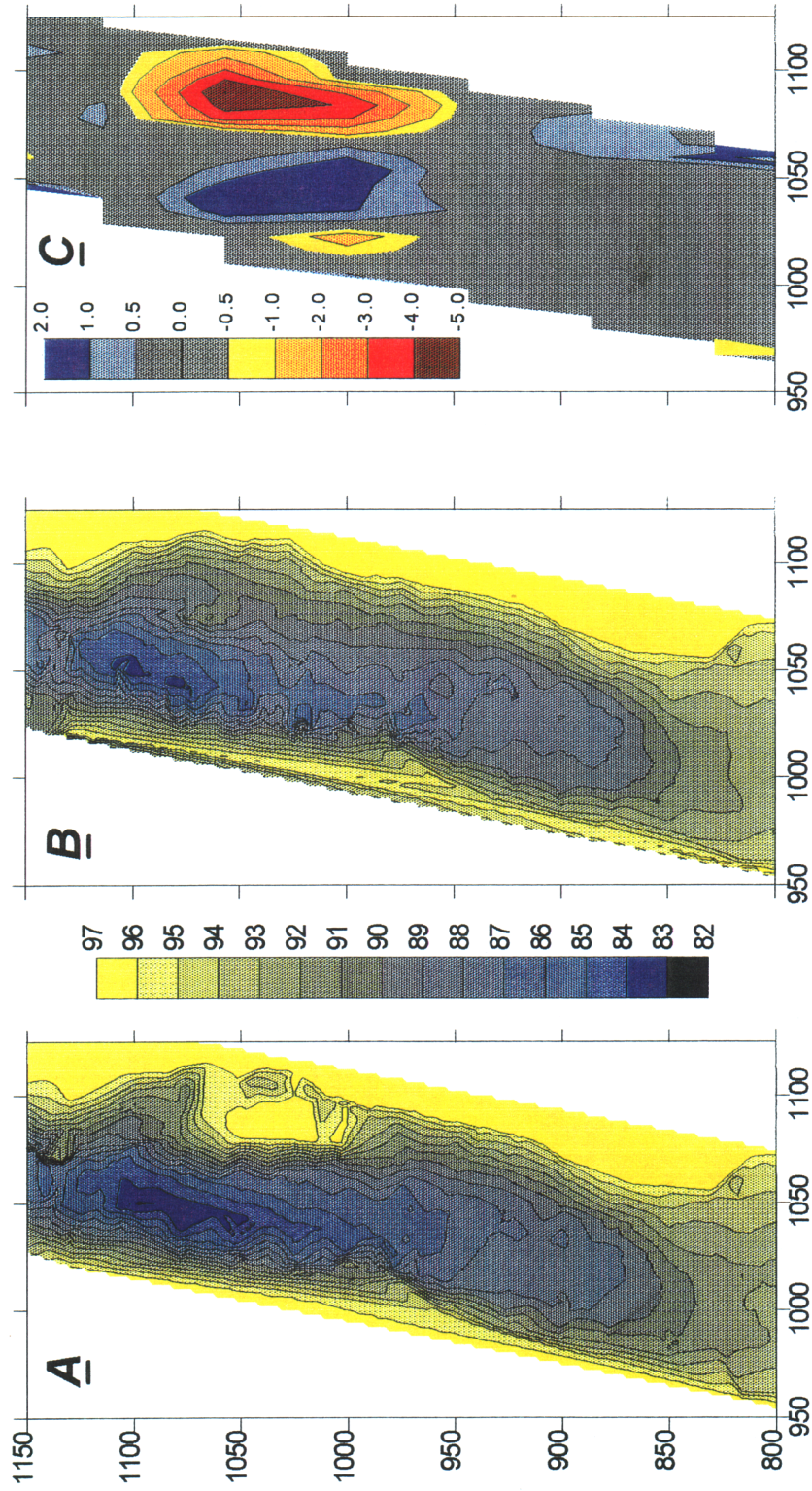


Figure 20. Topographic maps of Mohawk channel and sand bars from surveys MOE (A) and MOF (B), and residual surface topographic map (C) showing scour and fill pattern between surveys MOE and MOF.

rapid erosion event. These changes are best observed in profile and cross-section plots made by slicing the topographic maps along consistent lines.

Profiles of the channel thalweg (defined by the topographic axis of the channel) show that the thalweg profile was stable from survey MOA to MOB (figure 21). Between MOB and MOC there were small magnitude changes in the pool, which deepened approximately 0.5 meters upstream from the pool apex over 20-30 meters length. There was also a smaller amount of scour at the downstream end of the pool and a dune 0.7 meters high was removed from the pool exit slope.

Flow fluctuations between MOA, MOB and MOC were characteristic of the daily hydropower fluctuations for weekday load demands during that period (figure 18). Between MOC and MOD the fluctuation differed from the weekday pattern by smaller amplitude and lower trough. This pattern is often repeated on weekends due to the lesser power demands.

The thalweg profile during MOD differed considerably from MOC. The pool area was filled up to one meter deep over a length of approximately 175 meters. Also, the exit slope dune returned in much the same location and shape as during MOA and MOB. Between MOD and MOE the pool was scoured and closely resembled the MOC profile overall. The pool was unchanged in the upstream area but the downstream area and pool exit slope aggraded between 0.5 and 1 meters over 250 meters length. The aggradation was the result of erosion of the eddy bar which occurred shortly after survey MOD was completed. Topographic residual calculations indicate that of 11,500 m³ sand scoured from the eddy, approximately 5,000 m³ were deposited in the pool and pool-exit slope area (figure 20). Aggradation in the range 0.1-0.3 meters was mapped over the entire survey area downstream from the eddy, totaling approximately 8,000 m³ of sand redistributed on the channel bed from the eddy scour event. The remaining 3,500 m³ of sand were probably transported downstream from the survey reach before survey MOF was completed.

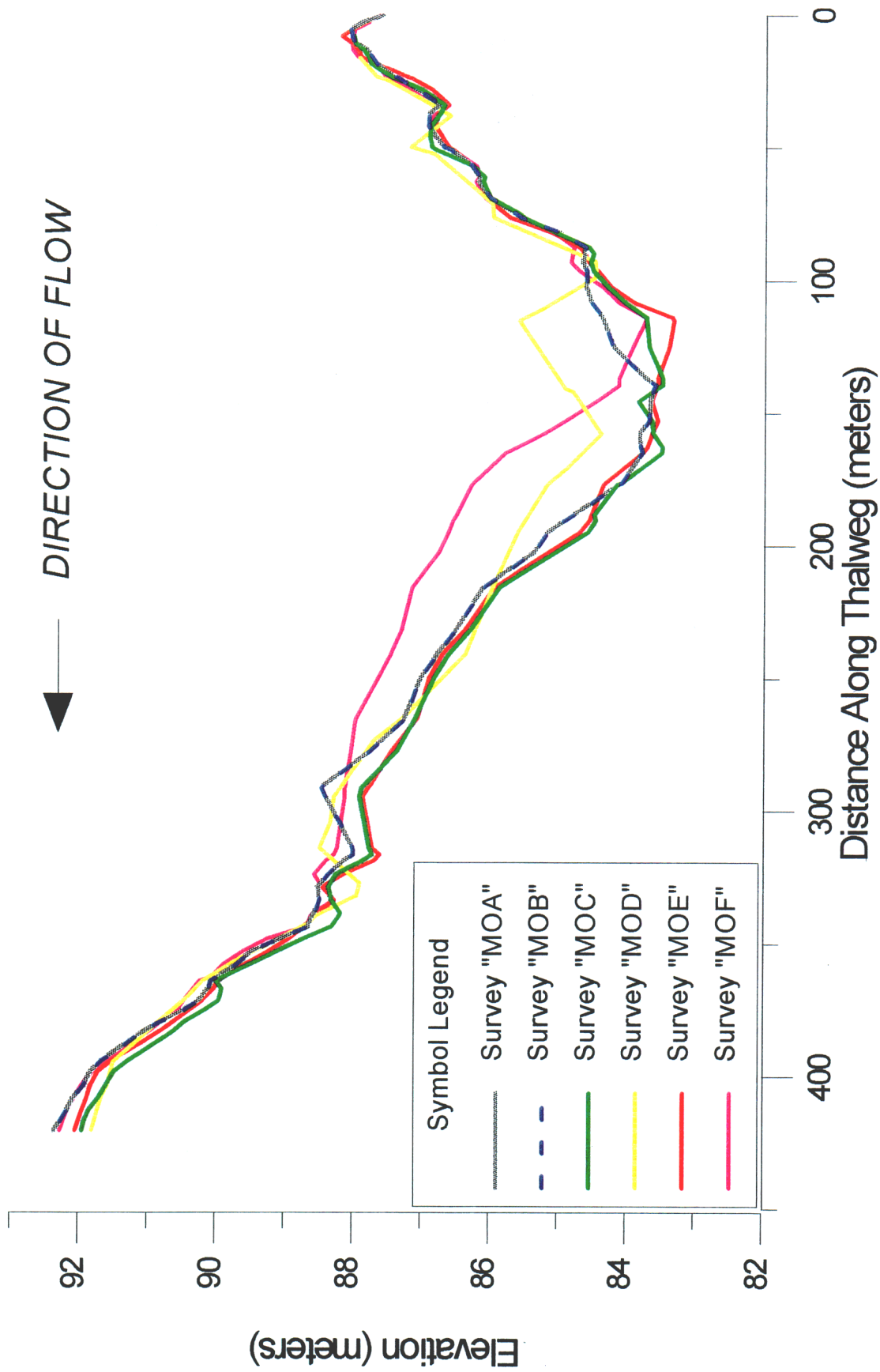


Figure 21. Thalweg profiles from Mohawk surveys MOA-MOF, as distinguished in legend.

Channel cross-sections were made by slicing the topographic maps along a line perpendicular to the channel that crossed the middle of the eddy deposit. These cross-sections show the eddy deposit and channel changes leading up to the rapid erosion event (figure 22). The right bank remained stable in location and shape during all the surveys at Mohawk, indicating the absence of mobile boundary materials on the right bank adjacent to the pool-eddy complex. The bottom of the pool underwent some adjustments to the different hydrodynamic conditions, just as the thalweg profiles showed.

Comparing cross-sections MOA and MOB shows that there were no noticeable differences between the two surveys. Between MOB and MOC the pool maintained its initial elevation but shifted right approximately five meters, and the toe of the eddy deposit migrated accordingly. The slope of the eddy bar steepened and the crest of the bar increased in elevation 0.1 to 0.5 meters. From MOC to MOD the pool aggraded approximately 1.1 meters over 100 meters length, indicating that the low weekend flow fluctuation caused pool filling. Also from MOC to MOD, the toe of the eddy bar shifted back to the right along the lines of MOA-MOB and the crest of the eddy bar was rounded and elevation reduced approximately 0.8 meters. Between MOD and MOE the pool scoured to the level previously surveyed during MOA, MOB and MOC. The bottom of the pool shifted back to the right along the profile lines defined by MOA-MOB, and the toe of the eddy bar was shifted left while the crest of the deposit attained the greatest elevation measured. The greatest change in the pool-eddy cross section was between MOE and MOF, resulting from erosion of the eddy bar.

A general trend is evident among the multiple changes described by the cross sections of figure 21. There was a progressive migration of the eddy deposit toe away from the pool and this correction was accompanied by steepening of the face of the eddy deposit. Between MOD and MOE the eddy bar elevation increased approximately 1 meter at its crest and the slope angle increased from 26 to 34 degrees (figure 23). The angle of incipient motion for well sorted sand is 26-28 degrees. The eddy deposit was scoured up to five meters deep and the slope angle was reduced to approximately five degrees following the rapid erosion event.

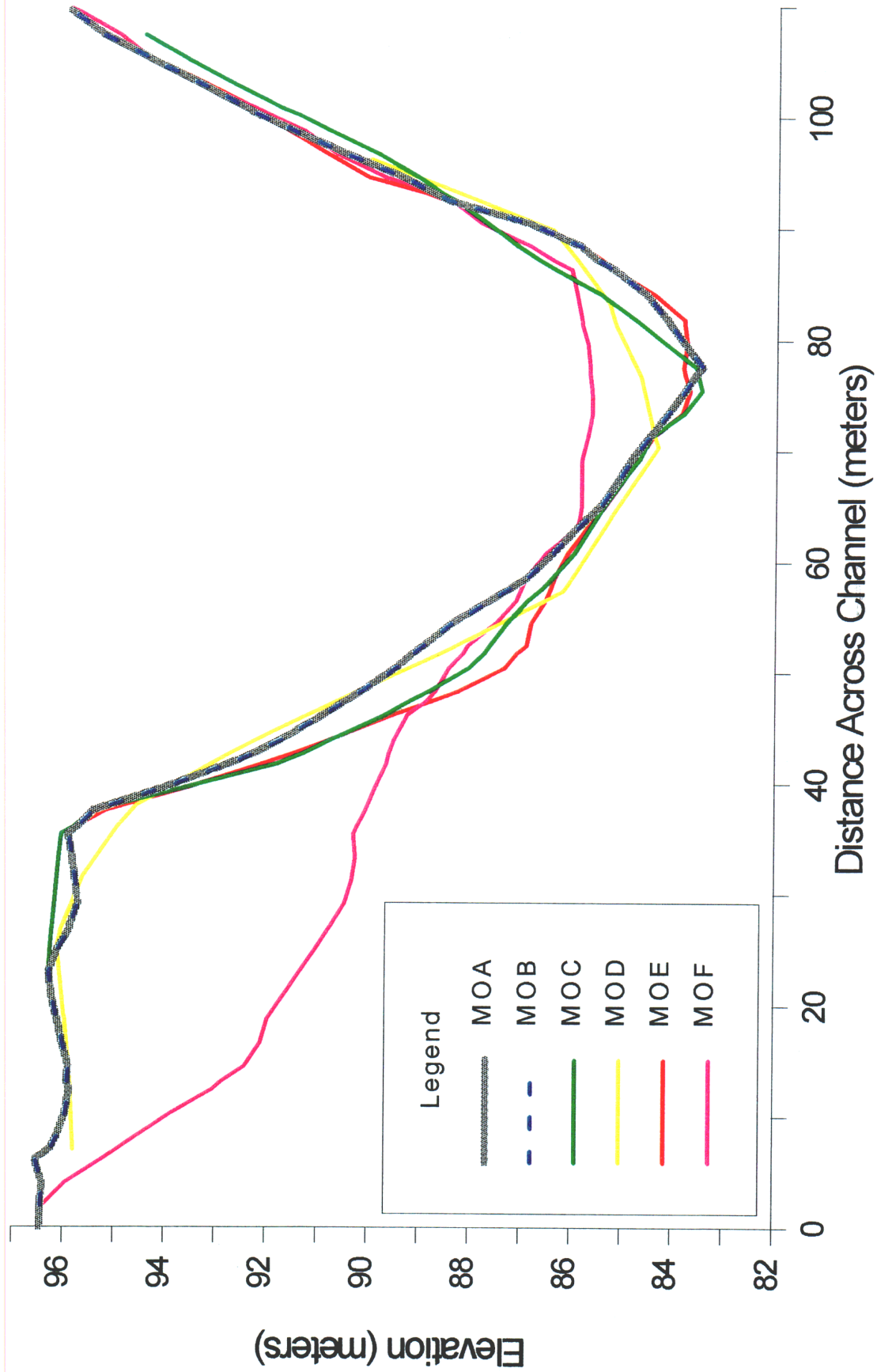


Figure 22. Cross sections from Mohawk across the pool and eddy bar for surveys shown in legend. View is looking downstream.

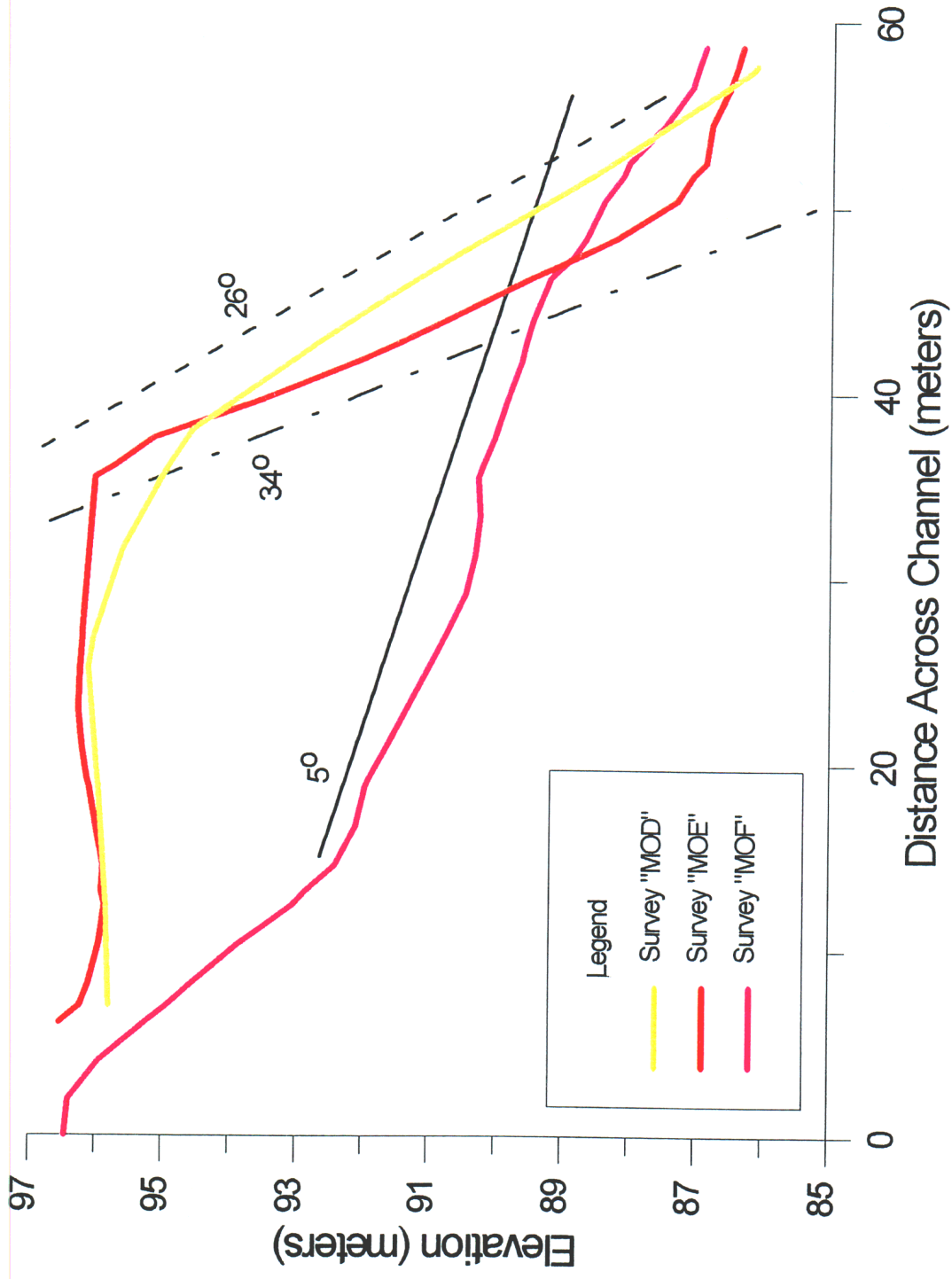


Figure 23. Cross sections from the Mohawk eddy bar for surveys shown in legend, and average slopes of the bar face.

Velocity Field-Particle Stability Maps

Velocity field maps for the various surveys show how velocity magnitude and direction vary spatially in the x - y plane at various depths. Comparison of such maps from different surveys shows how hydraulic patterns vary with discharge and with changing channel topography. An example of depth-averaged velocity is presented for illustrative purposes (figure 24). As informative as velocity field maps are in an investigation such as this, I decided to concentrate analysis on calculated shear stress and the determination of sand particle stability described in the methods section. Boundary shear stress is a combination of depth-averaged velocity and flow depth, whereas particle stability analysis compares available bed shear stress to the stress required to entrain specified particles. For this analysis the particle size chosen was the mean size of the sand sample dredged from the eddy deposit at Mohawk.

Particle Size

Figure 25 shows the results of sieve analysis of a 10.5-kilogram sand sample collected from the Mohawk eddy on August 5, 1993. The sample is not particularly well sorted because the size distribution is not uniform. However, the size range is relatively narrow, from 0.035 to 0.3 mm diameter, and the cumulative frequency curve shows that the lower and upper ten percentile range is from 0.09 to 0.2 mm diameter. The mean particle size (d_{50}) used for calculations of particle stability was 0.18 mm diameter.

Particle Stability

Map plots of particle stability show significant variation in hydrodynamic patterns between surveys prior to and after the erosion event (figure 26). These relatively easy to understand maps are made up of channel topography maps overlaid by particle stability color contour maps, which are overlaid by scaled vector plots of near-bottom velocities.

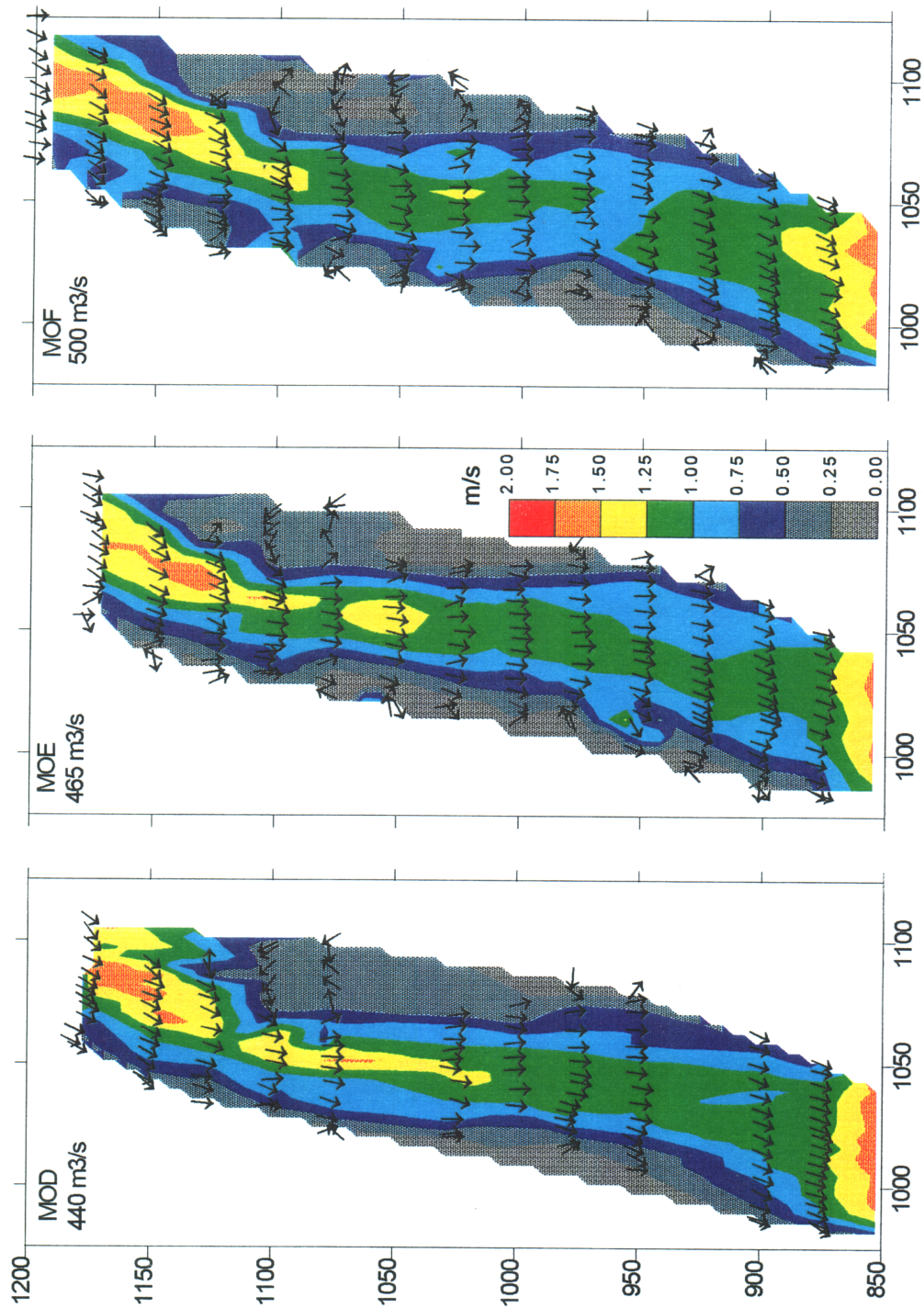


Figure 24. Depth-averaged velocity field maps from Mohawk for surveys indicated. Data from the BB-ADCP current velocity profiler, positioned with the bathymetric mapping system.

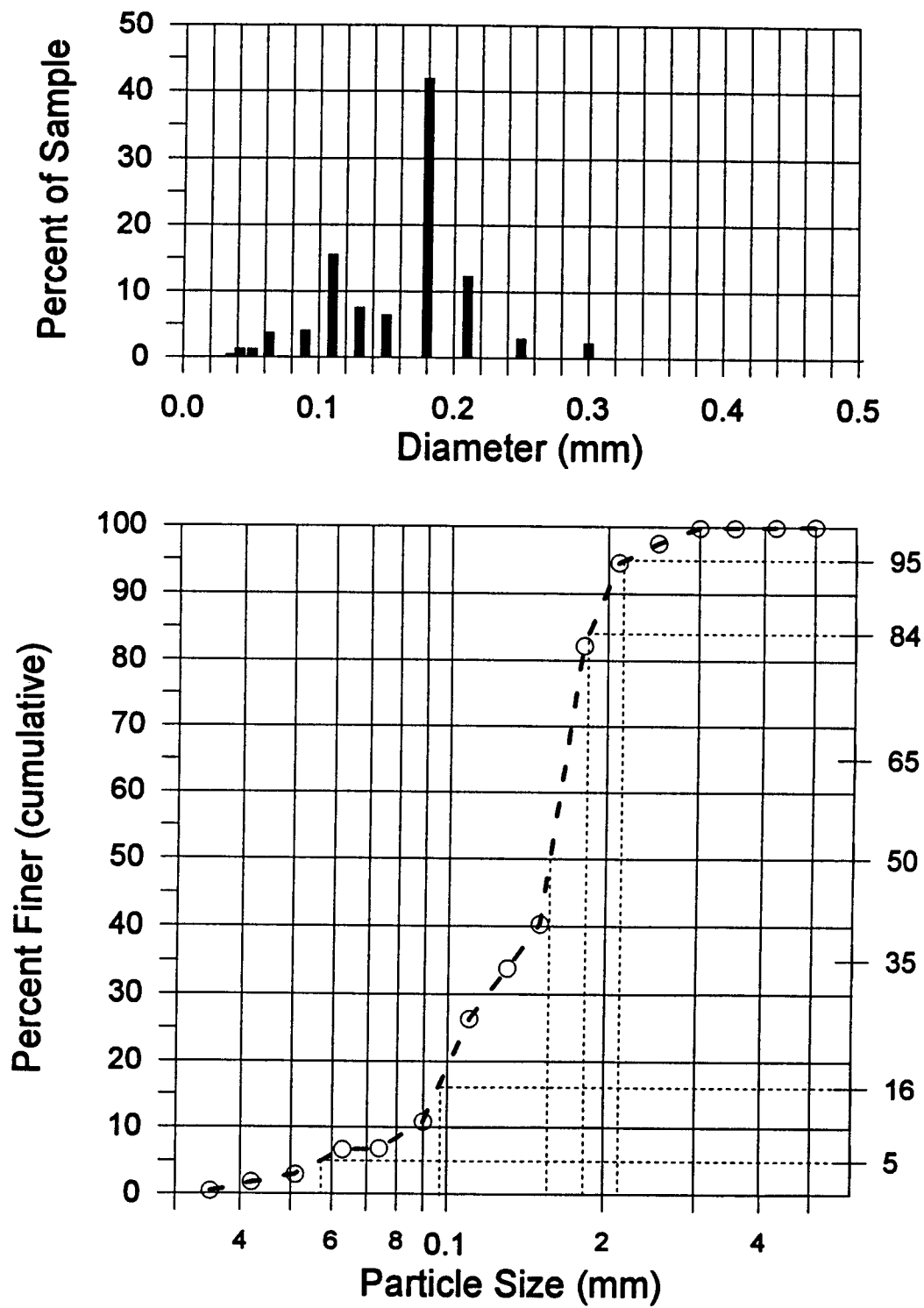


Figure 25. Sieve analysis for sediment sampled in Mohawk eddy.

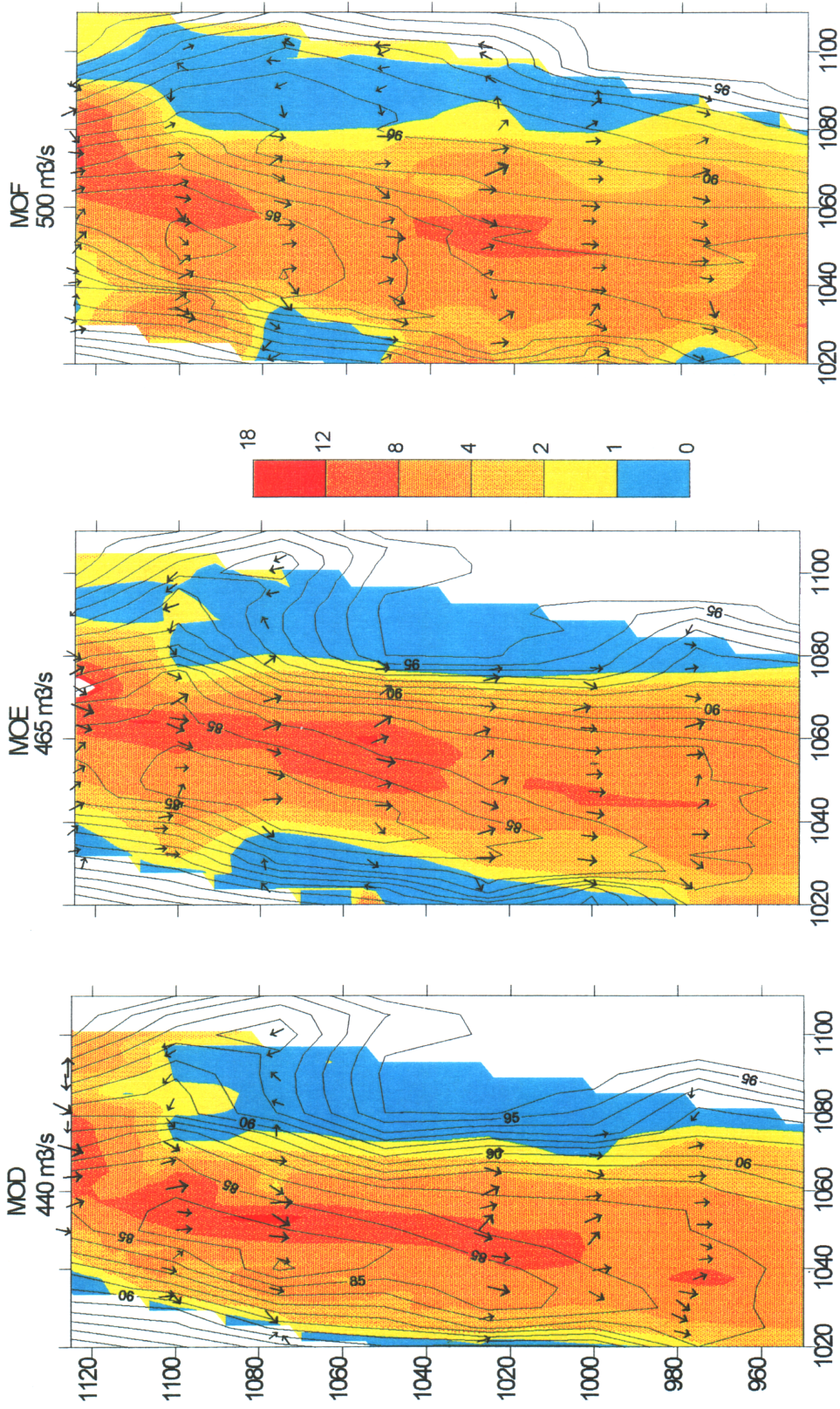


Figure 26. Maps of particle stability (color contours) and near-bed velocity vectors (scaled by magnitude) overlaid on channel topography contours (solid lines) for Mohawk surveys indicated. Particle stability values less than one show stable or depositional areas. Values greater than one are unstable or erosional.

The color contour scale is for relative particle stability, which is bed shear stress as compared to critical shear stress for d_{50} particles. Particle stability values less than one (light blue) occur where there is less than critical shear stress, and indicate zones where sand would be stable or deposition would occur. A transitional range from one to two (yellow) occurs where shear stress values are only slightly to not more than twice the critical shear stress value. Shades of orange to red are used to show zones of progressively greater shear stress. For example, a particle stability value of 12 indicates that bed shear stress is 12 times greater than the critical shear stress required to entrain sand of 0.18 mm diameter.

Velocity vectors in the x - y plane of the near-bed velocity bin were overlaid on the particle stability maps to provide an indication of the initial trajectory of a mobilized particle (assuming a planar bed). The vectors are scaled by magnitude and they also locate the positions of velocity measurement stacks along the ship's track. These maps show that highly variable hydrodynamic forces existed during surveys MOD, MOE and MOF, even though discharge varied only between 440 and 500 m^3s^{-1} .

Comparison of the particle stability pattern along the face of the eddy deposit between MOD and MOE shows that the mid-channel zone of greatest shear stress widened and shifted to the left. This resulted in a greater shear stress gradient along the eddy deposit face and shear stress values 2-8 times greater than the critical value. This pattern suggests that during MOE, sand at the toe of the eddy deposit was mobilized and the velocity vectors show that its trajectory was downstream or slightly toward the left. The particle instability along the toe of the eddy deposit caused by hydrodynamic forces is combined in MOE with an oversteepened slope which is unstable from gravitational forces (figure 23). As measured in survey MOE, the eddy deposit was at a threshold of gravitational slope failure whereas the hydrodynamic forces along the toe of the eddy bar were at a threshold of incipient sediment motion.

Following the rapid erosion event that occurred shortly after survey MOE, the eddy bar was scoured to a gentle slope of about 5 degrees and the MOF particle stability

map shows a large area conducive to sand deposition that closely defines the geomorphology of eddy bars observed in the past. Near-bed velocity vectors show that sand transported near the bed as bedload or as near-bed suspended load would be carried into the eddy zone where deposition would occur. The MOF particle stability map also predicts that an eddy return current channel would form along the extreme left bank of the channel.

Results From Hourly Surveys

Mapping and velocity profiling at hourly intervals following the rapid erosion event, documented changes in channel topography and flow patterns that occurred during hydropower flow fluctuations. Thalweg profiles (figure 27) made from four surveys during the rising limb of a typical power plant flood show that the pool was filled and subsequently scoured between hourly surveys 21A, 20A and 19A. The pool retained its maximum depth but 2-3 meters filling occurred in both the pool entry and exit slope areas.

The magnitude of pool deforming sediment changes observed at hourly time steps at Mohawk exceeded the magnitude of changes observed before and after the rapid erosion event, when a large volume of sand was scoured from the eddy. Comparing these changes to changes observed at the Moab location, the annual pattern of pool-eddy scour and fill was of the same magnitude in depth and volume as at Mohawk on hourly time scales. Flow modeling experiments for Mohawk used the magnitude of pool deformation measured during the hourly surveys to determine the effects of that magnitude of channel deformation on eddy bar stability.

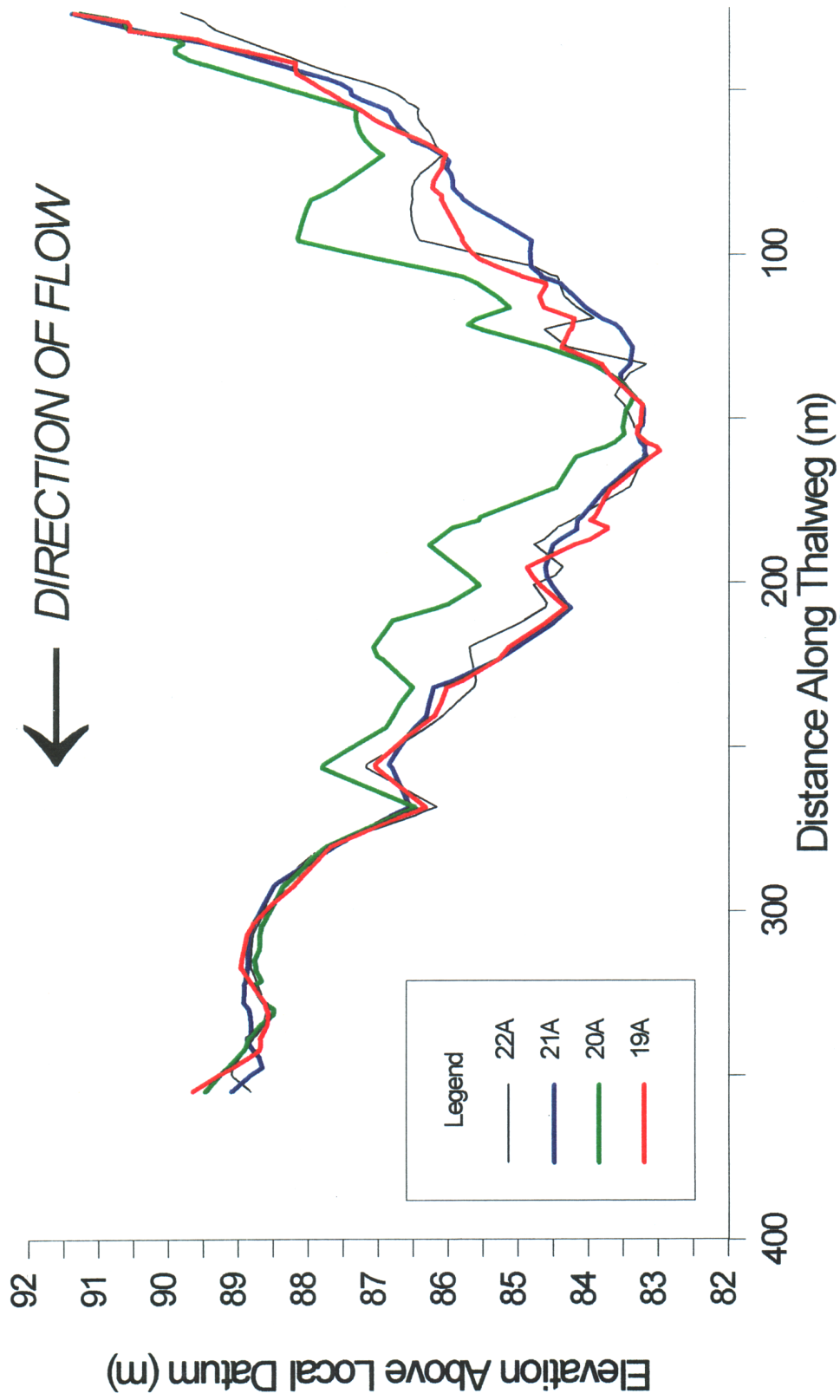


Figure 27. Thalweg profiles sliced from maps from Mohawk, for surveys shown in legend.

Modeling Results

Three series of models were set up and run to determine the effects that various patterns of channel deformation have on flow patterns, depth-averaged shear stress and sand grain stability in and near the eddy recirculation zone. The model runs simulated scour and fill patterns actually measured at the Mohawk study site for various eddy bar configurations. Discharge and outlet water-surface elevation were held constant in order to remove the effects of unsteady flow on pool-eddy hydraulics and to concentrate on the effects of observed channel deformation.

The initial condition model was first run at $465 \text{ m}^3\text{s}^{-1}$ discharge and 94.65 meters outlet elevation in order to compare the model results to field results for survey MOE. After only minor adjustment of the initial channel roughness value, the model results and field results agreed well using roughness values of $n=0.032$ for the channel, $n=0.035$ for the banks and $n=0.020$ for the sandy eddy deposit (figure 28). An isotropic eddy viscosity value of 150 Nsm^{-2} produced eddy recirculation zones in locations and with outlines in good agreement with the measured velocity field maps.

The calibrated model was then adjusted to discharge of $550 \text{ m}^3\text{s}^{-1}$ and outlet water-surface elevation of 95.4 meters. These values were selected from discharge at the time of greatest slump activity from the tilt sensor records and from a stage-discharge relationship established from the 24A hourly survey. The channel topography boundary condition was manually varied for different model runs and the model was set to automatically adjust the wetted boundary. The inflow and outlet water-surface elevation, and other model parameters, were held constant for all model runs. These experiments were designed to test the effects of relatively minor scour and fill of the pool entry and exit slopes on sand particle stability and flow fields in the eddy zone.

In the first set of runs the pool entry and exit slopes were filled (in a simple block experimental design) with the eddy deposit fully developed and intact as measured in survey MOE (table 4). The initial boundary conditions were defined by the channel topography measured in survey MOE. Fill and scour conditions used in the experiments

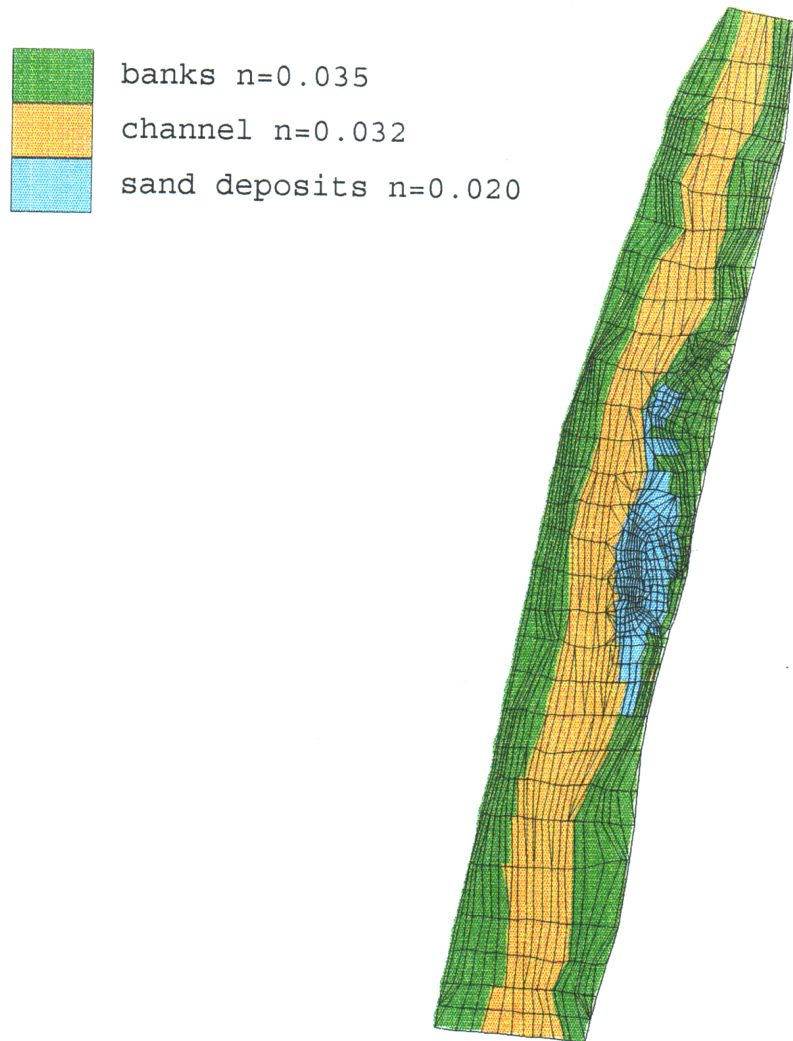


Figure 28. Layout of finite element mesh and material properties used in two-dimensional flow model.

followed conditions that were mapped at Mohawk during this investigation. When the entry slope was filled and the exit slope unchanged, stability in the eddy recirculation zone increased slightly and along the eddy bar face there was also increased stability over the baseline condition. Deposition on both the entry and exit slopes resulted in decreased stability along the eddy bar face and no change in stability pattern in the recirculating eddy zone. Deposition on the pool exit slope decreased stability along the eddy bar face in both entry slope configurations tested.

TABLE 4. Results of flow modeling experiments with fully developed eddy deposit compared to the baseline condition.

	Entry Slope as Measured in MOE	Entry Slope Filled
Exit Slope as Measured in MOE	1-Baseline condition. Figure 29	2-Increased stability along eddy bar face by 2 factors and eddy recirculation zone slightly more stable. Figure 30
Exit Slope Filled	3-Decreased stability along eddy bar face by 2 factors, no change in eddy stability pattern. Figure 31	4-Decreased stability along eddy bar face by 1-2 factors, no change in eddy stability pattern. Figure 32

The second set of runs was designed to test the hydraulic effects of slump failure on the face of the eddy deposit. This experiment consisted of multiple incremental adjustments to the eddy bar face simulating slump failure and deformation of the subaqueous sand deposit. The location and size of slumped areas was determined by examining particle stability maps at each iteration and decreasing elevations on nodes within the most unstable areas. First-hand experience with two rapid erosion events and the tilt sensor record for the rapid erosion event between surveys MOE and MOF provided additional basis for the incremental adjustments. Dimensions of the typical incremental ‘slump’ were approximately 2 meters wide, 10 meters deep and 25 meters long (500 m³).

Particle stability along the toe of the eddy bar was least in the downstream area under initial conditions (figure 29). The simulations of slope failure resulted in increased stability in the immediate area of slumping. Stability contours shifted away from the slumped areas and concentrated instability in new areas along the toe of the deposit. This resulted in a progression of simulated slump failures beginning at the downstream end of the eddy bar, switching to the upstream end of the bar and then progressing from downstream to upstream again. During all increments, flow along the eddy bar face was in the downstream direction so sand slumped from the bar would have been transported downstream.

The results of this set of experiments show that gravity-driven slope failure, initiated or accelerated by erosion of the toe of the eddy bar, can affect the local hydraulic patterns and result in additional localized slope failure. The progression of slumps followed the shifting of safety contours away from slumped areas and toward unslumped areas.

After removing approximately four meters width from the eddy bar face, the location of the safety factor one contour no longer was directly over the gravitationally unstable eddy bar toe. Consequently, stability of the eddy bar face was increased by the simulated slumping and erosion of four meters width. With all other hydraulic and boundary conditions held constant, the model predicts that the eddy bar would undergo no further erosion. At this point the first experiment was repeated to determine the effects of scour and fill of the pool entry and exit slopes on partially eroded eddy bar stability (table 5).

Filling the pool exit slope increased stability of the eddy bar face. Filling of the pool entry and exit slopes resulted in the formation of a long recirculating flow cell that extended along the length of the eddy bar face. The recirculation cell pushed the safety factor contours toward the channel and away from the eddy bar, substantially increasing the stability of the eddy bar. This result is opposite from results for the filled eddy configuration described above. However, by raising the exit slope approximately two

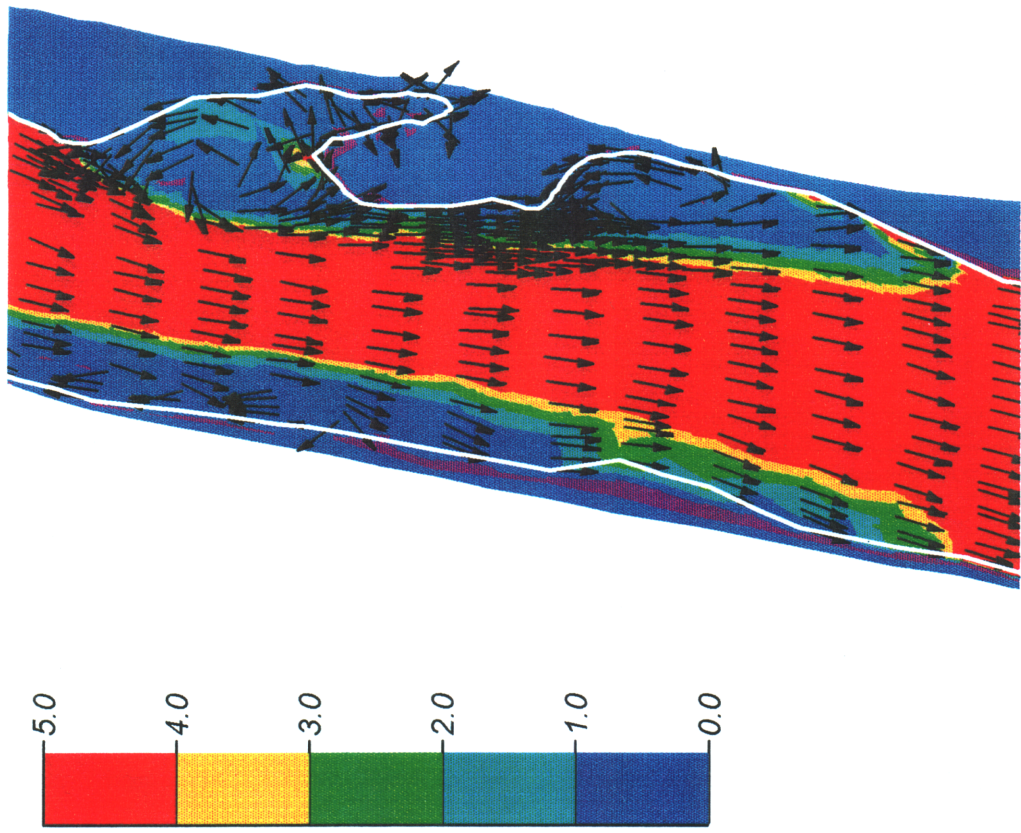


Figure 29. Particle stability and flow vector plot for initial condition of experiments listed in table 4. White lines show location of wetted boundary and information outside the boundaries should be ignored.

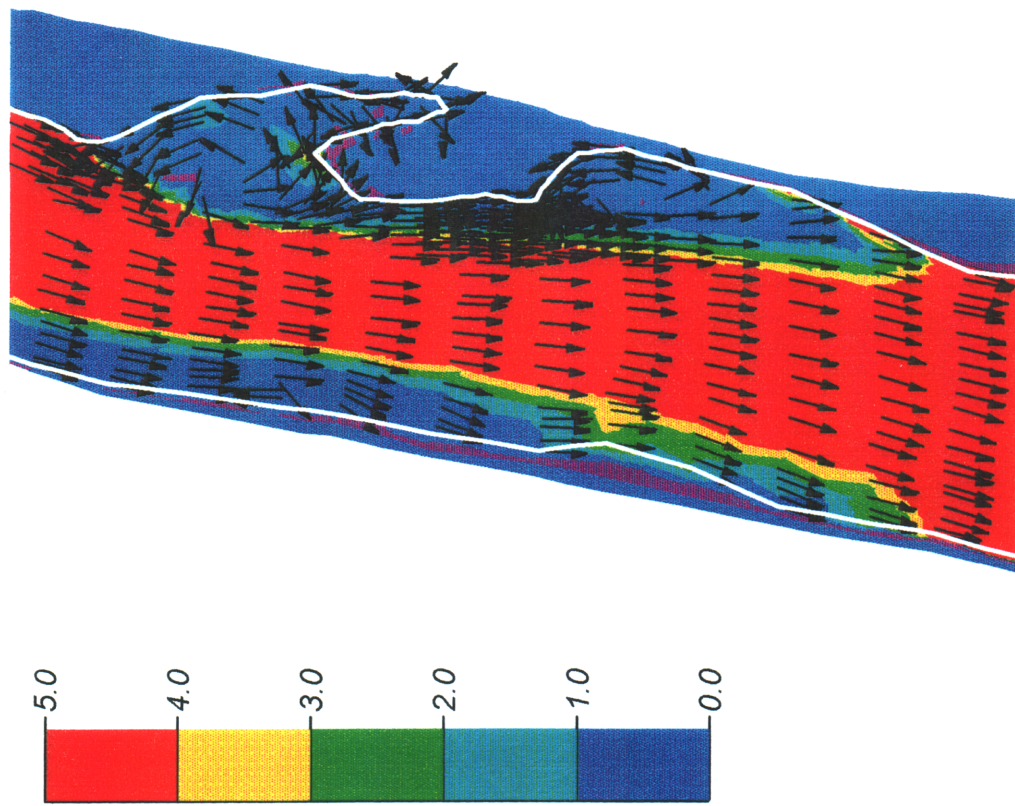


Figure 30. Particle stability and flow vector plot for entry slope filled condition of experiments listed in table 4. White lines show location of wetted boundary and information outside the boundaries should be ignored.

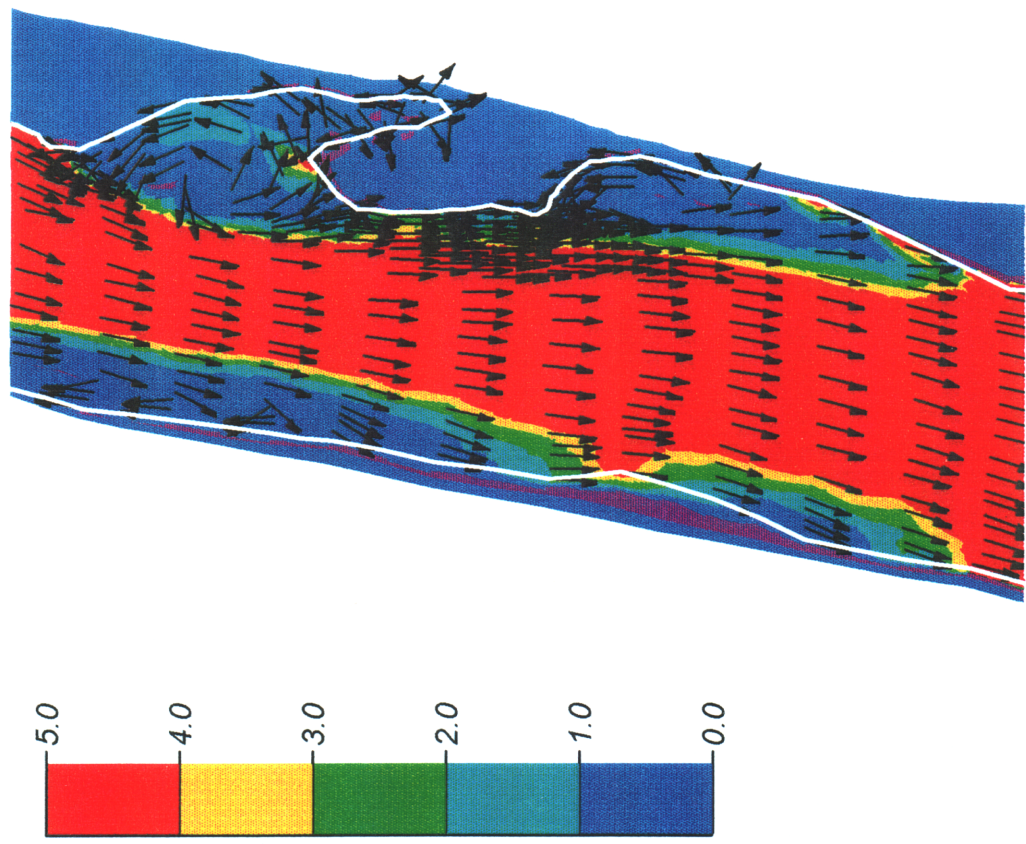


Figure 31. Particle stability and flow vector plot for exit slope filled condition of experiments listed in table 4. White lines show location of wetted boundary and information outside the boundaries should be ignored.

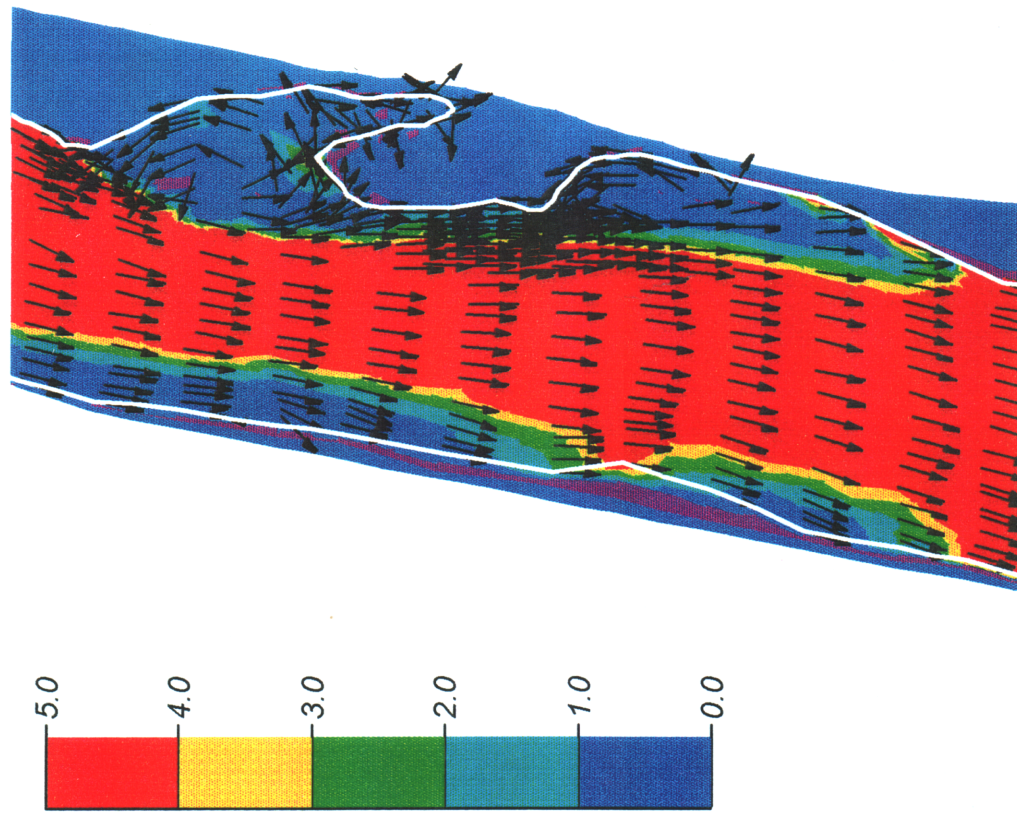


Figure 32. Particle stability and flow vector plot for entry and exit slopes filled condition of experiments listed in table 4. White lines show location of wetted boundary and information outside the boundaries should be ignored.

meters over the maximum configuration measured, instability returned along the face of the eddy bar.

TABLE 5. Results of flow modeling experiments with the eddy deposit partially eroded.

	Entry Slope as Measured in MOE	Entry Slope Filled
Exit Slope as Measured in MOE	1-Initial condition: downstream flow along bar face, face in equilibrium with tractive forces, small unstable areas on bar point and along left bank. Figure 33	
Exit Slope Filled	2-Downstream flow along bar face. Areas of instability in eddy along left bank and point of bar. Recirculating flow cell formed on right bank. Figure 34	3-Recirculating flow cell formed along length of eddy bar face, doubling width of stable area. Eddy stable except for small area on point. Figure 35

This experiment was taken to its logical conclusion, a completely eroded eddy bar, by continuing the process of decreasing elevations of nodes in unstable areas. The exit slope was incrementally raised to a maximum condition that was two meters higher than the configuration measured in survey 20A. Incrementally elevating the pool exit slope maintained unstable conditions along the eddy bar face. The unstable pattern persisted as the eddy bar was completely eroded by increments.

The model was then adjusted to the topographic condition measured in survey MOF. In the final configuration the eddy recirculation zone was a large stable zone from the reattachment point extending upstream to the debris fan. The eddy included an unstable area along the left bank predicting the location where return current flow channels typically form. This pattern is a good match to the particle stability pattern from measured conditions in survey MOF.

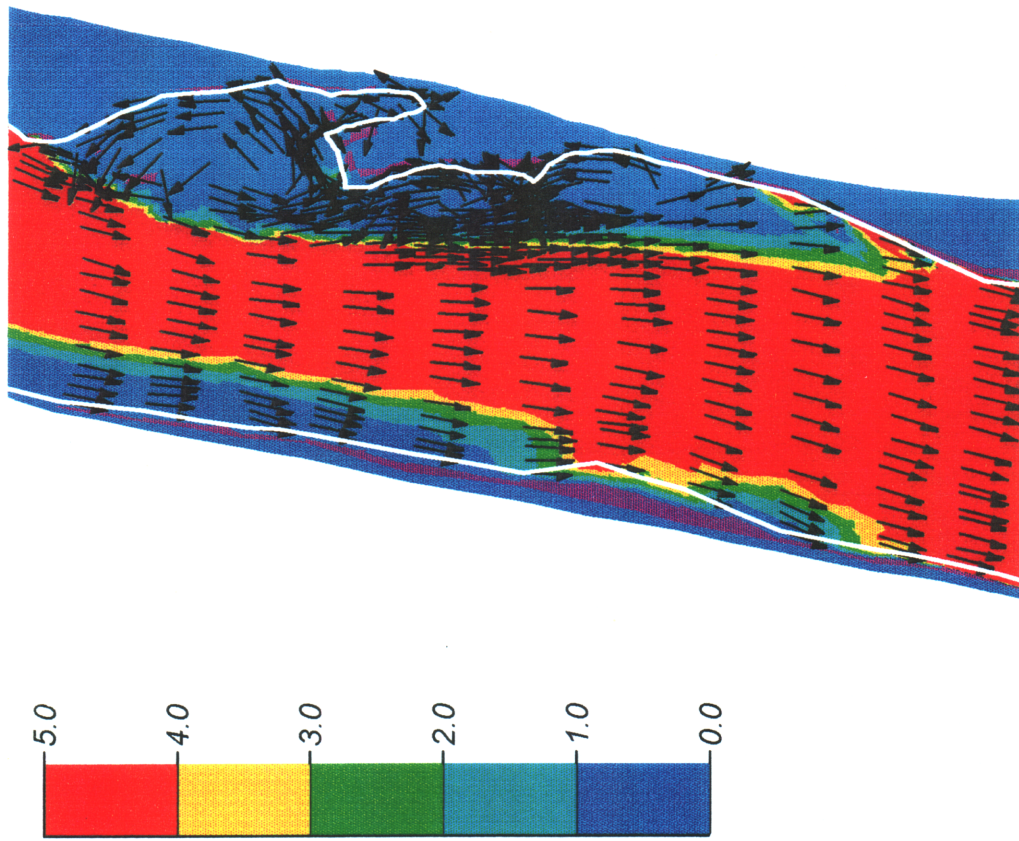


Figure 33. Particle stability and flow vector plot for initial condition of experiments listed in table 5. White lines show location of wetted boundary and information outside the boundaries should be ignored.

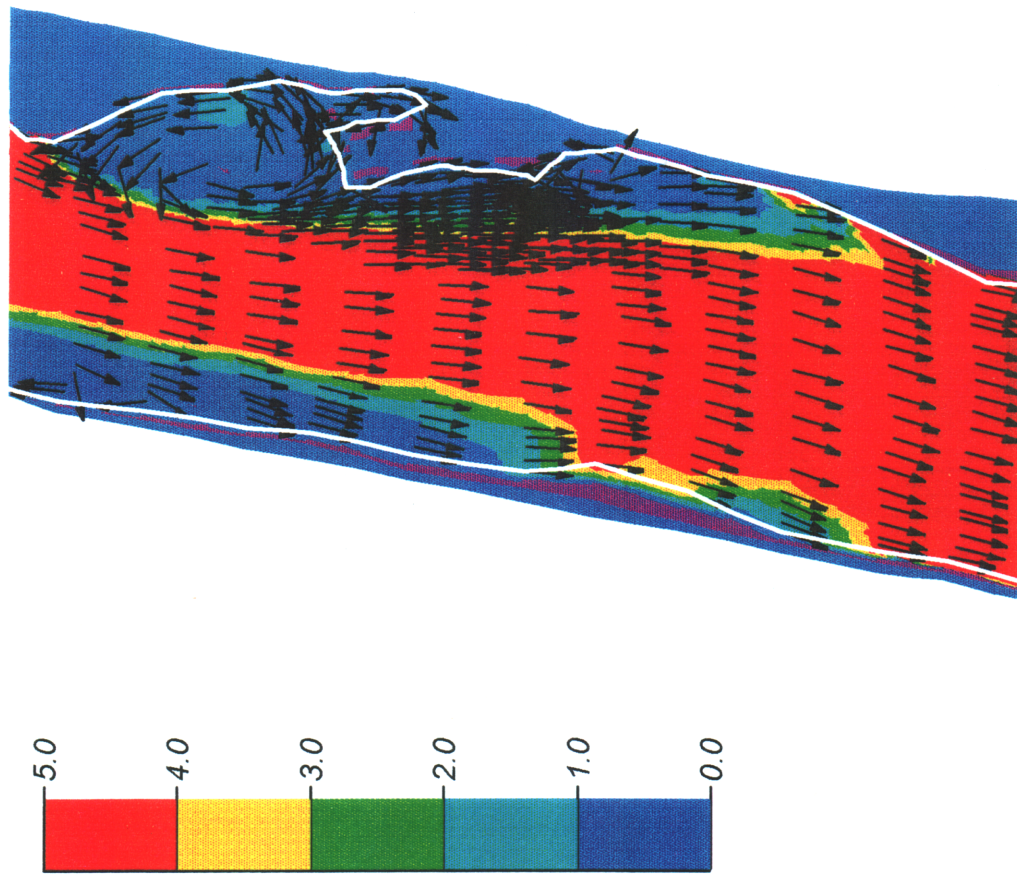


Figure 34. Particle stability and flow vector plot for exit slope filled condition of experiments listed in table 5. White lines show location of wetted boundary and information outside the boundaries should be ignored.

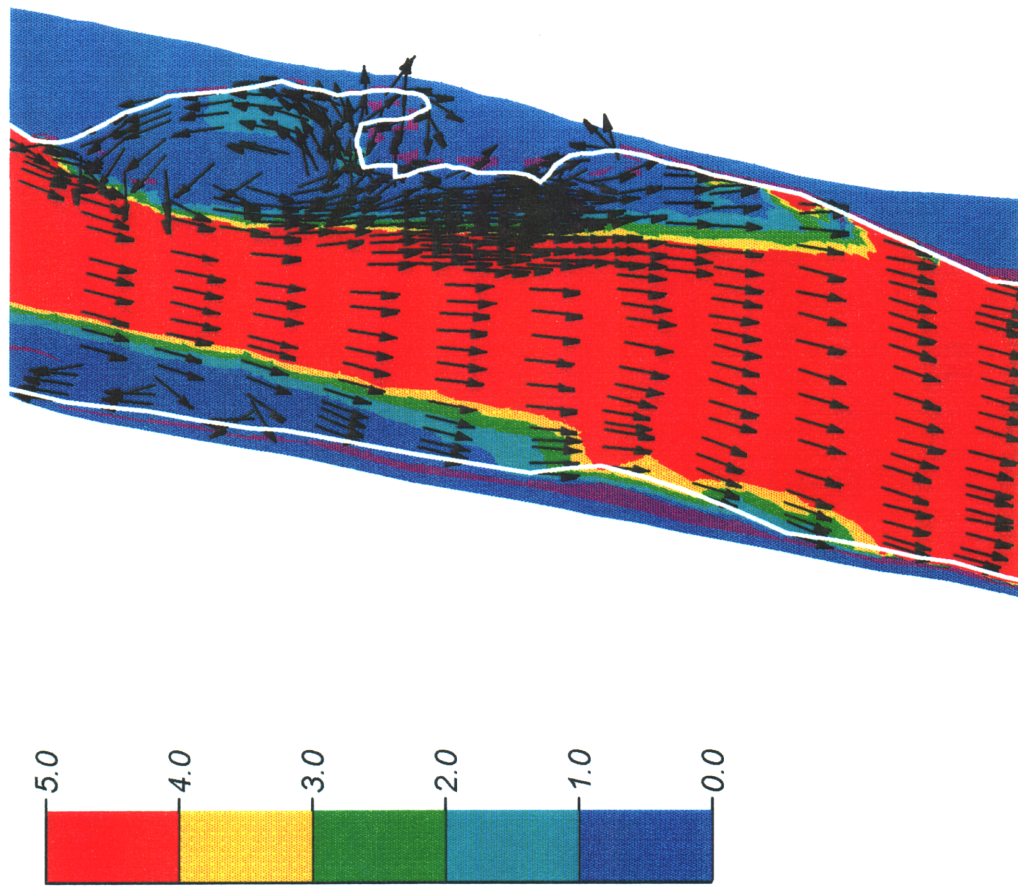


Figure 35. Particle stability and flow vector plot for entry and exit slopes filled condition of experiments listed in table 5. White lines show location of wetted boundary and information outside the boundaries should be ignored.

A fourth set of model runs tested the effects of various entry and exit slope configurations on particle stability and flow field patterns in the completely scoured eddy recirculation zone, as measured in survey MOF a few hours after rapid erosion of the eddy deposit. The effects of deformation of the entry and exit slopes were tested using a simple block experimental design as in the previous sets of model runs. The results are listed in table 6.

TABLE 6. Results of flow modeling experiments with the eddy bar completely eroded.

	Entry Slope Filled	Entry Slope Scoured (as measured in MOF)
Exit Slope Filled (as measured in MOF)	2-Predicts return current channel forms along left bank of large depositional eddy. Figure 37	1-Predicts unstable (factor 1) return current channel forms along left bank of large depositional eddy. Recirculating flow cell on right bank. Figure 36
Exit Slope Scoured	3-Enlarged and intensified unstable (factor 2) return current zone along left bank of eddy. Figure 38	4-Enlarged and intensified (factor 1-2) unstable return current zone along right bank of eddy. Recirculating flow cell on right bank. Figure 39

Scour of the pool entry slope resulted in development of a recirculating flow cell on the right bank opposite the channel constriction. Formation of this opposing flow cell resulted in increased flow velocities in the thalweg and in the main eddy, and the formation of an unstable zone along the left bank. This pattern predicts the formation of the return current flow channel that is a hydraulic feature of eddies and a geomorphic feature of eddy deposits. In this set of experiments, the eddy was more conducive to deposition when the pool exit slope was filled.

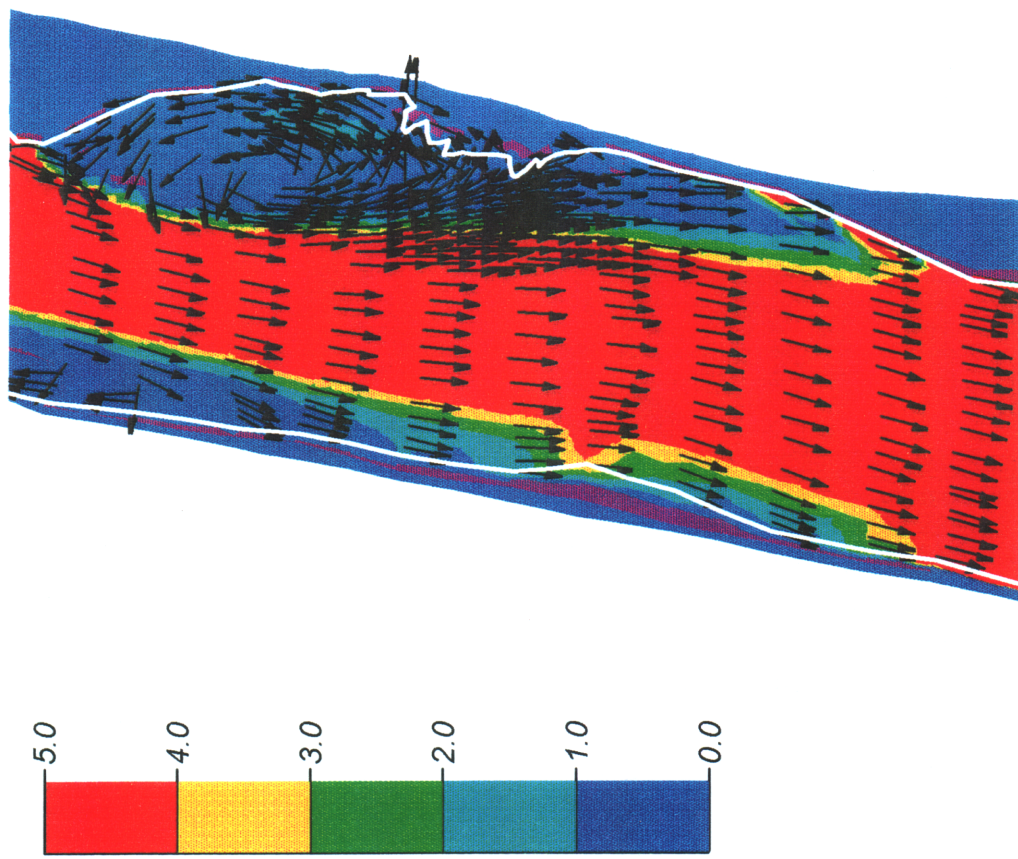


Figure 36. Particle stability and flow vector plot for exit slope filled and entry slope scoured condition of experiments listed in table 6. White lines show location of wetted boundary and information outside the boundaries should be ignored.

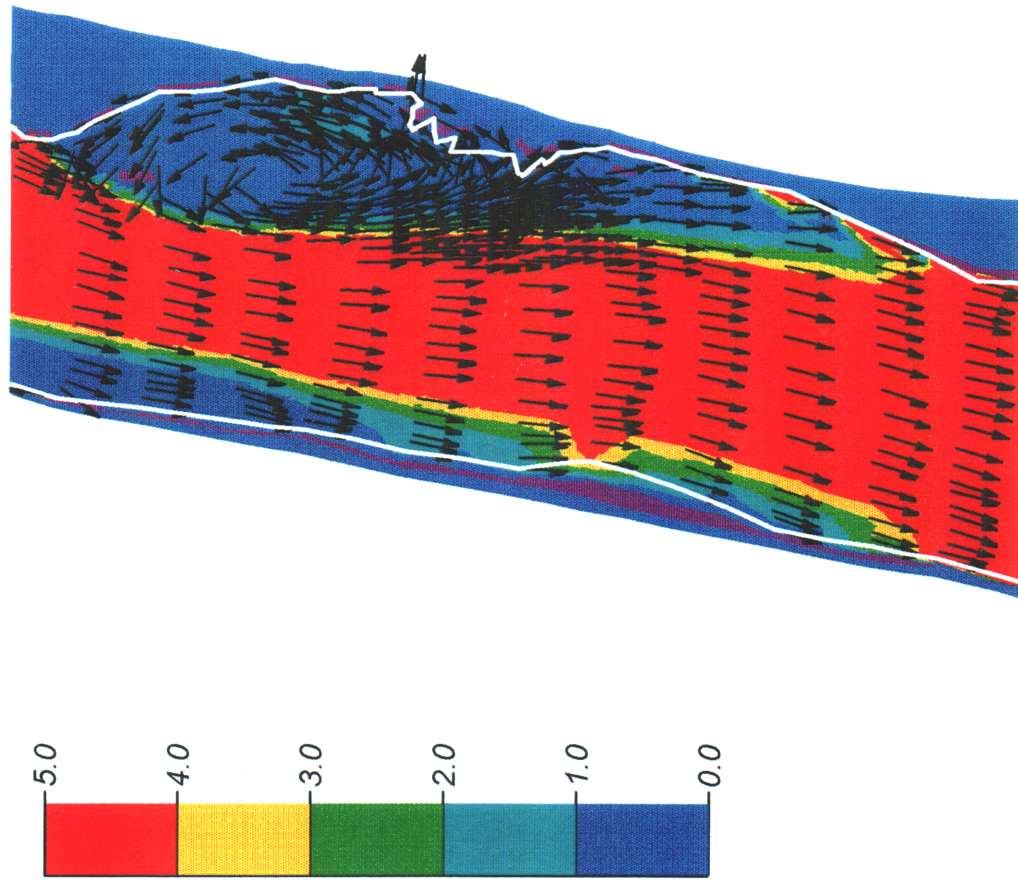


Figure 37. Particle stability and flow vector plot for entry and exit slopes filled condition of experiments listed in table 6. White lines show location of wetted boundary and information outside the boundaries should be ignored.

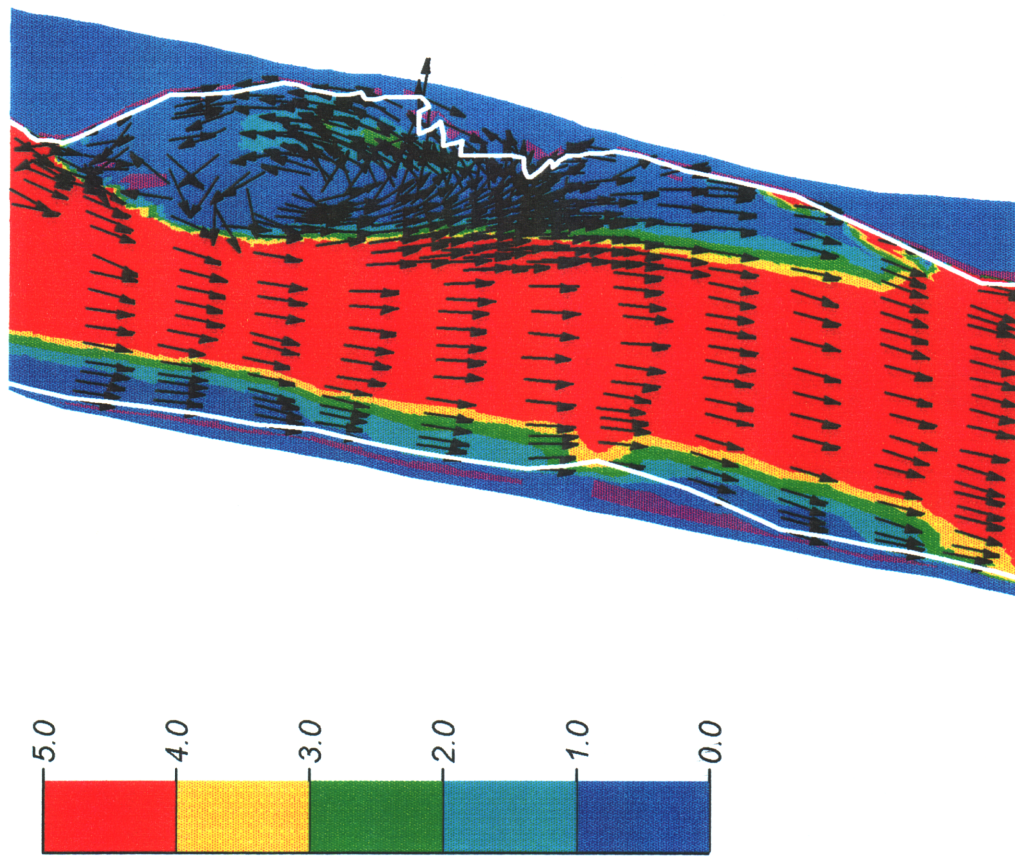


Figure 38. Particle stability and flow vector plot for entry slope filled and exit slope scoured condition of experiments listed in table 6. White lines show location of wetted boundary and information outside the boundaries should be ignored.

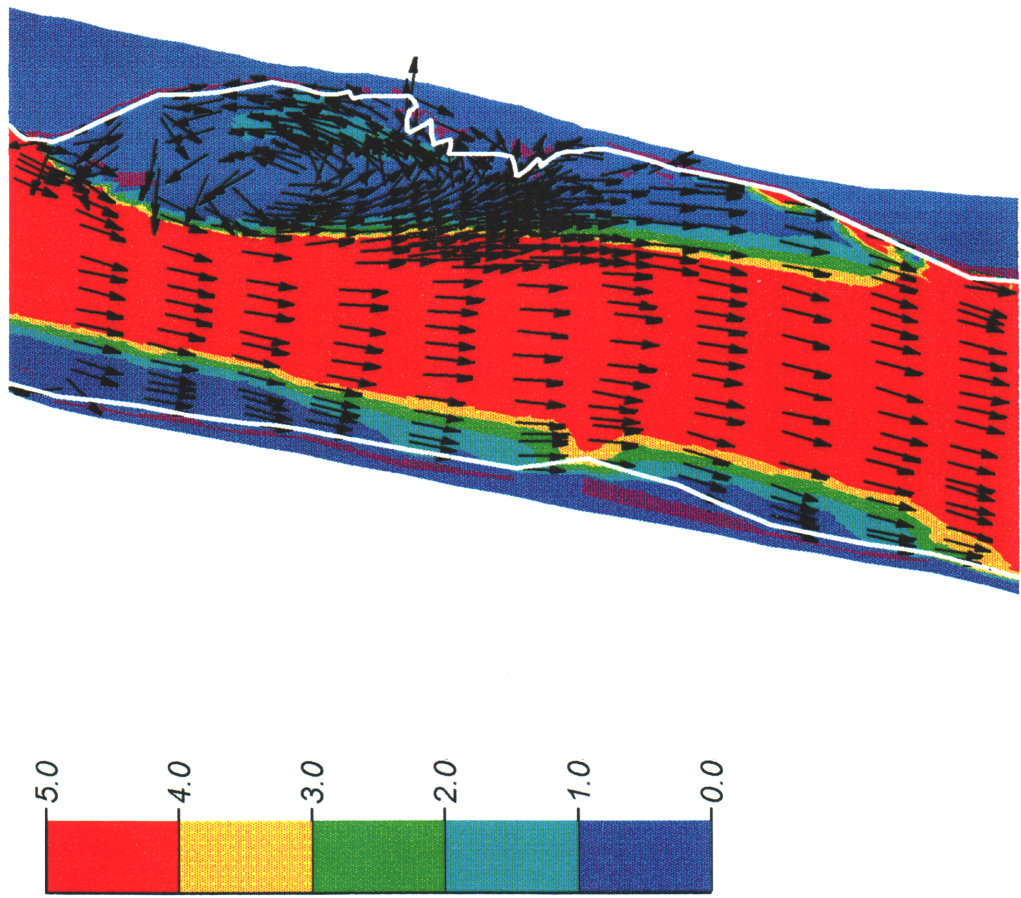


Figure 39. Particle stability and flow vector plot for entry and exit slopes scoured condition of experiments listed in table 6. White lines show location of wetted boundary and information outside the boundaries should be ignored.

DISCUSSION

Unregulated River Moab Reach

Field investigation of the unregulated river channel and sand deposits documented an annual progression of pool deformation culminating with erosion of the eddy bar during the rising limb of floods. The time-scale of change in the natural river setting was conducive to measurement of the progression with relatively simple equipment and techniques.

The Moab pool slowly scoured and elongated in the upstream direction between the period of 1993 flood recession and winter low flow. Throughout the winter low flow season the pool was relatively static. During the rising limb of the 1994 flood (1-2 year recurrence) the pool was slightly deepened and substantially shortened by deposition on the pool exit slope. The eddy bar was completely eroded as the flood continued to rise, and when the flood receded a new eddy bar emerged. During the receding limb of the flood, the pool entry slope was filled and the exit slope scoured. The channel profile strongly resembled the profile measured the prior summer following the previous year's flood. The eddy bar was stable throughout the 1994-1995 low flow season until the next annual flood when the eddy bar was again eroded. However, a new eddy bar did not emerge as the 1995 flood receded.

So what processes might explain the vast differences between the results of the 1993, 1994 and 1995 floods? Several possible reasons for the different responses of the sand bar are discussed in the following section.

The 1993 and 1995 peak magnitudes were very similar, $1,397$ and $1,456 \text{ m}^3\text{s}^{-1}$, respectively. This corresponds to a stage height difference of only 0.12 meters at the

Cisco gage, which would be less in the MP26 area where the channel is much less confined and very similar in slope. The debris fan is broad and low angle and is completely overtopped by discharges of $340 \text{ m}^3\text{s}^{-1}$. Daily photographs show that a recirculation zone existed throughout the flood flow of 1993, including during the peak discharge. Less frequent photos in 1995 also show a large and well developed recirculation zone at high discharges. These observations suggest that overtopping of the debris fan by high flows did not destroy the eddy recirculation zone. Consequently, recirculating flow existed throughout the range of discharges observed, so the slight differences between the peak discharges of 1993 and 1995 do not seem capable of producing such differing results. The 1995 peak discharge was not significantly greater than the 1993 peak but the duration was considerably longer. Flow volumes were 6.0×10^9 to 6.8×10^9 cubic meters for 1993 and 1995, respectively (calculated as cumulative flow greater than $227 \text{ m}^3\text{s}^{-1}$).

Another factor that may explain the different results is the duration of discharge over some specific value greater than the discharge at which the eddy deposit formed previously. The 1994 flood flow reached a peak value of approximately $425 \text{ m}^3\text{s}^{-1}$ and in 1995 the eddy bar was inundated at discharges around $340 \text{ m}^3\text{s}^{-1}$. Discharge of $567 \text{ m}^3\text{s}^{-1}$ was used for comparing flood durations. During the 1993 flood, discharge exceeded $567 \text{ m}^3\text{s}^{-1}$ for 48 days and for 71 days in 1995, an increase of 67%. The volume and duration differences between the 1993 and 1995 floods might explain the different bar responses through the dynamic balance between sediment supply and sediment transport.

This reach is essentially gravel bedded with sand as bedforms, patches of sand among the gravel on the channel bottom, and sand in temporary storage as sand bars along the channel margins. The prolonged flood duration in 1995 may have resulted in local depletion of the sand supply before flood recession. The 1993 flood built a large eddy bar and the 1994 flood was small by comparison to the 1993 and 1995 floods. Therefore sand should have remained abundant in the local reach following the 1994 flood. Sand storage may have actually increased beyond average conditions following the 1994 flood because the 1995 flood was one month later than normal and spring 1995 was wetter than average. Because of the longer flow duration of the 1995 flood, there was a

prolonged time period for deposition to occur in the eddy, and the bar should have become large before sediment depletion occurred in the channel. Also, if the local sand supply depletion theory was correct, adjacent eddy bars should record similar responses. An inventory of sand deposits in flow separation zones along the reach indicated that other deposits that existed in 1993 and 1994 still existed in 1995. They consisted of bare sand, were fully connected to adjacent reattachment bars, and appeared to have been reworked (emergent vegetation was scoured) and re-deposited at higher elevations by the 1995 flood. This line of reasoning leads to the conclusion that depletion of the local sediment supply is probably not the cause of failed eddy bar deposition at MP26 in 1995.

Other differences between the 1993 and 1995 floods were the timing. The initial rises from base flow to $227 \text{ m}^3\text{s}^{-1}$ were on March 27, 1993 and on April 29, 1995. Flow recession below $227 \text{ m}^3\text{s}^{-1}$ was on July 22, 1993 and August 17, 1995. Peak flood discharges were reached on May 18, 1993 and on June 19, 1995. Essentially, the 1995 flood was one month later than the 1993 flood. Might the timing have an effect on sediment supply? The tributaries supplying sediment to the river are formed in highly erodable, sparsely vegetated badlands between Grand Junction, Colorado and Green River, Utah. Such terrains are characterized by low annual precipitation and flash floods that occur most often in the summer months as a result of thunderstorms. That is when sediment would be delivered to the main channel. Because the 1995 flood was one month later than the 1993 flood, it is not likely that there was less sediment supply in the river channel.

Another aspect of the 1995 flood flow was two secondary peaks of approximately $1,133 \text{ m}^3\text{s}^{-1}$ following intermediate troughs of slightly less than $963 \text{ m}^3\text{s}^{-1}$ (figure 40). The scour of eddy deposits occurred during increasing discharge at MP26 during the 1993, 1994 and 1995 annual floods.

It has also been documented multiple times in the regulated Grand Canyon reach that eddy bars were scoured on the rising limb of daily fluctuating flows (Carpenter et al., 1991; Cluer, 1991; Cluer et al., 1993; Cluer and Dexter, 1994). I speculate that the reason the 1995 flood passage left the MP26 eddy stripped was either a diminished

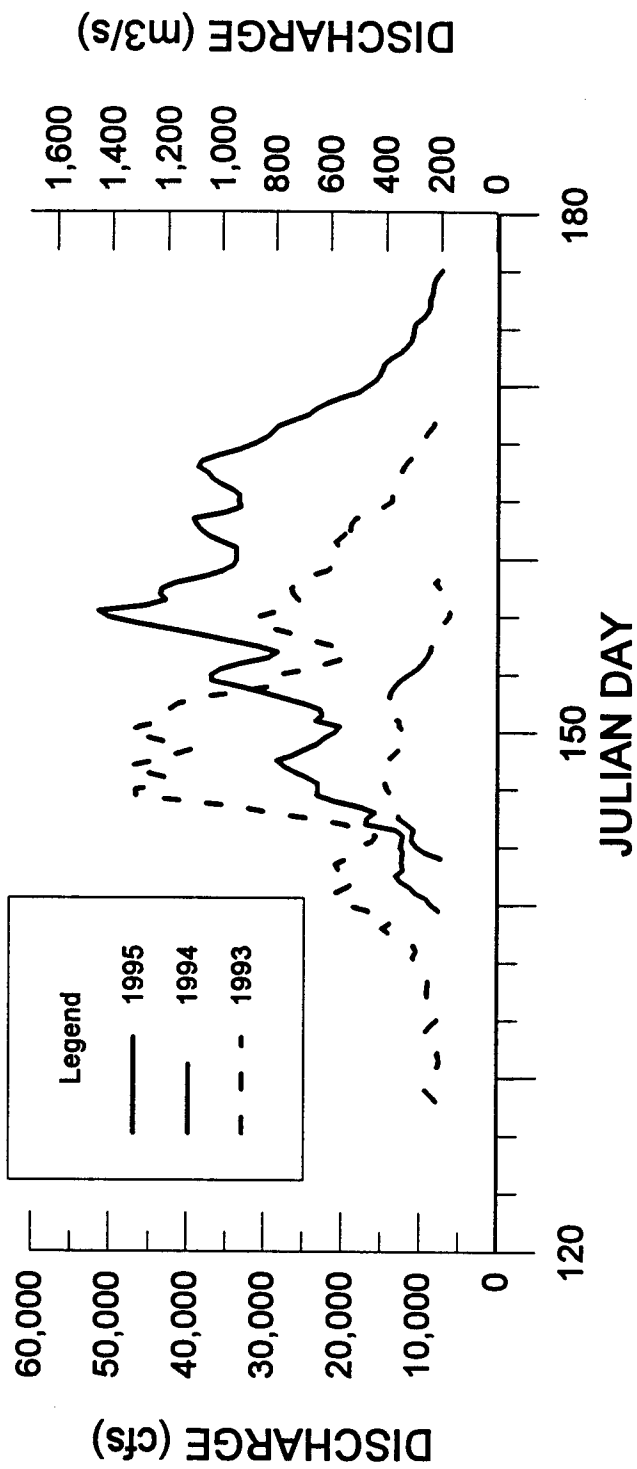


Figure 40. Hydrographs for the 1993-1995 floods for flows greater than $227 \text{ m}^3 \text{ s}^{-1}$.

sediment supply or a second stage of eddy bar scour, probably following eddy bar formation, caused by brief pool deformation from variation in sediment delivery associated with secondary flow peaks. These possibilities could be addressed if sediment transport measurements had not been discontinued in 1984 at the nearby Cisco gage, or earlier at the Dolores River near Cisco gage in 1964.

Regulated Mohawk Reach

Although the Moab sand bar underwent a seemingly anomalous pattern of scour that was not followed by deposition of a new eddy bar, similar sand bar erosion/deposition processes were observed in Grand Canyon during the 1996 habitat-building test flood (Ned Andrews, Dave Rubin, Jon Nelson and Julia Graf, personal communication July 25, 1996; Mike Carpenter, written communication July 1, 1996; Carpenter, 1996). These investigators observed that some sand deposits underwent rapid erosion during steady discharge, so unsteady sediment delivery might explain the phenomena.

Following the rapid scour of the Mohawk eddy bar, the sand that remained in the study reach 8-10 hours after the event was located on the pool exit slope. The sand lens was evident on the echosounder charts by the dune patterns on its surface. Of the approximately 11,500 m³ of sand scoured from the eddy bar, only 5,000 m³ still existed in the immediate area 8-10 hours after the scour event. The location of the sand lens was in the main channel and subject to downstream flow. The downstream flow field prevented any of the sand from returning to the eddy by recirculating flow. Eight days after the scour event, the sand lens was undetectable during the bathymetric survey MOO. During the period between scour of the eddy bar and the last survey (MOO), a new eddy bar was forming. The sand forming this bar must have been transported into the eddy from upstream sources.

The Causes of Rapid Sand Bar Erosion

Results from field measurements indicated, and modeling verified, that relatively minor deformation of pool geometry can result in wholesale erosion of eddy bars. The basic cause and effect relationship is that sand bars exist in zones of flow convergence adjacent to scour pools and upstream from areas of flow divergence that are created by riffles downstream. The zone of flow divergence is controlled by the location and geometry of the riffle and pool exit slope and modification to the channel in this area effects the location of flow divergence. Deposition on the pool exit slope results in upstream migration of the zone of flow divergence into the area where sand bars were previously in a convergence zone. Because this process occurs simultaneously with the downstream migration of the divergence zone due to increased discharge, there is a conflict between processes and the result is increased energy transfer to the eddy recirculation zone.

It is easy to see how pool filling on the rising limb of annual flood flows could be caused by non-linear variation in sediment load. In dryland rivers, such as occur throughout the arid western United States, sediment transport takes on a characteristic loop pattern known as a hysteresis loop. The sediment hysteresis loop shows that variation in sediment concentration for a given discharge can be an order of magnitude greater, or more, during the rising limb of flow than during the falling limb. This pattern is displayed in sediment records from the unregulated Colorado River at Cisco (figure 41), the Green River near Jensen, Utah; the Yampa River near Maybell, Colorado; the San Juan River near Bluff, Utah and others in the upper Colorado River basin.

A hysteresis pattern was also found in sediment records from the Colorado River near Grand Canyon gage (Phantom Ranch) for pre-dam periods. Extreme scour and fill behavior at the Grand Canyon gage was documented by Leopold and Maddock (1953) and by Leopold et al. (1964). Because the pattern at Grand Canyon gage was fill on the rising limb followed by scour during the peak, Leopold (1969) and Howard and Dolan (1981) debated the causes of scour and fill at the Grand Canyon and Lees Ferry gages. Howard and Dolan (1981) concluded that rising stage fill resulted partly from the location

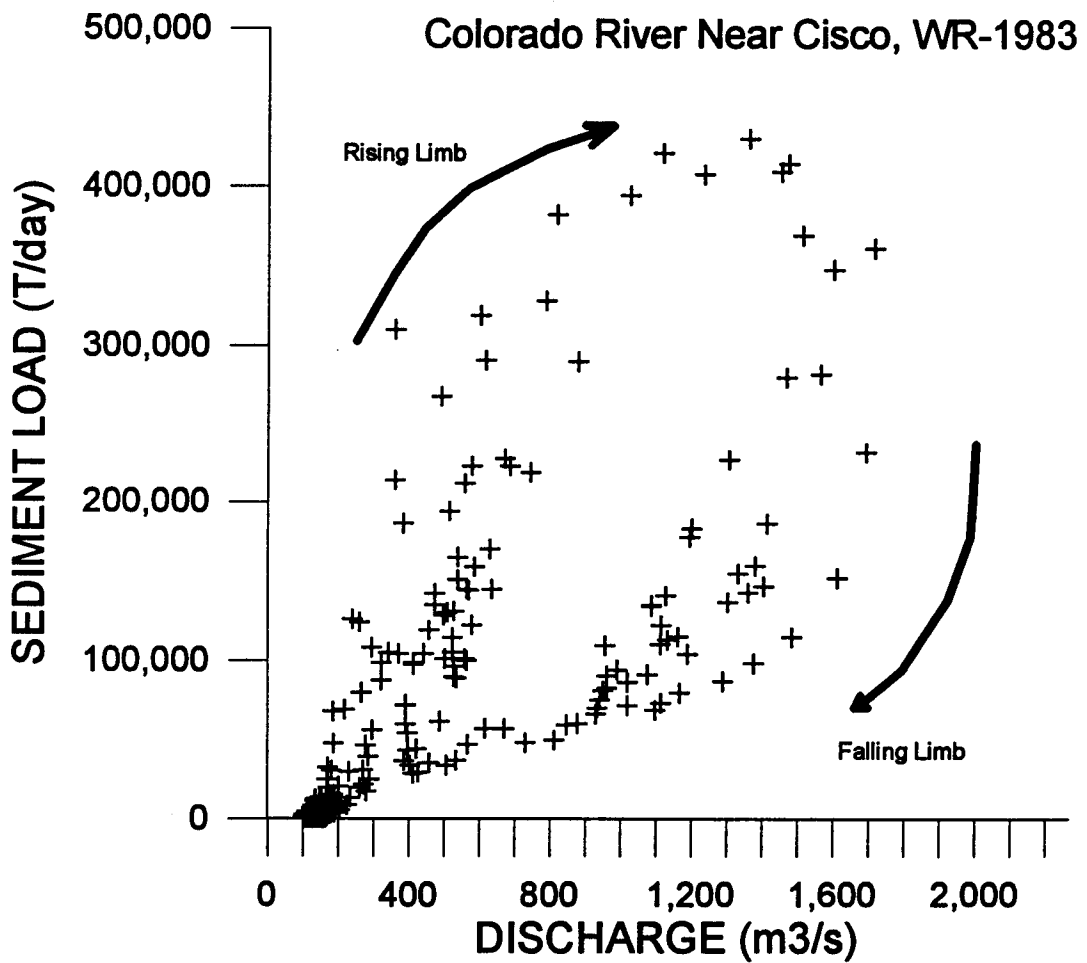


Figure 41. Sediment rating curve showing pronounced hysteresis for the 1983 flow, Colorado River near Cisco, UT.

of the gaging station near the downstream end of the pool, a location where temporary aggradation might occur in response to increased sediment load. Leopold (1994) used the Grand Canyon scour and fill example to illustrate the large variation of sediment load carried by the river during a flood passage. In pre-dam floods the sediment load was an order of magnitude greater on the rising limb than on the falling limb, for equivalent discharges. Sediment transport hysteresis is apparently capable of causing rising limb pool deformation but the question remains, is there significant sediment supply variation for hysteresis to occur on shorter time scales such as daily hydropower floods?

I am not aware of any data from high frequency sediment sampling that might directly answer this question of unsteady sediment load during powerplant flow fluctuations. Christiansen (1993) reported sediment measurements from a 1991 fluctuating flow period at National Canyon (river mile 163) but the measurements were made at the peak ($710 \text{ m}^3\text{s}^{-1}$) and trough ($280 \text{ m}^3\text{s}^{-1}$) of diurnal flow fluctuations. Gray and others (1991) measured low flow sediment transport under steady $312 \text{ m}^3\text{s}^{-1}$ discharge conditions at National Canyon in 1991. However, Jon Nelson (personal communication, July 1996) obtained continuous sediment concentration data during the 1996 spike flow in Grand Canyon using an optical backscatter device. He measured a significant reduction in suspended sediment concentration after two-three days of steady flow at $1,275 \text{ m}^3\text{s}^{-1}$. This still leaves open the question about sediment hysteresis during typical hydropower flow fluctuations.

The suspended sediment sampled by Christiansen (1993) at 0.15 meters above the bed was very similar in size frequency distribution and mean size ($d_{50} = 0.165 \text{ mm}$) to the sample taken from the Mohawk eddy bar ($d_{50} = 0.18 \text{ mm}$). Because this relatively fine sand size fraction is moving in near-bed suspension at flows from 280 to $710 \text{ m}^3\text{s}^{-1}$, it is likely that sediment of this size alternates between modes of transport depending upon minor variations in boundary shear stress. Dual mode transport of sand is supported at both locations by sand dunes that cover portions of the bed.

To explain the formation of short-lived pool-deforming sediment wedges during hydropower flow fluctuations, there has to exist in sufficient quantity, sediment of caliber

that is in transition between transport as bedload and transport as suspended load as flow fluctuates during powerplant releases, immediately upstream from a plunge pool. Christiansen's (1993) work shows that sand of slightly smaller size class than sand that makes up the Mohawk eddy bar is transported in near-bed suspension marginally above the incipient motion threshold. This suggests that larger caliber sand or reduced discharge would result in bedload as the predominant transport mode.

Results from the Mohawk investigation suggest that the effects of hysteresis do occur during normal power plant flow fluctuations. On August 31, 1993, as discharge increased from 430 to 500 m^3s^{-1} in one hour, sediment wedges were measured on the pool entry and exit slopes. One hour later, as discharge continued to increase to 530 m^3s^{-1} , the wedges had disappeared and the pool geometry was nearly indistinguishable from the geometry two hours before.

These observations lead me to hypothesize that pool deformation occurs during a narrow range of discharge where sand is mobilized upstream, perhaps in the pool above Mohawk/Gateway rapid, and transported to the study reach where it settles in the pool in response to locally reduced boundary shear stress. The sand resides briefly on the pool slopes until further discharge and shear stress increases are sufficient to re-entrain the sand and transport it out of the pool environment.

The phenomenon occurs during the rising limb of floods because there is a greater supply of sand on the channel bed than during the receding limb. This also explains the observation that most rapid erosion events occur 1-2 days after a weekend low flow or after an evaluation flow (Cluer and Dexter, 1994), which would increase the supply of sand in depositional areas of the channel and increase the delivery of sand to pools when flow next increased. Rapid erosion events have also been temporally correlated with nearby tributary flows that probably introduced a pulse of sediment to the channel, resulting in temporary pool deformation.

The discharge corresponding to formation of the pool-filling wedges was approximately 460 to 500 m^3s^{-1} . At discharge of approximately 530 m^3s^{-1} , the wedges were scoured and the pool returned to very similar geometry measured two hours prior.

The discharge range 460 to 530 m³s⁻¹ corresponds to local river stage range of approximately 11.5 to 12.5 meters during surveys 21A, 20A and 19A (figure 27). The rapid erosion event that began shortly after survey MOE was completed occurred within the range of river stage from 11.5 to 12.5 meters.

Flow converges in pools and diverges in riffles (Keller and Melhorn, 1978). Temporary formation of sediment wedges on the pool entry and exit slopes would cause increased flow convergence in the pool and a corresponding increase in divergence downstream from the pool. Increased flow divergence would be evident by upstream migration of the point of flow reattachment to the bank. Because one bank is non-deformable (the right bank at Mohawk and the left bank at Moab), and the erosion process occurred at stages well below that needed to overtop the eddy bar and create a large eddy recirculation zone, increases in flow divergence downstream from the reattachment point would result in greater velocity and correspondingly greater shear stress along the toe and face of the eddy deposit. These processes were verified by flow modeling experiments which showed increased shear stress along the toe of the eddy bar when a sediment wedge was formed on the pool exit slope.

The phenomenon of rapid erosion of sand bars occurs with the culmination of two critical conditions. The conditions are: (1) a relatively large sand deposit compared to the size of the low velocity zone in which it is deposited, and (2) non-linear sediment transport patterns that briefly modify the pool-eddy geometry. Theoretically, eddy bars attain maximum elevation with respect to river stage as a result of the critical combination of depth of flow and velocity where incipient motion of sand occurs. Once this threshold is realized, sand can no longer be deposited on the top of the bar and is simply transported across the bar, into the return current channel, and returned to the pool, where it continues downstream transport with some fraction making return trips through the recirculating eddy.

At the Moab site each year's eddy deposits had different elevations and volumes directly related to the magnitude of the previous flood flow. It has been shown that Grand Canyon eddy deposits also attain elevations and volumes directly related to flow

magnitude and adjust vertically according to seasonal and annual or operational adjustments in flow magnitude (Kaplinski et al. 1994). Schmidt and Graf (1990) reported that eddy bars accreted vertically to within 0.3 meters of maximum river stage.

As the eddy bar approaches its maximum elevation relative to the maximum river stage, and maximum volume relative to the volume of the recirculation zone, the slope of the bar facing the river increases until another limiting threshold is reached - the angle of repose. The angle of repose is the angle of internal friction ϕ , which is governed by the gradation of particle size and roundness. For well sorted and well rounded sand particles such as those that compose eddy deposits, ϕ is approximately 28 degrees for dry as well as saturated conditions. This relationship has been determined theoretically and experimentally by many investigators. Budhu and Gobin (1994) tested sand samples from Mohawk taken in 1991 using standard techniques and reported $\phi = 32$ degrees, ± 2 degrees.

The angle of the eddy bar measured during surveys prior to the rapid erosion event at Mohawk increased progressively from 26 degrees (MOD) to 34 degrees (MOE). The critical stable slope angle ϕ existed within 1-2 hours before the rapid erosion event at Mohawk. Budhu and Gobin, in a series of papers (1994, 1995a, 1995b, 1996), showed that saturated sand deposits slide or slump through Mohr-Coulomb failure and can be further destabilized during river drawdown periods by outward flowing pore-water and associated forces of lift measured by Carpenter et al. (1995). Budhu and Gobin's work predicts two important conditions; (1) slope failures most likely occur during periods of deep river drawdown when bank-stored water head and associated seepage forces reach maximum values, and (2) the seepage slope intersects the slope of the deposit at the elevation of lowest river stage.

Seepage and Mohr-Coulomb failure may provide a mechanism that initiates slope failure, but slope failure alone does not explain the observations made in this and other investigations. Rapid erosion events occur in the absence of seepage forces as documented at Moab and in the Grand Canyon under steady discharges as documented

during the beach/habitat rebuilding spike flow in 1996. Documented rapid erosion events in the Grand Canyon, including the examples used by Budhu and Gobin, occurred during increasing discharges when seepage forces would be increasing the strength of sand deposits (Iverson and Major, 1986). Also, the Mohawk eddy deposit was scoured four meters deeper than the lowest river stage elevation in July 1993. The modeling results in this investigation indicated that slumping of the eddy bar, without simultaneous deformation of the pool exit slope, would decrease shear stress along the face of the bar and would be a self limiting process. Given the contradictory evidence, seepage-induced slope failure is probably not the most important agent in wholesale erosion of eddy bars, although slope failure may provide an important triggering mechanism for rapid erosion through pool deformation.

Large eddy deposits are already in a state of impending slope failure due to the high angle ϕ of the slope facing the river. Once an eddy deposit has attained maximum dimensions and reached the critical slope ϕ , a minor perturbation in the local particle stability field would initiate slope failure. The initial slope failure, whether from internal stresses due to seepage or external stresses due to tractive forces, locally increases the eddy deposit slope. Additional slope failure would result from increased local slope angles or upturned flow paths if seepage forces exist. When the toe of a slope fails, the slope failure process translates up slope and involves ever larger volumes of sand. If the volume of sand is great enough to itself affect local flow patterns, then a chain reaction might occur which continues to deliver sand to the pool and pool exit slope, which increases the adverse effect of pool deformation. Results from flow modeling experiments suggest that deposition on the pool exit slope simultaneously with erosion of the eddy bar maintains an unstable shear stress field in the vicinity of the eroding eddy bar.

The self enhancing feedback process continues until either (1) the temporary pool modification is transported downstream, (2) the river stage overtops the eddy deposit which immediately increases recirculation area and proportionately reduces velocity along the eddy deposit face or (3) the entire eddy deposit is scoured.

Other geomorphic processes are known to behave similarly. For example, in arid climates valleys fill with alluvium through slow vertical accretion of flood plains. As deposition occurs in some channel reaches, local gradients increase and erosion ultimately occurs. Gradual deposition is punctuated by rapid erosion and the formation of gullies or arroyos (Bryan, 1927). Nanson (1986), looking at laterally confined channels in Australia, proposed a model of flood plains formed episodically by vertical accretion over long periods of time, followed by catastrophic erosion and repetition of the cycle. In this model, flood plains accrete vertically by overbank deposition to a size threshold where their dimensions begin to constrict flood flows. Once a maximum size is attained, even normal floods may scour incredible quantities of the channel margin sediments. Nanson found that erosion events were temporally and spatially discontinuous because flood plain deposits were in unique stages of development.

Eddy deposits of the Colorado River in Grand Canyon can be described by a similar model, with asymptotic vertical accretion to a maximum size which is maintained for various time periods until catastrophic erosion occurs. Vertical limits are constrained by the maximum river stage and lateral limits are constrained by the angle of internal friction and the size of the recirculating eddy. Once the maximum limits are attained, channel margin deposits exist in a tenuous state between maintenance at the maximum size and abrupt erosion, sometimes to the minimum size. The minimum size is ultimately controlled by the geometry of immobile material underlying the sand bars along the channel margins. Whereas small vertical adjustments are possible in the positive direction (deposition), eddy bars adjust in the negative vertical direction through rapid and often complete erosion, and then through deposition to a new elevation in equilibrium with the maximum stage.

One ingredient required to make eddy deposits dynamic, at any time scale, is sediment in the river channel that can be mobilized. The relative dynamic frequency (number of rapid erosion events per year) ranges from zero to ten or more in the Grand Canyon. Cluer and Dexter (1994) found that the distance from sediment supplying tributaries was a major factor in the relative dynamic frequency. Beus and Avery (1991) and Kaplinski and others (1994) also found distance downstream from the Little Colorado

River correlated to relative variability in sand bar volumes. More recently, Hoeting and others (1997) found a temporal correlation, with reasonable lag times, between flow from the Little Colorado River and increased sand bar size variance downstream. They also report a negative response of sand bars to tributary sediment input during powerplant fluctuations.

Without mobile sediment in the channel, the pool deformation effect cannot occur, and rapid scouring of eddy bars will not occur. Over a three-year period of daily photography, an eddy deposit 4.2 kilometers downstream from Lees Ferry was found to become very dynamic for periods immediately following large flows from the nearby Paria River (Cluer and Dexter, 1994), as were deposits downstream from the Little Colorado River following flood flows in 1993 (Kaplinski and others 1994; Wiele et al., 1996).

Conceptual Model

Silverston and Laursen (1976) developed a hypothetical model of scour and fill for a pool-rapid river (using the Colorado River in Grand Canyon as a prime example) which consists of short and medium length reaches at subcritical flow separated by rapids where the flow rate is supercritical. The rapids behave as hydraulic controls and flows alternate between supercritical and subcritical between respective rapid-pool sequences. A pool will eventually scour with an increase in flow and fill with a decrease in flow because the change in head on a rapid is less than the change in equilibrium depth in the pool upstream. With increased flow, initially there may be either scour or fill in the downstream pool because the supply of sediment to a pool is dependent on the conditions at the outlet of the pool upstream. As a reach scours during rising discharge this results in non-equilibrium inputs of sediment to the next reach downstream. As a result, a reach that eventually will scour may first fill, temporarily.

Silverston and Laursen's (1976) model suggests that a pool downstream from other pools may behave in an erratic manner because its sediment supply is affected by

what happens in each of the upstream pools. Because with increasing discharge, the equilibrium depth increases faster than does the head on the control, there will be scour in all pools if the flood lasts long enough. With decreasing discharge, fill is to be expected, but fill takes longer to occur than scour because the difference between sediment supply and capacity to transport sediment is much smaller. Silverston and Laursen (1976) conclude that if the hydrograph is not long enough, the scour or fill to the equilibrium condition will be interrupted, and locally the system will be out of equilibrium, and the disequilibrium will migrate through the system. The complex response of pools will be further complicated by an elaborate hydrograph.

Building upon this basic conceptual model, Jackson and Beschta (1982) developed a model explaining bed-material routing in sand and gravel bedded channels with sequences of pools and armoured riffles. They hypothesized that bedload transport occurs in two distinct phases, at distinct flow levels, and characterized by two distinct material sizes. Their Phase I bedload transport of sand-sized material concept has application in this investigation. Phase I bedload transport begins as discharge increases and mobilizes sand that previously settled out in pools, along channel edges, and behind obstructions. The sand-sized material is transported over stable riffles and transport rates may be non-uniform, resulting in local minor adjustments in pools. As discharge continues to increase, sand temporarily deposited in pools is transported out of pools and downstream.

A conceptual model based in part on the models of Silverston and Laursen (1976) and Jackson and Beschta (1982) is developed to explain episodic pool deformation and eddy bar scour with respect to the dynamics of sediment transport during powerplant flow fluctuations. The model presented integrates many of the observations made in this and other Grand Canyon sand bar investigations. The basic channel profile described previously can be idealized as follows (figure 42). The gently sloping longitudinal profile of the river is modified by debris fans which locally raise the channel and dam the river. Upstream from these dams, pools conducive to sedimentation extend for several kilometers. These pools are the main sediment storage reservoirs where sand accumulates during powerplant discharges. Downstream from debris fans the rapids have

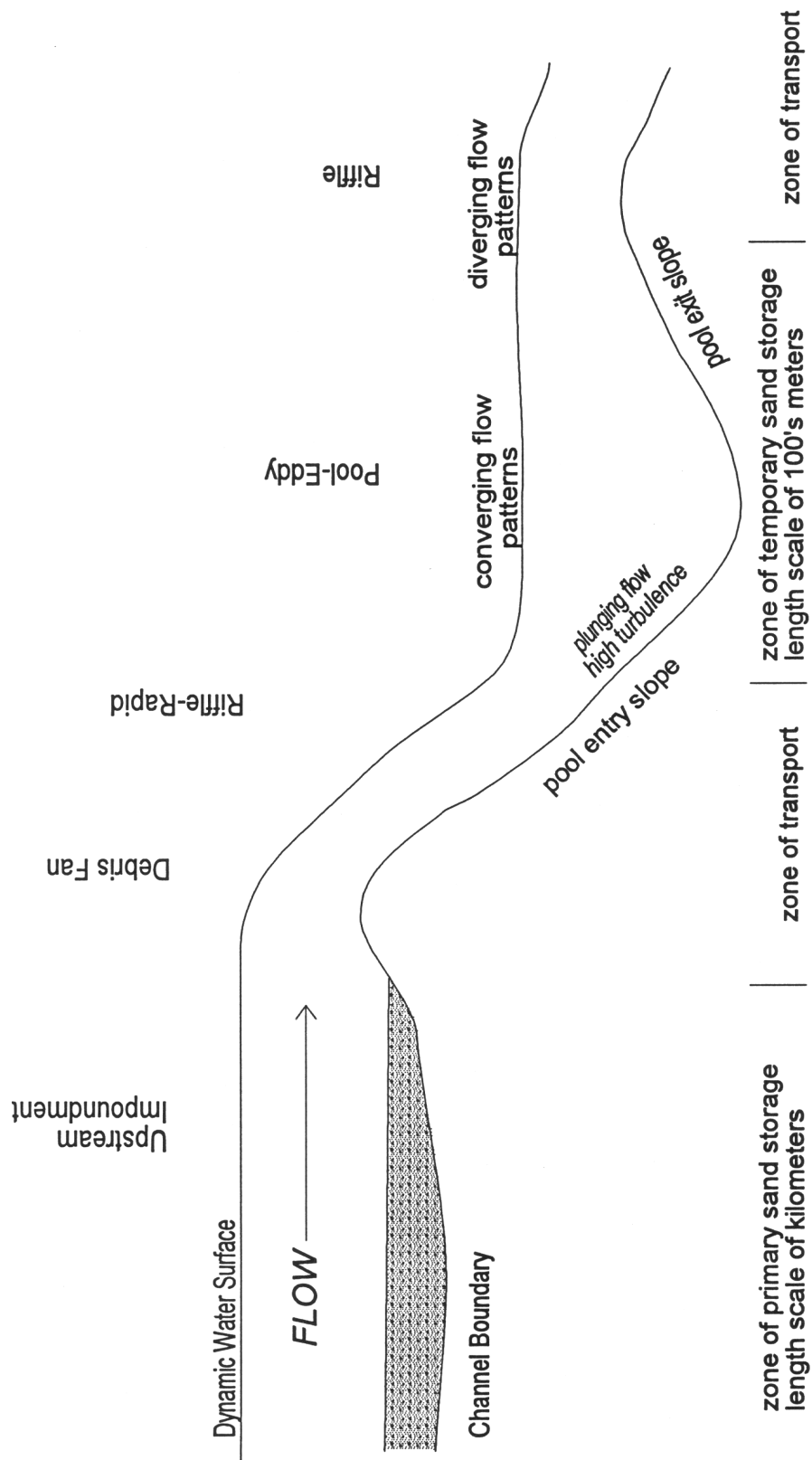


Figure 42. Explanatory river profile diagram for conceptual model of non-uniform sediment transport and episodic eddy bar scour. Sediment storage reservoir is shaded region on left.

greater capacity to transport sand than can be delivered from the pool upstream, but the plunge pools adjacent to eddy bars oscillate between transport and deposition zones depending on discharge.

During low flow, the upstream sediment storage reservoir is a trap for sand delivered from upstream and no sand is transported to the plunge pool. Consequently, even though transport capacity is also low in the plunge pool, the capacity exceeds supply and the pool is scoured. The eddy bar is stable except for minor adjustments due to collapse of the flow recirculation cell.

The sand storage was increased in the upstream storage reservoir during low flow. As flow begins to rise, transport capacity increases in the upstream sand storage reservoir coincident with the recently increased storage and a large load is delivered to the plunge pool. Transport capacity in the plunge pool is less than the supply, resulting in local storage of sand. As discharge continues to increase, the load from upstream continues but at some critical condition the capacity of the plunge pool equals the supply. Upon further increase in discharge the capacity exceeds the supply and the pool begins to scour.

During the brief period when conditions are conducive for sand storage in the plunge pool, the local flow patterns are disturbed. The eddy bar is destabilized by the local changes in flow pattern during intermediate flows that have not yet overtopped the bar, particularly if the bar is large and at a threshold of stability. If the disturbed flow patterns persist long enough, the eddy bar is completely scoured. The duration of pool deformation depends on the duration of flows in the critical range where pool deformation occurs and on the continued delivery of sand to the pool. However, once the eddy bar begins scouring, the local erosion process may deliver sand to the pool that enhances bar scouring regardless of the delivery of sand from upstream.

During peak flow, sand storage in the upstream reservoir is significantly reduced as transport capacity increases logarithmically with discharge. Sand delivery to the plunge pool is reduced and the pool is scoured, if it was not previously. As flow recedes

through the range that coincided with pool deformation on the rising limb, the plunge pool is not deformed because the sediment supply has been reduced.

The sediment reservoir is replenished during low flow and the cycle is repeated with each flow fluctuation. This series of processes and responses of the channel and eddy bars is summarized in table 7.

Interpretation For Various Reaches

The eddy bars in the 24 kilometer Glen Canyon reach downstream from the Glen Canyon Dam, due to their proximity to the Dam and downstream flood wave attenuation, have been subjected to more extreme floods and hydropower flow fluctuations than the deposits downstream. Yet they persist and are thought to be very stable. The apparent stability of the Glen Canyon eddy bars may be because they are relatively small compared to their respective eddy recirculation zones. Also, there is little if any sand-sized sediment left in the gravel-bedded reach, and no significant supplies of sediment to the reach (Pemberton, 1976). Because of a lack of pool deforming sediment available in the Glen Canyon reach, the eddy bars would be expected to remain stable under hydropower and greater flow releases from the Dam.

At the other end of the dynamic frequency spectrum are the Mohawk eddy bar and other bars in lower Grand Canyon. This reach contains comparatively large volumes of sand-sized sediment in the river channel and sand accumulation occurs during hydropower releases (Randle and Pemberton, 1987). Eddy bars in the lower Grand Canyon would be expected to be dynamic on time scales driven by dam operations that vary discharge through ranges that locally scour and fill pools. These conditions may be enhanced by weekend flows and seasonal adjustments to flow patterns.

Intermediate dynamic frequency would be expected for eddy bars in reaches where sediment supplies are intermediate or ephemeral. Sediment supply in the reach

downstream from the ephemeral Paria River is often depleted but when supplies are available, dynamic activity of pools and eddy bars will occur.

Table 7. Sequential changes in sediment transport and changes in flow during powerplant flow fluctuations for the regulated river, and during annual flood cycles for the naturally flowing river.

<p>Stage 1 Low Flow</p> <ul style="list-style-type: none"> • upstream sand storage reservoir full • minimum sand transport over debris fan 	<ul style="list-style-type: none"> • eddy pool fully scoured and stable by plunging/turbulent flows and very low sediment load (capacity > supply) • eddy bar fairly stable, minor adjustment to low flow pattern and collapse of eddy
<p>Stage 2 Initial Rising Flow</p> <ul style="list-style-type: none"> • sand transport from upstream storage reservoir at 'near capacity' • rapid transport capacity >> supply 	<ul style="list-style-type: none"> • transport capacity < supply in pool • deposition of sand wedges on eddy-pool slopes • modification of flow patterns and destabilization of eddy bar • if eddy bar is at stability threshold: scour of eddy bar increases local sand supply to pool and pool exit slope
<p>Stage 3 Continued Rising Flow</p> <ul style="list-style-type: none"> • sand transport from upstream storage reservoir at 'near capacity' • rapid transport capacity >> supply 	<ul style="list-style-type: none"> • transport capacity = or > supply in pool • scour of sand wedges, return pool to undeformed geometry • eddy becomes depositional setting • sand scoured from pool transported to next pool downstream • eddy bar rebuilding if scoured during stage 2
<p>Stage 4 Peak Flow</p> <ul style="list-style-type: none"> • upstream storage reservoir waning • supply < capacity 	<ul style="list-style-type: none"> • eddy bar enlarging if not scoured during stage 2 • eddy bar rebuilding if scoured during stage 2
<p>Stage 5 Receding Flow</p> <ul style="list-style-type: none"> • supply > capacity in upstream storage reservoir • sand reservoir begins refilling 	<ul style="list-style-type: none"> • eddy bar stable if not scoured during stage 2 • eddy continues rebuilding, at slower rate, if scoured during stage 2

CONCLUSIONS

The investigation of unregulated river eddy bars and pools resulted in understanding a progression of natural events leading up to rapid erosion of the eddy bar. The time scale of change in the natural river setting was conducive to measurement and documentation of the progression with relatively simple equipment and techniques. What was learned in the natural river setting is directly applicable to the problem investigated in the regulated river setting in Grand Canyon.

Results from the unregulated and regulated river environments document clearly that rapid erosion of sandy eddy deposits and re-deposition in repeating cycles are naturally occurring phenomena involving sand deposits in lateral flow separation zones. At Moab there was one cycle per year, corresponding to one flood per year. At Mohawk and many other locations in the Grand Canyon, there are many cycles occurring throughout a year (Cluer and Dexter, 1994). What is unnatural in the regulated river environment are the frequency and timing of rapid erosion and deposition cycles.

Annual cycles of rapid erosion and subsequent deposition of eddy bars are natural processes of dynamic equilibrium in naturally flowing incised rivers where debris fan-eddy complexes occur. The cycle is strongly linked to the annual flow cycle and is caused by variation in sediment load between the rising and falling limbs of floods. Regulated river eddy bars also eroded during the rising limb of daily hydropower floods and variation in sediment load was found in the regulated river at hourly time scales. Observations and multiple avenues of detailed investigation from both the regulated and unregulated rivers suggest that the common cause of rapid eddy bar erosion is diverging flow patterns in response to the temporary formation of sediment wedges on the pool entry and exit slopes, which is explained by hysteresis effects.

Flow modeling experiments conducted on the regulated river pool-eddy complex showed that eddy bar stability is directly influenced by minor topographic changes in the pool's entry and exit slopes. The formation of a two-meter thick wedge on the pool exit slope caused stability in the eddy bar zone to transition from quasi-stable to unstable under steady flow. Because large eddy bars exist at the threshold of slope instability, minor hydraulic pattern changes can trigger slope failure. Slope failure, combined with temporary formation of sediment wedges on the pool exit slope, ultimately leads to scour of the entire eddy bar. The scour of sand from eddy storage zones results in delivery of the sand to the main channel where it is transported downstream. New eddy bars are formed from sediment delivered from upstream.

The frequency of erosion/deposition cycles is important from a sediment storage and sediment transport perspective. The longevity and long term stability of high elevation sand deposits (important natural resources in the Grand Canyon for riparian vegetation, backwater formation, protecting archaeological sites, and for recreation) are directly related to the frequency and magnitude of erosion cycles affecting the lower elevation eddy deposits. During periods when the low elevation deposits are re-depositing following erosion events, high elevation deposits retreat. Because high discharges are required to deposit sand at high elevations, and high discharges are infrequent in the regulated river environment, minimizing erosion cycles of low elevation deposits could prolong high elevation deposits.

On the unregulated river, the long-term variability in eddy bar size was much less than the short-term variability. Sand bars are spatially persistent through time because their hydraulic controls (debris fans) are stable over long time spans, as shown by Webb (1996) through century-interval re-photography. However, the unregulated river eddy bars are completely reworked each year and return to similar size and morphology after a wide variety of flood magnitudes. Monitoring at a consistent time each year, after flood recession and before significant wind erosion, would allow detection of long term trends in sediment storage because the period of stasis is 10-11 months long. Regulated river sand bars also experience cycles of erosion and deposition, but the cycles are not

synchronized because there is not an annual hydrologic event. Furthermore, some regulated river bars undergo several cycles of erosion/deposition annually. This creates problems for sediment transport measurement, modeling and sediment storage monitoring programs.

Monitoring regulated river sand bars on a calendar schedule unknowingly includes but does not quantify the significant effects of erosion/deposition cycles. The effects are significant because the variance caused by an erosion/deposition cycle greatly exceeds the variance of long term adjustments. Quantifying the short term variance leads to different interpretations of long term information, and that information is needed to document trends caused by river management actions and dam operations. Monitoring changes in high elevation deposits (above the influence of dam operations) such as volume or event cut-bank migration may be more productive than monitoring the dynamic low elevation or high and low elevation deposits together.

Processes associated with annual erosion and deposition of large volumes of sand along the river margins may affect biological processes. For example: the sudden release of sediment to the river during the rising limb of floods may introduce rich nutrients downstream; return current channels used by juvenile fish may be rejuvenated on an annual basis, and perhaps other processes not identified yet may also be important. Wind processes during the extensive low flow season on unregulated rivers are important in forming and maintaining high elevation sand deposits. These processes are diminished along rivers that are regulated for peaking hydropower, because the sand bars are either frequently wetted or become vegetated. Return current channels, or backwaters, along the unregulated river support biological processes that have not been observed in the regulated river return current channel environment.

As floods become a valuable tool for regulated river resource management, predicting the outcome of floods is important. This is a difficult task because the result of a flood at an individual eddy depends on local variables such as sediment supply and the

dynamic hydraulics of eddy recirculation and channel geometry adjustments in response to a vacillating sediment supply-sediment transport relationship.

Summary

There were three goals in this investigation. The first was to determine if rapid erosion processes were unique to the regulated river. It was found that rapid erosion of eddy bars also occurs on naturally flowing rivers, but with return periods and timing driven by the annual flood cycle, significantly different than those observed on the regulated river which are driven by daily powerplant flow fluctuations.

The second goal was to determine if sand scoured from eddy bars during rapid erosion events was transported downstream. Repeated channel mapping and velocity field mapping showed that sand scoured from eddy bars is transported into areas of downstream flow.

The third goal was to determine what processes cause rapid erosion of eddy bars. The master hypothesis tested was that transient deformation of the pool adjacent to eddy bars results in flow pattern changes that cause eddy bar scour. This investigation found that pool deformation preceded eddy bar scour in the natural and regulated river settings. Flow modeling experiments showed that eddy bar stability is sensitive minor changes in pool geometry.

Recommended Improvements

The results of this investigation could be verified by repeating the field measurements or by conducting physical model experiments with different discharge and sediment delivery rates. One of the greatest limitations of the investigation was the absence of sediment transport data. Therefore, it is recommended that future studies of this nature attempt to obtain sediment transport measurements. The broad-band acoustic Doppler current profiler may contribute sediment data in the near future as the developers

learn to quantify the energy backscattered from suspended sediment. Also, recent advances in echosounder technology have resulted in discrimination of rocks versus sand on the channel boundary by the intensity of the reflected energy. This technique will allow mapping the extent of these two bed materials.

It is recommended that future investigations thoroughly test their field equipment and data reduction programs before embarking on a Grand Canyon scale expedition. Also, analysis would improve if changes in sediment storage in the upstream reservoir could be measured.

MANAGEMENT CONSIDERATIONS

Investigating Natural Rivers Improves Understanding Regulated Rivers

Investigation of a naturally flowing river channel and its sand deposits resulted in understanding a natural progression of events leading up to annual scour of the eddy deposit. The time scale of change in the natural river setting was conducive to measurement and documentation of the progression with relatively simple equipment and techniques. The natural river provides a reliable annual flood flow free of water claims or political maneuvering, and one of the most inaccessible rivers on this continent is the Colorado River in Grand Canyon. For these reasons one could make the case that basic river mechanics research is best conducted outside the regulated river setting where frequent flow fluctuations disrupt processes and create confusing patterns of responses. What was learned in the natural river setting is directly applicable to the problem investigated in the regulated river setting in Glen and Grand Canyons, and also provided a much needed comparison between the rivers upstream and downstream from Lake Powell.

Annual cycles of rapid erosion and subsequent deposition of eddy bars are natural processes of dynamic equilibrium in naturally flowing incised rivers where debris fan-eddy complexes occur. The scour/fill cycle is driven by the annual flood flow cycle which is accompanied by increased sediment load during the rising limb of floods (hysteresis) and deformation of the pool-eddy system. Regulated river eddy bars also eroded during the rising limb of daily hydropower floods and pool deformation at hourly time scales can be explained by variation in sediment load. Observations and multiple avenues of detailed investigation from both the regulated and unregulated rivers suggest that the common cause of rapid eddy bar erosion is tractive forces directed along the toe

of over-steepened eddy deposits, which is explained by pool deformation/channel modification due to hysteresis effects in sediment transport. The sediment hysteresis effect is enhanced by the dam operation practices of low fluctuating 'weekend' flows, holiday flows and even low constant evaluation flows because sand storage is increased in the channel in direct proportion to the duration of low flow.

The frequency of erosion/deposition cycles is important from a sediment storage and sediment transport perspective for management and monitoring of these resources. The longevity and long term stability of high elevation sand deposits, important natural resources in Glen and Grand Canyons, are directly related to the frequency and magnitude of erosion cycles affecting the lower elevation eddy deposits. During periods when the low elevation deposits are re-depositing following erosion events, high elevation deposits retreat. Because high discharges are required to deposit sand at high elevations, and high discharges are infrequent in the regulated river environment, minimizing the frequency of erosion cycles that effect low elevation deposits could prolong high elevation deposits.

Monitoring Regulated River Sand Bars

Sand bars are spatially persistent through time because their hydraulic controls (debris fans) are stable over long time spans. However, the unregulated river eddy bars are completely reworked each year and return to similar size and morphology after a wide variety of flood magnitudes. On the unregulated river, the long-term variability in eddy bar size was much less than the short-term variability. Even without accounting properly for sampling variability, monitoring at a consistent time each year after flood recession would allow detection of long term trends in sediment storage because the period of stasis is 10-11 months long. However, in order to critically compare repeated measurements of sand bar size, the sampling variability has to be quantified. This basic principle of

scientific investigation must be controlled in order to allow comparison of results and to define trends which are indisputable.

Regulated river sand bars also experience cycles of erosion and deposition but the cycles are not synchronized because there is not an annual hydrologic event. Furthermore, some regulated river bars undergo several cycles of erosion/deposition annually. Cluer and Dexter, in a series of contract reports, have attempted to address the variability issue but have met with limited support or interest in this fundamental sampling/monitoring issue. Monitoring regulated river sand bars on a calendar schedule does not quantify the significant effects of short term erosion/deposition cycles. The effects are significant because the variance caused by an erosion/deposition cycle greatly exceeds the variance measured over longer time spans. Quantifying the short term variance leads to different interpretations of long term information, and that information is needed to document trends caused by river management actions and dam operations. An alternative monitoring approach may focus on measuring changes in high elevation deposits (above the influence of dam operations) such as volume or event cut bank retreat. Such an approach could rely on annual time span measurements and may be more productive than monitoring the dynamic low elevation or high and low elevation deposits together, which is the current practice.

Because sediment transport in the Colorado River downstream from Glen Canyon Dam is supply limited, not capacity limited, cycles of erosion and deposition also create problems for sediment transport measurements and modeling. Modeling programs will need very detailed sediment supply information to be accurate and it is probably not feasible to obtain such information over appreciable reaches. Therefore, model predictions will have high uncertainty.

Processes Missing On The Regulated River

Sand transported by wind processes during the extensive low flow season on the unregulated river was important for forming and maintaining high elevation sand deposits. Wind processes are diminished along rivers that are regulated for peaking hydropower, because the sand bars are either frequently wetted or become vegetated.

Processes associated with annual erosion and deposition of large volumes of sand along the river margins may affect biological processes, for example: the sudden release of sediment to the river during the rising limb of floods may be rich in nutrients and provide feeding opportunities for aquatic organisms or trigger biological processes based on an environmental cue. There is also rejuvenation of the return current channels, or backwaters, used by juvenile fish on an annual basis, and perhaps other processes not identified yet. Return current channels along the unregulated river were observed to be producing biomass primarily during winter months because of their remarkable stability throughout the winter low flow season. They were supporting biological processes that have not been observed in the regulated river return current channel environment.

The Role Of Floods And Realistic Expectations Of Their Results

As floods become a tool for regulated river resource management, predicting the outcome of floods is important. This is a difficult task because the result of a flood at an individual sand bar, or site specific benefits, depends on the local variables of sediment supply and the dynamic hydraulics of flow recirculation and channel geometry adjustments in response to a vacillating sediment supply-sediment transport relationship. However, this investigation and observations made following the 1996 spike flow in Grand Canyon are consistent with the hypothesis and conceptual model of this report which provides a framework for understanding the range of results.

The basis of the model is that sand is required in the channel to make the channel a dynamic hydraulic environment, which causes dynamic changes in sand storage along the channel margins in sand bars. Where and when sand is not available in the channel, the channel is stable under dam operations and spike flows and consequently, the channel margin deposits are stable also. Field evidence supporting this prediction of the model comes from sand bars in the Glen Canyon reach which were only minimally changed during the 1996 spike flow. Where sand is in large supply in the channel the model predicts that sand bars would scour on the rising limb of hydropower floods or spike flows. As flow continues to rise the effect of channel modification is reduced and sand bars begin rebuilding. Sand bars will rebuild to elevations approaching the maximum river stage provided an adequate sediment supply and duration of high flow.

Given sufficiently long flow duration, all scoured sand bars will rebuild. However, long duration high flows can deplete sediment supplies because the depletion rate of the sediment supply depends on the duration of high flows which have the greatest transport capacity. Short duration floods could result in insufficient time for sand bar rebuilding following the initial scour. This effect would be most prominent where sediment supply was low.

The magnitude of floods controls the maximum elevation at which sand can be deposited. Also, high elevation deposits are less directly influenced by scour and fill processes related to dam operations. Therefore it is reasonable that greater magnitude floods would deposit sand in more stable environments and those sand deposits would have greater longevity. Low magnitude floods would create low elevation sand deposits that would be very unstable during powerplant flows and the duration of flood benefits would short. There is some question about scouring sand bars by large magnitude floods that overtop debris fans. Often presented as general knowledge is the idea that flows over debris fan elevations contract the recirculating eddy, resulting in scour of the sand bars. However, observations made in this investigation at the naturally flowing river study reach near Moab provide conflicting evidence. The Moab debris fan is low elevation and

is completely inundated by flows with 1-2 year return period but the eddy recirculation zone persists and sand bars persist through a wide range of flood discharges, although the sand bars are scoured and rebuilt by each flood. Very short duration floods might scour sand bars but not completely rebuild them. This question could be addressed with additional flow modeling experiments.

The frequency of floods in the regulated river is a question asked of and by managers and scientists. The greatest concern is about the 'adequacy' of sediment supply in order to realize 'benefits' from a flood. This investigation shows that sand bars will not scour during floods where or when sand supply is very low, as is the case in the Glen Canyon reach, because the channel is stable. Where a large sand supply exists in the channel, we can expect sand bars to scour on the rising limb of floods because the channel is deformed, but deposition of new bars begins once the channel regains conducive geometry. Where sediment supply is greatest we can expect the greatest range of sand bar responses to floods because of the locally variable sediment supply and sorting processes and the resultant variation in channel deformation (and the duration of deformation) at individual eddies. Because the sand supply is not evenly distributed throughout the Grand Canyon, a range of results is expected from individual floods and managers need to recognize that there will be non-uniform results regardless of the sediment supply or design of a flood. Benefits of frequent floods are that they allow the river to naturally limit the colonization of sand bars by invasive plants and they rejuvenate backwater environments. Infrequent floods allow vegetation to become so established on sand bars that even very large magnitude floods are incapable of removing it.

If general benefits to the river 'system' are the goal of managed floods then the case can be made that large magnitude floods are a good approximation of the natural processes that incised river channel ecosystems evolved to. On the other hand, if site specific benefits are the yard sticks which measure the success or failure of floods, then

the opportunities to rejuvenate individual sites will be rare, and there will always be large uncertainty about the sediment supply and local responses.

Additional Work

The conceptual model presented in this investigation could be verified through additional field studies that included high frequency sediment transport measurements in the sediment storage and sediment transport environments. Also, additional understanding of the processes of hysteresis and pool-eddy deformation could be gleaned from physical model studies. It is possible to evaluate questions about various spike flow alternatives using the techniques and concepts developed in this investigation. For example, resource managers may want to know the effects of 1,275 vs. 1,700 m^3s^{-1} (45,000 vs. 60,000 cfs) in an eddy and its associated sand bars.

REFERENCES CITED

- Andrews, E.D., 1991a. Deposition rate of sand in lateral separation zones, Colorado River. EOS, Trans. Am. Geophys. Union, v.72, p.212.
- Andrews, E.D., 1991b. Sediment transport in the Colorado River Basin. *In: Colorado River Ecology and Dam Management*, National Academy Press, pp.54-74.
- Baars, D.L., 1972. Red Rock Country-The Geologic History Of The Colorado Plateau. Doubleday/Natural History Press, New York, 73 p.
- Bates, P.D., Anderson, M.G., Baird, L., Walling, D.E., and Simm, D., 1992. Modelling floodplain flows using a two-dimensional finite element model. *Earth Surface Processes and Landforms*, v.17, pp.575-588.
- Bauer, B.O., and Schmidt, J.C., 1993. Waves and sandbar erosion in the Grand Canyon: applying coastal theory to a fluvial system. *Annals Assoc. Amer. Geogr.*, v.83, pp.475-497.
- Beus, S.S., and Avery, C.C., (eds) 1991. The influences of variable discharge regimes on Colorado River sand bars below Glen Canyon Dam. United States Department of Interior Bureau of Reclamation Glen Canyon Environmental Studies Program Report P3. Flagstaff, AZ.
- Beus, S.S., Avery, C.C., and Cluer, B.L., 1991b, Beach erosion studies under discrete controlled releases: Colorado River through Grand Canyon National Park: EOS, Trans. Am. Geophys. Union, v.72, pp.223.
- Beus, S.S., Biddle, J.W., Iaquinto, P., Lojko, F.B., and McAfee, B, 1982, Study of beach profiles as a measure of beach erosion on the Colorado River : Colorado River Investigations I, Northern Arizona University/Museum of Northern Arizona, pp.16-19.
- Beus, S.S., Bogart, R., Flick, L., Brinkhuif, S., Possen, B., Ringhiser, S., and Kuhl, M., 1988a, Chapter IV-topographic changes on selected beaches in the Grand Canyon, 1986-1987: Colorado River Investigations VI, July-August 1987, Northern Arizona University/Museum of Northern Arizona, pp.2-32.

- Beus, S.S., Bogart, R., Flick, L., Brinkhuif, S., Possen, B., Ringhiser, S., and Kuhl, M., 1988b, Chapter I-topographic changes on selected beaches in the Grand Canyon, 1987-1988: Colorado River Investigations VI, July-August 1987, Northern Arizona University/Museum of Northern Arizona, pp.16-41.
- Beus, S.S., Burmaster, B., Byars, B., Dancis, D., Hasenbuhler, P., and Pauls, J., 1984a, Changes in beach profiles along the Colorado River in Grand Canyon 1974-1983: Colorado River Investigations II, July-August 1983, Northern Arizona University/Museum of Northern Arizona, pp.85-105.
- Beus, S.S., Cardon, R., Fulton, F., Pastrick, A., and Stock, M., 1987, Chapter II-beach profile data from July-August 1986 surveys in Grand Canyon: Colorado River Investigations V, July-August 1987, Northern Arizona University/Museum of Northern Arizona, pp.3-33.
- Beus, S.S., Carothers, S.W., and Avery, C.C., 1985, Topographic changes in fluvial terrace deposits used as campsite beaches along the Colorado River in Grand Canyon: *Jour. Ariz.-Nev. Acad. Sci.*, v.20, pp.111-120.
- Beus, S.S., Coffin, J., Doty, A., Messina, P., and Mail, D., 1986, Chapter II-changes in selected beach profiles along the Colorado River, Grand Canyon, 1984-1985: Colorado River Investigations II, July-August 1983, Northern Arizona University/Museum of Northern Arizona, pp.3-69.
- Beus, S.S., Lojko, F., Holmes, M.F., Penner, D., and Renken, S., 1984b, Topographic changes in fluvial terrace deposits used as campsite beaches along the Colorado River in Grand Canyon: Colorado River Investigations II, July-August 1983, Northern Arizona University/Museum of Northern Arizona, pp.23-84.
- Beus, S.S., Stevens, L.E., and Lojko, F., 1989, Chapter II-topographic changes on selected beaches in the Grand Canyon, 1988-89: Colorado River Investigations VII, July-August 1989, Northern Arizona University/Museum of Northern Arizona, pp.35-61.
- Beus, S.S., Beus, S.S., Beus, S.S., 1991a. Chapter II-topographic changes on selected beaches in the Grand Canyon, 1989-1990: Colorado River Investigations VIII, July-August 1990, Northern Arizona University/Museum of Northern Arizona, pp.25-50.
- Breed, W.J., (ed) 1974. Geology of the Grand Canyon. Museum of Northern Arizona, Flagstaff, AZ.
- Brigham Young University, 1995. SMS User's Manual. BYU-Engineering Computer Graphics Laboratory, Provo, UT.

- Bryan, K., 1927. Channel erosion of the Rio Salado, Socorro County, NM. U.S. Geological Survey Bulletin 790, pp.17-19.
- Budhu, M., and Gobin, R., 1994. Instability of sandbars in Grand Canyon. *ASCE J. Hyd. Eng.*, v.120, n.8, pp.919-933.
- Budhu, M., and Gobin, R., 1995a. Seepage erosion from dam-regulated flow: case of Glen Canyon Dam, Arizona. *ASCE J. Irr. Drain Eng.*, v.121, n.1, pp.22-33.
- Budhu, M., and Gobin, R., 1995b. Seepage-induced slope failures on sandbars in Grand Canyon. *ASCE J. Geotech. Eng.*, v.121, n.8, pp.601-609.
- Budhu, M., and Gobin, R., 1996. Slope instability from ground-water seepage. *ASCE J. Hyd. Eng.*, v.122, n.7, pp.415-417.
- Carpenter, M.C., 1996. Monitoring erosion and deposition using an array of load-cell scour sensors during the Spring 1996 controlled-flood experiment on the Colorado River in the Grand Canyon. *EOS, Trans. Am. Geophys. Union*, v.77, p.F271.
- Carpenter, M.C., Carruth, R.L., and Cluer, B.L., 1991. Beach erosion and deformation caused by outward flowing bank storage associated with fluctuating flows along the Colorado River in the Grand Canyon. *EOS, Trans. Am. Geophys. Union*, v.72, p.222.
- Carpenter, M.C., Carruth, R.L., Fink, J.B., Boling, J.K., and Cluer, B.L., 1995. Hydrogeology and deformation of sandbars in response to fluctuations in flow of the Colorado River in the Grand Canyon, Arizona. U.S. Geological Survey Water-Resources Investigations Report 95-4010, 16p.
- Christiansen, T., 1993. Suspended sediment transport in the Colorado River. Unpublished M.S. thesis, University of Washington.
- Clifford, N.J., 1993. Formation of riffle-pool sequences: field evidence for an autogenetic process. *Sedimentary Geology* v.85, pp.39-51.
- Cluer, B. L., 1991. Catastrophic erosion events and rapid deposition of sandbars on the Colorado River, the Grand Canyon, Arizona. *EOS, Trans. Am. Geophys. Union*, v.72, p.223.
- Cluer, B.L., 1995a. Cyclic fluvial processes and bias in environmental monitoring, Colorado River in Grand Canyon. *The Journal of Geology*, v.103, pp.411-421.

- Cluer, B.L., 1995b. Aerial photography of the GCES-II test flows and interim flows. Final Report, U.S. Department of the Interior, National Park Service. Flagstaff, AZ.
- Cluer, B.L., Carpenter, M.C., Martin, L.J., Wondzell, M.A., Dexter, L.R., and Manone, M.F., 1993. Rapid erosion and slow redeposition of sand bars along the regulated Colorado River in Grand Canyon, Arizona. EOS, Trans. Am. Geophys. Union, v.74, p.321.
- Cluer, B.L., and Dexter, L.R., 1994. Daily dynamics of Grand Canyon sandbars; monitoring with terrestrial photogrammetry. Final Report, U.S. Department of the Interior, National Park Service. Flagstaff, AZ. 200p.
- Dexter, L.R., Cluer, B.L., and Manone, M.F., 1995. Using land based photogrammetry to monitor sandbar stability in Grand Canyon on a daily time scale. In, VanRiper, C., III, ed.: Proceedings of the Second Biennial Conference of Research in Colorado Plateau National Parks. Transactions and Proceedings Series, National Park Service. pp. 67-86.
- Dolan, R. Howard, A., and Trimble, D., 1978. Structural control of the rapids and pools of the Colorado River in Grand Canyon. *Science*, v. 202, pp. 629-631.
- Dynesius, M., and Nilsson, C., 1994. Fragmentation and flow regulation of river systems in the northern third of the world. *Science*, v.266, pp.753-761.
- Froelich, D.C., 1988. Finite element surface water modeling system: 2-dimensional flow in the horizontal plane - User's manual, Federal Highways Administration Publication No. FHWA-RD-88-177.
- Gauger, R.W., 1996. River-stage data, Colorado River, Glen Canyon Dam to Upper Lake Mead, Arizona, 1990-94. U.S. Geological Survey Open-File Report 96-626.
- Gore, J.A., and Petts, G.E., (eds), 1989. Alternatives in Regulated River Management. CRC Press, Inc., Boca Raton, FL.
- Graf, W.L., 1987. Rapids in canyon rivers. *The Journal of Geology*, v.87, pp.533-551.
- Gray, J.R., Webb, R.H., and Hindman, D.W., 1991. Low-flow sediment transport in the Colorado River, in *Proceedings of the Fifth Federal Interagency Sedimentation Conference*, Las Vegas, Nevada, pp. 4-63 to 4-71.
- Hereford, R., Fairley, H.C., Thompson, K.S., and Balsom, J.R., 1993. Surficial geology, geomorphology, and erosion of archaeological sites along the Colorado River, eastern Grand Canyon, Grand Canyon National Park, Arizona. U.S. Geological Survey Open-File Report 93-517, 46p.

- Hirsch, R.M., Walker, J.F., Day, J.C., Kallio, R., 1990. The influence of man on hydrologic systems, *in* Surface Water Hydrology, Wolman, M.G., and Riggs, H.C., eds., Geological Society of America, volume O-1, pp.329-359.
- Howard, A.D., 1975, Establishment of benchmark study sites along the Colorado River in Grand Canyon National Park for monitoring of beach erosion caused by natural forces and human impact: University of Virginia Grand Canyon Study, Technical Report no.1, 182p.
- Howard, A.D., and Dolan, R., 1976. Alterations of terrace deposits and beaches of the Colorado River in the Grand Canyon caused by Glen Canyon Dam and by camping activities during river float trips: summary, management implications, and recommendations for future research and monitoring. University of Virginia, Grand Canyon Study, Technical Report 7. 29p.
- Howard, A., and Dolan, R., 1981. Geomorphology of the Colorado River in the Grand Canyon. *Journal of Geology*, v.89, n.3., pp.269-298.
- Hoeting, J.A., Varga, K., and Cluer, B., 1997. Predicting Colorado River sandbar size using Glen Canyon Dam release characteristics: Final Report. National Park Service, Flagstaff, AZ, 55p.
- Iverson, R.M., and Major, J.J., 1986. Ground water seepage vectors and the potential for hillside failure and debris flow mobilization. *Water Resources Research*, v.22, pp.1543-1548.
- Jackson, W.L., and Beschta, R.L., 1982. A model of two-phase bedload transport in an Oregon Coast Range stream. *Earth Surface Processes and Landforms*, v.7, pp.517-527.
- Julien, P.Y., 1995. Erosion and Sedimentation. Cambridge University Press. 280p.
- Kaplinski, M.A., Beus, S.S., Hazel, J.E., and Kearsley, L., 1994. Monitoring the effects of interim flows from Glen Canyon Dam on sandbar dynamics and campsite size in the Colorado River corridor, Grand Canyon National Park, Arizona. Draft Final report. National Park Service, 38 p. plus appendix.
- Kearsley, L.H., Schmidt, J.C., and Warren, K.D., 1994. Effects of Glen Canyon Dam on Colorado River sand deposits used as campsites in Grand Canyon National Park, USA. *Regulated Rivers*, v.9, pp.137-149.
- Keller, E.A., and Melhorn, W.N., 1978. Rhythmic spacing and origin of pools and riffles. *Geological Society of America Bulletin*, v.89, pp.723-730.
- Keller, E.A., 1971. Areal sorting of bed-load material: the hypothesis of velocity reversal. *Geological Society of America Bulletin*, v.82, pp.753-756.

- Kieffer, S.W., 1985. The 1983 hydraulic jump in Crystal Rapid: Implications for river-running and geomorphic evolution in the Grand Canyon. *The Journal of Geology*, v.93, pp.385-406.
- King, I.P., 1990. Program Documentation: RMA2 - a two dimensional finite element model for flow in estuaries and streams, version 4.3. Resource Management Associates, Lafayette, CA.
- Le Mehaute, B., 1976. An Introduction to Hydrodynamics and Water Waves. Springer-Verlag, New York.
- Leopold, L.B., 1969. The rapids and pools-Grand Canyon. U.S. Geological Survey Professional Paper 669-D, pp.131-145.
- Leopold, L.B., 1994. A View of the River. Harvard University Press, Cambridge, MA., 298p.
- Leopold, L.B., and Maddock, T., Jr., 1953. The hydraulic geometry of stream channels and some physiographic implications. U.S. Geological Survey Professional Paper 252, 57p.
- Leopold, L.B., Wolman, M.G., and Miller, J.P., 1964. Fluvial Processes in Geomorphology. San Francisco, Freeman, 522p.
- Lisle, T.E., 1979. A sorting mechanism for a riffle-pool sequence. *Geological Society of America Bulletin*, v.90, pp.1142-1157.
- Lyons, J.K., Pucherelli, M.J., and Clark, R.C., 1992. Sediment transport and channel characteristics of a sand-bed portion of the Green River below Flaming Gorge Dam, Utah, USA. *Regulated Rivers: Research and Management*, v.7, pp.219-232.
- Miller, A.J., 1994. Debris-fan constrictions and flood hydraulics in river canyons: some implications from two-dimensional modelling. *Earth Surface Processes and Landforms*, v.19, pp.681-697.
- Miller, A.J., 1995. Valley morphology and boundary conditions influencing spatial patterns of flood flow, in Costa et al., eds., Natural and Anthropogenic Influences in Fluvial Geomorphology, Geophysical Monograph 89, American Geophysical Union, Washington, DC.
- Nanson, G.C., 1986. Episodes of vertical accretion and catastrophic stripping: A model of disequilibrium flood-plain development. *Geological Society of America Bulletin*, v.97. pp.1467-1475.

- National Research Council, 1987. River and dam management: a review of the Bureau of Reclamation's Glen Canyon Environmental Studies. National Academy Press, Washington, D.C.
- National Research Council, 1996. River resource management in the Grand Canyon. National Academy Press, Washington, D.C.
- Nelson, J.M., McDonald, R.R., and Rubin, D.M., 1994. Computational prediction of flow and sediment transport patterns in lateral separation eddies. EOS, Trans. Am. Geophys. Union, v.75, pp.268.
- Norton, W.R., King, I.P., and Orlob, G.T., 1973. A finite element model for lower Granite Reservoir, Water Resources Engineers, Inc., Walnut Creek, CA.
- Oberg, K.A., and Mueller, D.S., 1994. Recent applications of acoustic Doppler current profilers. Fundamentals and Advancements in Hydraulic Measurement and Experimentation, ACSE Conf. Proc., Clifford A. Pugh, ed., pp.341-350.
- Pemberton, E.L., 1976. Channel changes in the Colorado River below Glen Canyon Dam, *in* Proceedings of the Third Inter-Agency Sedimentation Conference. Water Resources Council Sedimentation Committee, v.5, pp.61-73.
- Powell, J.W., 1875. Exploration of the Colorado River and the West and its Tributaries. U.S. Government Printing Office.
- Randle, T.J., and Pemberton, E.L., 1987. Results and analysis of STARS modeling efforts of the Colorado River in Grand Canyon, Glen Canyon Environmental Studies Technical Report. Bureau of Reclamation, Salt Lake City, UT.
- RD Instruments, 1993. Direct-reading broadband acoustic Doppler current profiler technical manual. RD Instruments. San Diego, CA. 52p.
- Richards, K., 1982. Rivers: Form and Process. Methuen and Co.
- Richardson, E.V., Simons, D.B., and Julien, P.Y., 1990. Highways in the river environment. U.S. Dept. Transportation, Federal Highways Administration.
- Rubin, D.M., Schmidt, J.C., and Moore, J.N., 1990. Origin, structure, and evolution of a reattachment bar, Colorado River, Grand Canyon, Arizona. *Journal of Sedimentary Petrology*, v.60, n.6, pp.982-991.
- Rubin, D.M., Schmidt, J.C., Anima, R.A., Ikeda, H., McDonald, R., and Nelson, J.M., 1991. Depositional processes and structures in recirculation zones in the Colorado River, Grand Canyon, Arizona (abst.), *in* AGU 1991 Fall Meeting

- Program and Abstracts. American Geophysical Union EOS Transactions, v.72, n.44, pp.218.
- Rubin, D.M., Schmidt, J.C., Anima, R.A., Brown, K.M., Ikeda, H., Jaffe, B.E., McDonald, R., and Nelson, J.M., Reiss, T.E., Sanders, R., and Stanley, R.G., 1994. Internal structure of bars in Grand Canyon, Arizona, and evaluation of proposed flow alternatives for Glen Canyon Dam. U.S. Geological Survey Open-File Report OF94-594, 16p.
- Schmidt, J.C., 1990. Recirculating flow and sedimentation in the Colorado River in Grand Canyon, AZ. *The Journal of Geology*, v.98, pp.709-724.
- Schmidt, J.C., and Graf, J.B., 1990. Aggradation and degradation of alluvial sand deposits, 1965 to 1986, Colorado River, Grand Canyon National Park, Arizona. U.S. Geological Survey Professional Paper 1493, 74p.
- Schmidt, J.C., Grams, P.E., and Webb, R.H., 1995. Comparison of the magnitude of erosion along two large regulated rivers. *Water Resources Bulletin*, v.31, n.4, pp.617-631.
- Schmidt, J.C., and Rubin, D.M., 1995. Regulated streamflow, fine-grained deposits, and effective discharge in canyons with abundant debris fans, in Costa et al., eds., *Natural and Anthropogenic Influences in Fluvial Geomorphology*, Geophysical Monograph 89, American Geophysical Union, Washington, DC.
- Schmidt, J.C., Rubin, D.M., and Ikeda, H., 1993. Flume simulation of recirculating flow and sedimentation. *Water Resources Research*, v.29, pp.2925-2939.
- Silverston, E., and Laursen, E.M., 1976. Patterns of scour and fill in pool-rapid rivers. Proc. Third Federal Inter-agency Sedimentation Conference, Denver, CO., pp.5-125 to 5-136.
- Smith, J.D., and Andrews, E.D., 1993. Channel margin and eddy bar deposition along the Colorado River in Grand Canyon NP. *Park Science*, Winter 1993, pp.3-4.
- Smith, J.D., and Wiele, S., *in press*. Flow and sediment transport in the Colorado River between Lake Powell and Lake Mead. U.S. Geological Survey Professional Paper.
- Smith, W.O., Vetter, C.P., Cummings, G.B., et al., 1960. Comprehensive survey of sedimentation in Lake Mead, 1948-1949. U.S. Geological Survey Professional Paper 295, 254p.
- Soong, T.W., and Bhowmik, N.G., 1991. Two-dimensional hydrodynamic modeling of a reach of the Mississippi River in Pool 19, in Shane, R.M., ed., *Hydraulic*

- Engineering: Proceedings of the 1991 National Conference, American Society of Civil Engineers, New York, pp.900-905.
- Stevens, L.E., Schmidt, J.C., Ayers, T.J., and Brown, B.T., 1995. Geomorphic influences on fluvial marsh development along the dam-regulated Colorado River in the Grand Canyon, Arizona. *Ecological Applications*, v.5, pp.65-74.
- Stevens, M.A., and Simons, D.B., 1971. Stability analysis for coarse granular material on slopes, *in* River Mechanics. Water Resources Publications, Littleton, CO.
- Stockstill, R.L., and Berger, R.C., 1994. HIVEL2D: a two-dimensional flow model for high-velocity channels. Technical Report REMR-HY-12, 53pp., US Army Corps of Engineers Waterways Experiment Station, Vicksburg, MS.
- Thomas, W.A., and McAnally, W.H., Jr. 1991. User's manual for the generalized computer program system: open-channel flow and sedimentation, TABS-2. U.S. Army Engineer Waterways Experiment Station, Vicksburg, MI.
- USBOR, 1995. Operation of Glen Canyon Dam, Final Environmental Impact Statement. Bureau of Reclamation, Salt Lake City, UT.
- van Rijn, L.C., 1984. Sediment Transport, Part III: Bedforms and alluvial roughness. *J. Hyd. Div., ASCE*, v.10, n.12.
- Webb, R.H., Pringle, P.T., and Rink, G.R., 1989. Debris flows from tributaries of the Colorado River, Grand Canyon National Park, Arizona. U.S. Geological Survey Professional Paper 1492.
- Webb, R.H., 1996. Grand Canyon, a Century of Change. University of Arizona Press, Tucson, AZ, 290p.
- Wegner, D.L., Stevens, L., and Melis, T., 1996. Controlled flood studies, Glen Canyon Dam, Spring 1996. Glen Canyon Environmental Studies Office, Bureau of Reclamation, Flagstaff, AZ.
- Werrell, W., Inglis, R., Jr., and Martin, L., 1993. Geomorphic stability of sandbar 43.1L on the Colorado River in the Grand Canyon in response to ground water seepage during fluctuating flow releases from Glen Canyon Dam. National Park Service Technical Report 92/10.
- Wiele, S.M., Graf, J.B., and Smith, J.D., 1996. Sand deposition in the Colorado River in Grand Canyon from floods in the Little Colorado River. U.S. Geological Survey Open-File Report, in press.

Wilson, R.P., 1986. Sonar patterns of Colorado riverbed, Grand Canyon. Proc. Fourth Federal Inter-agency Sedimentation Conference, Las Vegas, NV, v.2, pp.5-133 to 5-142.